Towards Improving Electron Recovery and Coulombic Efficiency of Microbial Electrochemical Cells Fed with Fermentable Electron Donors

by

Mohamed Mahmoud Ali Mohamed

A Dissertation Presented in Partial Fulfillment
of the Requirements for the Degree
Doctor of Philosophy

Approved October 2016 by the
Graduate Supervisory Committee:

Bruce E. Rittmann, Co-Chair
César I. Torres, Co-Chair
Paul Westerhoff
Prathap Parameswaran

ARIZONA STATE UNIVERSITY

December 2016

ABSTRACT

The microbial electrochemical cell (MXC) is a novel environmental-biotechnology platform for renewable energy production from waste streams. The two main goals of MXCs are recovery of renewable energy and production of clean water. Up to now, energy recovery, Coulombic efficiency (CE), and treatment efficiency of MXCs fed with real wastewater have been low. Therefore, the overarching goal of my research was to address the main causes for these low efficiencies; this knowledge will advance MXCs technology toward commercialization.

First, I found that fermentation, not anode respiration, was the rate-limiting step for achieving complete organics removal, along with high current densities and CE. The best performance was achieved by doing most of the fermentation in an independent reactor that preceded the MXC. I also outlined how the efficiency of fermentation inside MXCs can be enhanced in order to make MXCs-based technologies cost-competitive with other anaerobic environmental biotechnologies. I revealed that the carbohydrate and protein contents and the BOD_5/COD ratio governed the efficiency of organic-matter fermentation: high protein content and low BOD_5/COD ratio were the main causes for low fermentation efficiency.

Next, I showed how a high ammonium concentration can provide kinetic and metabolic advantages or disadvantages for anode-respiring bacteria (ARB) over their competitors, particularly methanogens. When exposed to a relatively high ammonium concentration (i.e., > 2.2 g total ammonia-nitrogen (TAN)/L), the ARB were forced to divert a greater electron flow toward current generation and, consequently, had lower net biomass yield. However, the ARB were relatively more resistant to high free ammonia-nitrogen (FAN) concentrations, up to 200 mg FAN/L. I used FAN to manage ecological interactions among ARB and non-ARB in an MXC fed with fermentable

substrate (glucose). Utilizing a combination of chemical, electrochemical, and genomic tools, I found that increased FAN led to higher CE and lower methane (CH_4) production by suppressing methanogens. Thus, managing FAN offers a practical means to suppress methanogenesis, instead of using expensive and unrealistic inhibitors. My research findings open up new opportunities for more efficient operation of MXCs; this will enhance MXC scale-up and commercial applications, particularly for energy-positive treatment of waste streams containing recalcitrant organics.

ACKNOWLEDGMENTS

I believe that I have reached a point that I can write this section freely without any concern about the validity, logic, and reproducibility of experimental data. Being the first and only Ph.D. holder in my extended family, I would like to write some thoughts for myself, my family, and a lot of people to whom I owe thanks.

I was completing my masters at Cairo University and beginning to think about graduate school, when I came across a few papers on microbial electrochemical cells, which was a "sexy" topic at that time. Among a few hundred papers I had collected, I found that the articles from Dr. Bruce Rittmann's laboratory at Arizona State University were the most existing. This was the main motivation for me to join his laboratory. That decision proved, over the past 4.5 years or so, to be right; his teaching, support, and mentorship has been unwavering. He always points out how it is important to "think like microorganisms, so they can work for us." Here, I was able to blend my Chemistry background with Engineering, Microbial Ecology, and Mathematical Modeling to mimic the microorganisms' thinking. I can't thank him enough for being such an unconditional, endless supporter in my academic life, making the transition from a Ph.D. student to an independent researcher easier and smoother. I will remember his grammar and writing lessons for the entirety of my academic life as well as his focus on the "take-home messages" and how to make my wordy writing more concise. I also grateful to could work closely with Dr. César Torres, once I joined Swette Center for Environmental Biotechnology. Dr. Torres always challenged me to critically dig into my research data, and he taught me to improve my communication skills. He was always eager to help me simplify the problem at hand, to provide full support and guidance in my research, to always be mindful of the fundamentals, and to inspire me to perform research I have never thought about doing.

I must also thank my committee members: Dr. Paul Westerhoff and Dr. Prathap Parameswaran for giving me invaluable input on my work. Their feedback after my research proposal was critical in reminding me to tie my work back into the big picture.

Next, I acknowledge Diane Hagner – our Lab Manager – and Carole Flores – our Business Operations Manager. You are the "true heroes" of the Swette Center for Environmental Biotechnology. Diane: thank you for picking me and my wife up from airport once we arrived Arizona; for your endless support to ensure that our research environment is safe, efficient, and organized; and for ensuring that I, and others, can perform their experiments efficiently. Carole: thank you for all your administrative assistance, especially with travels, that saved my time; and your desire to help me (and other, too), which is a very special trait of yours. I also would like to thank my current mentee: Omar Arafa. Your unstoppable passion for my research and learning excited me to teach and perform more research. I thank past and present members of the MXC team, especially Andrew Marcus and Michelle Young, for all of their help, discussion, and support. A big thanks to Juan Maldonado Ortiz for his expertise on bioinformatics.

I thank Waste Management Inc. team, especially Nicole Bisacchi and Clay Carroll for helping with landfill leachate procurement from the Northwest Regional Landfill facility.

Lastly, for their love, patience, and support, I thank my family close by: my wife, Marwa, and two daughters: Tala and Celine. I also thank my family far away: my beloved mother, my father, and my sister.

My research was funded by an Egyptian government fellowship from the Egyptian Ministry of Higher Education, by a Graduate Completion Fellowship and Faculty Emeriti Fellowship from Arizona State University, by an Arizona Water

Association Scholarship, by the Graduate and Professional Student Association (GPSA) at Arizona State University and by the Swette Center for Environmental Biotechnology.

TABLE OF CONTENTS

Page

LIST OF TABLES

LIST OF FIGURES

Figure Page

LIST OF ABBREVIATIONS

ARB	Anode-respiring bacteria
BES	2-bromoethanesulfonic acid
BMP	Biochemical methane potential
BOD_5	5-day biochemical oxygen demand
CE	Coulombic efficiency
COD	Chemical oxygen demand
COS	Carbon oxidation state
CR	Coulombic recovery
CV	Cyclic voltammetry
EET	Extracellular electron transfer
FAN	Free-ammonia nitrogen
HRT	Hydraulic retention time
j	Current density
MEC	Microbial electrolysis cell
MFC	Microbial fuel cell
MXC	Microbial electrochemical cell
OTU	Operational taxonomic unit
PC	Principal Component
PCoA	Principal Coordinate Analysis
qPCR	Quantitative real-time polymerase chain reaction
SHE	Standard hydrogen electrode
$SUVA_{254}$	Specific ultraviolet absorption at 254 nm
VFAs	Volatile fatty acids

CHAPTER 1

INTRODUCTION AND SIGNIFICANCE

1.1 Fossil fuels and greenhouse gases

In 2003, late-professor Richard E. Smalley, the Chemistry Nobel laureate in 1996, created a list of the most important challenges of humanity for the next 50 years (Smalley, 2003). Not surprisingly, water, environment, and energy are among the major resource challenges facing humanity on his list.

Concerning energy, our current annual global energy demand is ~13500 million tons of oil equivalent (Mtoe) (or ~5.7×10^{20} J), with the majority of this demand (~81.4% in 2013) being extracted by the combustion of fossil fuels: oil (31.1 %), coal (28.9 %), and natural gas (21.4 %) (IEA, 2015). Approximately 44% of the global energy supply (~6000 Mtoe, or 2.5×10^{20} J) is used to produce 2000 Mtoe (or 8.4×10^{19} J) of electricity with a conversion efficiency of ~33 % (IEA, 2015). While our fossil fuel reservoirs remain enormous – the proven untapped reserves are ~9.1×10^{22} J, which might be enough to supply energy for hundreds of years (BP, 2011) – fossil fuels will result in significant emissions of greenhouse gases (GHG), particularly carbon dioxide (CO_2) and methane (CH_4), into the atmosphere (IEA, 2015; IPCC, 2014; Rothausen and Conway, 2011).

The agreement at Paris in December 2015 signals a political acceptance among the developed countries, including the United States, that net greenhouse gas emissions must be reduced to zero during the second half of the 21st century. In this context, the Intergovernmental Panel on Climate Change (IPCC) has suggested a range of possibilities for climate-change mitigation, including increased use of biomass-based technologies for efficient energy generation (IPCC, 2014). Therefore, our major

challenge is to reduce drastically our use of fossil fuel, and simultaneously replace them with carbon-neutral sources (Rittmann, 2008).

1.2 Biomass as a renewable energy source

Interest in biomass as one of the renewable resources for energy, chemicals, and fuel production, is growing, since it could result in substantial reduction in GHG emissions (Hatti-Kaul et al., 2007; Ragauskas et al., 2006; Kamm and Kamm, 2004). Biomass is still the main source of energy in many developing countries, such as Nepal (~97 %), Bhutan (~86 %), and the eastern part of the African Sahel (~81 %), where it is mainly used for cooking and heating (Hoogwijk et al., 2005). These "old-fashioned" technologies are inefficient in that they contribute to local air pollution and land degradation, sometimes even desertification (Holdren and Smith, 2000). Overcoming these drawbacks was the main motivation to develop modern, sustainable technologies that can be used to convert biomass into high-quality energy-value products, such as electricity and transportation liquid fuels, from relatively-concentrated biomass (i.e., wood and agricultural byproducts) (Ail and Dasappa, 2016; Heidenreich and Foscolo, 2015; Faaij, 2006; van Wyk, 2001; Kheshgi et al., 2000; Hall and Scrase, 1998). The modern biomass-based technologies have the potential to generate a significant share of global-energy need, perhaps up to 50% of global-energy demand (Hoogwijk et al., 2005; Berndes et al., 2003; Fischer and Schrattenholzer, 2001; Williams, 1995; Shell, 1995; Johansson et al., 1993; Lazarus, 1993; Lashof and Tirpak, 1990), mainly due to their high conversion efficiency, expectation to reduce their cost, and increase in the demand of sustainable, carbon-neutral energy source. Another possibility is to extract energy from less-concentrated organic wastes, such as wastewater, although current technologies are not efficient enough (Li et al., 2015; Shoener et al., 2014; Smith et al., 2014; McCarty et al., 2011; Iranpour et al., 1999).

1.3 Wastewater treatment: common practice

Over the past few decades, the activated-sludge process has become the dominant method to treat domestic wastewater in the United States. In activated sludge, air or oxygen is continuously supplied in order to oxidize the contaminates aerobically (Metcalf and Eddy, 2003; Rittmann and McCarty, 2001). Although the activated-sludge process is efficient at removing most organic compounds (85–95%) and nitrogen (70–85%) (Metcalf and Eddy, 2003), it is only suitable to treat low-strength wastewater, such as domestic wastewater, and it also has a high-energy demand (i.e., ~1.2 kWh per each 1 m^3 of wastewater treated for aeration, pumping, and other processes), which makes it expensive process in terms of O&M costs (McCarty et al., 2011). Theoretically, the wastewater's organic content is sufficient to generate approximately 3 to 4 times more energy than is required for wastewater treatment (Logan and Rabaey, 2012; Heidrich et al., 2011). Thus, our society could help minimizing its fossil fuel extraction and consumption through capturing part of energy in organic waste streams energy.

1.4 Can wastewater be a renewable energy source?

One possibility for wastewater treatment that generates net energy is methanogenesis, where microorganisms break down complex organic matter anaerobically (i.e., in the absence of oxygen) into a variety of organic acids, which are subsequently converted into CH_4 gas by methanogens (Smith et al., 2014). The CH_4 can be combusted in a separate system to generate electricity (with a relatively-low efficiency, i.e., < 40%), with the remainder converted to heat, which may or may not be used beneficially (McCarty et al., 2011). CH_4 is a potent GHG – with a global warming potential of nearly 25 times that of CO_2 (Forster et al., 2007) – and it cannot be allowed to escape to the atmosphere. A traditional limitation of methanogenic treatment that is

needs a concentrated organic waste stream and warm temperatures (> 20°C). Thus, methanogenesis has mainly been employed to anaerobically digest waste sludge from conventional wastewater-treatment processes, not the main flow directly (Peccia and Westerhoff, 2015; Smith et al., 2014; Logan and Rabaey, 2012; McCarty et al., 2011). This traditional combination (i.e., activated sludge process with anaerobic digestion of sludge) recovers only a small fraction of the energy stored in wastewater's organic matter (Owen, 1982), which makes the current wastewater treatment technologies energy-negative even when they use anaerobic digestion.

These bottlenecks can be avoided with application of the anaerobic membrane bioreactor (AnMBR), where porous membranes are used to retain biomass inside the reactor and to maintain longer sludge age, leading to capture most of particulate organics, degradation of more than 90% of the dissolved organics, and increase the methane generation (Li et al., 2015; Stephenson et al., 2000). However, the cost associated with membrane cleaning and maintenance impairs the scaling-up of these technologies. A new AnMBR design – the anaerobic fluidized membrane bioreactor (AFMBR) – may overcome the fouling problem by combining the advantages of a membrane bioreactor with an anaerobic fluidized bed reactor (McCarty et al., 2011). The fluidized GAC particles naturally clean the membrane and prevent fouling. Experiments by Kim et al. (2011a) revealed that total energy of AFMBR to treat low-strength domestic wastewater (i.e., chemical oxygen demand (COD) = 500 mg/L) was ~0.058 kWh per cubic meter of treated wastewater, approximately 10-times lower than the energy requirement for typical aerobic membrane bioreactor. More research is required to evaluate and optimize the efficiency of AFMBR to treat different waste streams under ambient conditions and to meet the discharge requirements into water bodies, but the AFMBR is a promising option.

A nascent technology to extract the energy value in organic waste streams is the 'microbial electrochemical cell (MXC).' The MXC is a platform technology that can recover energy value as electric current in the mode of microbial fuel cells (MFCs) (Figure 1.1A); as hydrogen gas (H_2) in the mode of microbial electrolysis cell (MEC) (Figure 1.1B); or in a variety of valuable chemicals, such as hydrogen peroxide (H_2O_2) (Logan and Rabaey, 2012; Rittmann, 2008). The hallmark of an MXC is the ability of anode-respiring bacteria (ARB) to oxidize organic matter internally and transfer the resulting electrons beyond their outermost membranes to a solid electron acceptor i.e., the anode surface (Malvankar and Lovley, 2014; Borole et al., 2011; Franks and Nevin, 2010; Lovley, 2008; Logan and Regan, 2006). Perhaps except for electric current, their products are more valuable than methane gas (Logan and Rabaey, 2012; McCarty et al., 2011; Rozendal et al., 2008a). However, a current drawback of MXCs is that electron recovery often is low when wastewater has complex organic matter, compared to simple substrates, such as acetate (Logan and Rabaey, 2012).

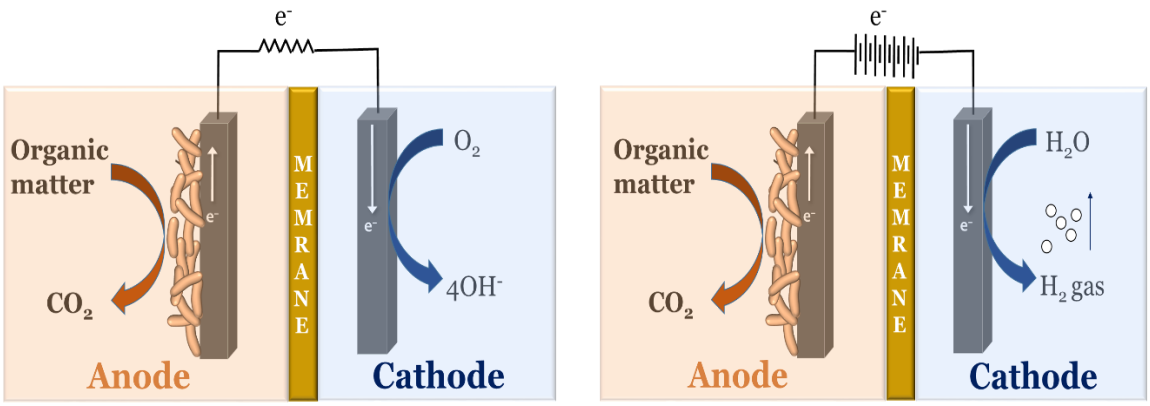

Figure 1.1 Schematic diagram of two different types of MXC. (A) microbial fuel cell (MFC). (B) microbial electrolysis cell (MEC).

1.5 Can MXCs be scaled-up?

Only a handful of studies have addressed pilot or semi-pilot MXCs, and most of studies were performed using small-volume reactors (i.e., tens to hundreds of milliliters) (Tota-Maharaj and Paul, 2015; Heidrich et al., 2014; Cusick et al., 2011; Logan, 2010; Qian et al. 2009; Li et al. 2008; Scott et al. 2007). Thus, a main challenge facing researchers for bringing MXCs to practical applications is to achieve fast kinetics so that the high cost associated (i.e., capital and O&M costs) are offset by the high-value of the generated energy (Logan and Rabaey, 2012; Logan, 2010; Rittmann, 2008). Although the current density and electron recovery have steadily improved over the past decade, today's MXCs are far from being commercially viable, mainly because no single part of MXCs is solely controlling their efficiency. Thus, more research is needed to optimize the MXCs efficiency in many areas – such as type of separator used, kinetics and metabolic activity of ARB, the cathode catalyst and electron acceptor, and the physical design of the system (Torres, 2014). Therefore, the overarching goal of my research is to maximize the electron recovery of MXCs and study the organic matter degradation in the MXCs' anodes, especially when real wastewater, such as landfill leachate, is used as an electron donor.

1.6 Fundamentals of an MXC

In an MXC, the complex organic compounds are biodegraded through a series of reactions that are illustrated in Figure 1.2. A variety of microorganisms are needed and, thus, found in MXCs: fermenters, homoacetogens, methanogens, and ARB. First, fermenters convert complex organic substrates, such as carbohydrate and protein, into a variety of short-chain volatile fatty acids (VFAs), alcohols, H_2, and CO_2 (Logan and Rabaey, 2012; Rittmann, 2008). Then, most of the fermentation products (i.e., VFAs

and alcohols) are further fermented into acetate and H_2 – the main products of fermentation in any anaerobic environmental biotechnology systems – although some of the H_2 can be converted to more acetate by homoacetogens (Schuchmann and Müller, 2014; Parameswaran et al., 2009; Diekert and Wohlfarth, 1994). Finally, acetate and H_2 are channeled either into methane by methanogens or electric current by ARB (McCarty et al., 2011; Parameswaran et al., 2010; Parameswaran et al., 2009; Thauer et al., 2008; Rittmann and McCarty, 2001; Reeve et al., 1992; Jones et al., 1987).

In an MXC, methanogenesis is an undesired process that often is a factor behind the low electron recovery (Parameswaran et al., 2009). Previous research studies proposed different strategies to inhibit methanogenesis in laboratory-scale MXCs, including thermal treatment, periodic exposure to oxygen, pH treatment, and use of chemical inhibitors, such as 2-bromoethanesulfonate (BES) (Rago et al., 2015; Parameswaran, et al., 2011; Chae et al., 2010).

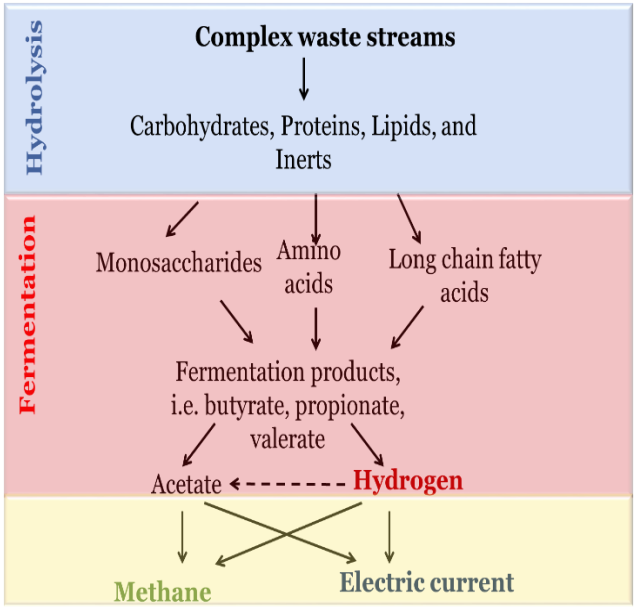

Figure 1.2 Anaerobic food web. Several groups of microorganisms mediate biotransformation processes – depicted as arrows – that stepwise convert complex waste streams into energy-conserving end-products: electrons in electric current or methane gas.

The MXC's performance is often characterized by current density (*j*) or power density (PD), Coulombic efficiency (CE), and treatment efficiency. CE is the fraction of electrons recovered as electric current at the anode of an MXC compared to the electron removed from the substrate, indicating the conversion efficiency of substrates into useful energy. It can be represented by the following equation:

$$CE = \frac{Q_{output}\ (C)}{96{,}485\ \left(\frac{C}{e^- eq}\right) \text{ x } (S_{influent} - S_{effluent})\ \left(\frac{g\ COD}{L}\right) \text{x } \frac{1\ e^- eq}{8\ g\ COD} \text{ x V (L)}} \qquad \text{(Eq. 1.1)}$$

where Q_{output} is the total charge recovered as electric current (C), $S_{influent}$ is the organic matter concentration in the initial substrate (expresses as g COD/L), $S_{effluent}$ is the organic matter concentration in the final effluent (expresses as g COD/L), and V is the volume of the reactor (L).

Aimed at wastewater treatment, treatment efficiency reflects the ability of MXCs to remove organic matter, and is often expressed as COD and BOD_5 (5-day biochemical oxygen demand) removals, which can be represented by the following equation:

$$\text{Treatment efficiency (\%)} = \frac{S_{influent} - S_{effluent}}{S_{effluent}} \text{ x } 100 \qquad \text{(Eq. 1.2)}$$

where $S_{influent}$ and $S_{effluent}$ are the influent and effluent organic matter concentration (expressed as g COD/L or mg BOD_5/L), respectively.

1.7 Dissertation objectives and outline

The optimization of MXCs fed with complex organic substrates, in terms of CE and treatment efficiency, requires a comprehensive understanding of pathways of organic substrates degradation in MXCs. The degradation pathway involves cooperation among ARB, fermenters, and homoacetogens, as well as competition with methanogens. Therefore, I will focus in this dissertation to answer a number of research questions that relate directly to maximize the electron recovery of MXCs and organic-matter degradation in the MXCs' anode chamber: (1) What is the main limiting step for the degradation of wastewater organics in MXCs? (2) Can pre-treatment of wastewater improve the MXCs performance in terms of *j*, CE, and organic matter removal? (3) What is the main component (i.e., protein and carbohydrate) in wastewater that controls the overall fermentation in MXCs? And (4) Can I inhibit methanogens using means that are practical for large-scale application of MXCs, instead of using expensive chemical inhibitors in laboratory experiments?

Chapter 2 provides extensive background on wastewater treatment in MXCs, the limited factors affected the anode performance, and the main microbial processes occurred in mixed-culture MXCs, which describes the goals of the research data presented in Chapters 3–7.

In Chapter 3, I use the Fenton reaction as pre-treatment to improve the biodegradability of organic matter in landfill leachate that is subsequently fed to an MEC. The Fenton reaction is one of the most commonly used advanced oxidation processes (AOPs). It relies on electron transfer between H_2O_2, the initiating oxidant, and ferrous ions (Fe^{2+}), a homogenous catalyst, to yield hydroxyl radicals ($OH^{\cdot}$), which attacks the recalcitrant organic matter (Duesterberg and Waite, 2006; Deng and Englehardt, 2006). I evaluate whether or not Fenton oxidation of landfill leachate can

enhance MEC performance and how Fenton pre-treatment alters the microbial community in ways that explain the enhanced performance. The content of Chapter 3 was published in an altered format in *RSC Advances* (Mahmoud et al., 2016).

Based on the results obtained in Chapter 3, I use Chapter 4 to investigate the impacts of doing most of the fermentation in an independent reactor that preceded the MEC. Findings from Chapter 4 indicate that the complex organic matter in the leachate was transformed to simple volatile fatty acids in the pre-fermentation reactor, leading to much better MEC performance compared to an MEC fed with raw leachate. The content of Chapter 4 was published in an altered format in *Bioresource Technology* (Mahmoud et al., 2014).

Building on Chapters 3 and 4, I use Chapter 5 to optimize Fenton oxidation of leachate. The concept is to feed different partially treated leachates into fermenting batch-culture reactors to evaluate whether the carbohydrate-to-protein ratio, inhibitory compounds, or both control the overall fermentation of the leachate's organic matter. Findings from Chapter 5 indicate that altering the BOD_5/COD and carbohydrate-to-protein ratios significantly increase the fermentation efficiency and the distribution of fermentation organic acids, with acetate, butyrate, and propionate being the dominant products, compared to raw leachate. This chapter will be submitted for publication in the *Waste Management Journal*.

In Chapters 6 and 7, I investigate the possible role of ammonia to promote the desired syntrophy in MXCs fed with fermentable substrates, such as glucose, by inhibiting H_2-consuming methanogens. The suppression of methanogenesis should promote the accumulation of homoacetogens, which convert H_2 and CO_2 to acetate, the substrate for ARB. This concept requires that a free ammonia nitrogen (FAN; NH_3) concentration that inhibits methanogens not have a significant inhibitory effect on ARB.

My literature search did not yield a consensus about the toxicity of ammonia on ARB in MXCs. Therefore, in Chapter 6, I test how ammonia can alter the ARB metabolism and extracellular electron transport in MXCs fed with non-fermentable substrate (i.e., acetate). My findings reveal that ARB are resistant to relatively high free ammonia concentrations, but sensitive to total ammonia-nitrogen (TAN), which is the sum of FAN and ionic ammonium nitrogen (NH_4^+). I also show that relatively high TAN concentration imposed a significant stress on the ARB biofilm. When induced with relatively high ammonium concentration (i.e., 2.2 g TAN-N/L), the anode biofilm boosted the electron fluxes toward current generation, a likely result of an energetic penalty, and consequently lowered biomass yield. The content of Chapter 6 was submitted to *Biotechnology & Bioengineering*.

Based on the findings from Chapter 6, I investigate how ammonia can be used to manage interactions among ARB and other members of the communities, particularly the fermenters and methanogens, in an MXC fed with fermentable substrate (i.e., glucose). In Chapter 7, I show that FAN altered the glucose fermentation pathways in batch MECs, minimizing the production of H_2, the "fuel" for hydrogenotrophic methanogens, leading to a significant increase in CE. Increasing FAN concentration was associated with the accumulation of higher organic acids (e.g., lactate, iso-butyrate, and propionate), which was accompanied by increasing relative abundances of phylotypes that are most closely related to anode respiration (*Geobacteraceae*), lactic-acid production (*Lactobacillales*), and syntrophic acetate oxidation (*Clostridiaceae*). Thus, the microbial community established syntrophic relationships among glucose fermenters, acetogens, and anode-respiring bacteria (ARB). I reveal that methanogenesis does not need to be completely suppressed to achieve high current production and CE from MXCs fed with fermentable substrates. Using FAN to suppress

methanogenesis is a realistic option for scaling-up MXCs during the biodegradation of fermentable substrates, particularly when the feed stream has a high nitrogen content, such as animal manures and landfill leachate. The content of Chapter 6 was submitted to *Environmental Science & Technology*.

In Chapter 8, I summarize the key findings, the significance of my work, and some concluding remarks that link the results in Chapters 3–7. I also make recommendations for future studies that would be a natural progression from or parallel research in this dissertation.

CHAPTER 2

BACKGROUND

2.1 MXCs as sustainable wastewater treatment technology

The main function of MXCs can be broken into two main categories: (1) Recovery of renewable energy in the form of electric current, hydrogen gas, or valuable organic compounds; and (2) production of clean treated water that can be discharged safely into water bodies, by removing the biodegradable organic contaminants (Rittmann, 2008). Despite the growing interest in MXCs over the past decade, they have not been successfully scaled-up compared to other mature environmental biotechnologies, such as anaerobic digestion (Logan and Rabaey, 2012; Logan, 2010). Although it has been recently demonstrated that MXCs can be considered an energy-neutral or -positive technology (Li et al., 2014; Zhang et al., 2013), my literature search yielded little information on energetically self-sustained wastewater treatment using MXCs. Therefore, our main challenge, as a scientific community, is to bring the MXC technology out the laboratory in ways that maximize energy output, while keeping the cost relatively low. What are the main factors that have limited scaling-up of this technology? The main obstacles for scaling-up MXCs include high cost of materials (e.g., precious catalysts), high internal resistance, transport limitations in anode and cathode chambers, and low efficiency of MXCs employed mixed-culture microbial community (Popat and Torres, 2016; Torres, 2014; Logan, 2010; Fornero et al., 2010).

Among the different types of MXCs, the anode reactions are the same. They involve cooperation among different trophic guilds to break down organic matter into simple fermentation by-products that are the “fuel” for ARB. Regardless of the significant improvements that have been made in the anode performance over the past decade or so, its performance is still not good enough to make MXCs a competitor to

more mature anaerobic environmental biotechnologies. For example, Sleutels and his co-workers proposed a target current density of 25 A/m^2 that has to be achieved to support the commercialization of MXCs (Sleutels et al., 2012). Their analysis suggested that MECs have superiority over MFCs for scale-up, since their current densities can be easily increased by increasing the applied voltage, whereas the MFCs' current densities suffering from high internal resistance that have to be remarkably decreased. However, the maximum current densities reported for MXCs treating different substrates were < 15 A/m^2 (Borole et al., 2011; Torres et al., 2009; Rozendal et al., 2008a; Torres et al., 2007; Fan et al., 2007). Thus, boosting the current density and coulombic efficiency are the utmost goals for MXCs commercialization.

2.2 MXC's microbial community: teamwork or coexistence?

As summarized in Chapter 1, the biodegradation of complex organic compounds proceeds through a series of reactions under strict anaerobic conditions. Some of these reactions are essential to produce electric current; however, a few reactions can contribute only to organic matter biodegradation, but not to anode respiration. All of these reactions must be catalyzed by specific groups of microorganisms that can be present in the suspension phase and/or biofilm of MXCs; they may work as a team or as competitors.

2.2.1 Fermenting bacteria. Fermenting bacteria, or fermenters, are the main trophic guild responsible to biodegrade the complex organic compounds, such as carbohydrate and protein, into simple organic acids, such as acetate, propionate, and butyrate, as well as H_2 (Hallenbeck, 2009; Angenent et al., 2004; Rittmann and McCarty, 2001). Generally, organic matter fermentation is more thermodynamically favorable compared

to other anaerobic respiration processes, such as anode respiration (Freguia et al., 2008; Thauer et al. 1977), which is the most-likely reason for why ARB do not directly consume complex organic compounds, such as carbohydrate (Zhang et al., 2009).

In an early study, Lee et al. (2008) observed an ~1.45-fold decrease in CE when glucose was used as an MFCs feed compared to acetate, and the decrease in CE was associated with a much lower *j*. They suggested that acetate was quickly consumed by ARB compared to glucose, which needs to be fermented first. Later, experimental evidence supported the need for metabolic cooperation between fermenters and ARB (Parameswaran et al., 2010; Parameswaran et al., 2009; Freguia et al., 2008).

Further evidence from microbial-community analysis revealed that members of phyla *Bacteroidetes* and *Firmicutes,* which are well-known fermenting bacteria, dominated the suspended phase and biofilm of MXCs fed with complex organic matter (Siegert et al., 2015; Sanchez-Herrera et al., 2014; Rismani-Yazdi et al., 2013; Zhang et al., 2012). This contrasted to the dominance of Phylum *Proteobacteria*, which are known to be ARB, in MXCs fed with acetate (Torres et al., 2009).

Although fermenting bacteria are needed for fully functional MXCs, they can compete ARB for space as they can grow in the suspended phase and the biofilm of MXCs (Mahmoud et al., 2016; Siegert et al., 2015), and they necessarily consume some of donor's electrons for growth and maintenance (Parameswaran et al., 2010). This might lead to thick anode biofilms, hindering the transport of electron to the anode surface and the by-products (e.g., protons) out of the biofilm. Behera and Ghangrekar (2009) showed stable performance of an MFC fed with sucrose when suspended phase was entirely removed, although with a slight decrease in maximum power density (~30%).

2.2.2 ARB. ARB, which perform a unique type of respiration different from other anaerobes, have the ability to oxidize organic matter internally and transfer the resulting electrons to the anode as their terminal electron acceptor (Borole et al., 2011; Logan and Regan, 2006). So far, 3 main mechanisms are known for electron transfer to the anode surface. As illustrated in Figure 2.1, they are (1) direct electron transfer, (2) an electron shuttle, and (3) a solid conductive matrix (Torres et al., 2010). Several studies showed that ARB can generate *j* over a wide range: << 1 up to 15 A/m^2 (Lusk et al., 2015; Badalamenti et al., 2013; Torres et al., 2010; Xing et al., 2008; Marsili et al., 2008; Nevin et al., 2008; Malki et al., 2008; Bretschger et al., 2007; Bond and Lovley, 2005; Holmes et al., 2004; Chaudhuri and Lovley, 2003). This discrepancy in current generation is mainly a result of the electron-transport mechanism used. For example, *Shewanella oneidensis* is a model ARB that is known to perform anode respiration through producing e^- shuttles (Kotloski and Gralnick, 2013; Marsili et al., 2008; von Canstein et al., 2008). This type of anode respiration limits their *j*, usually to < 1 A/m^2, regardless of their ability to use a variety of electron donor, such as acetate, lactate, and glucose. In contrast, *Geobacter sulfurreducens* is an ARB that performs anode respiration using the solid conductive matrix mechanism, which results in the highest *j* values; however, it is known to oxidize only simple substrates (e.g., acetate and H_2).

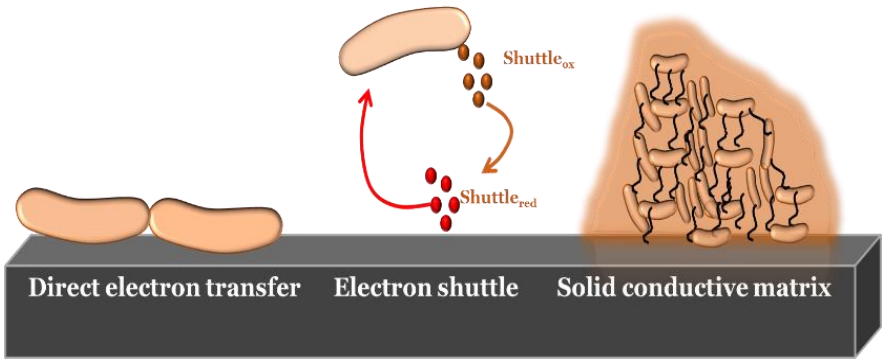

Figure 2.1 Schematic of three proposed electron transport mechanisms used by ARB (Adopted from Torres et al., 2010).

The majority of earlier studies were limited to exploring pure-culture ARB, although pure-culture ARB are usually unable to produce as much current densities as mixed-culture communities (Call et al., 2009; Ishii et al., 2008a). More importantly, MXC's biofilm anodes fed with complex substrates, such as real wastewater, are not comprised solely of ARB (Ishii et al., 2012; Kiely et al., 2011; Parameswaran et al., 2010). Generally, the microbial community of a mixed-culture MXC includes ARB, but has high community diversity (Kiely et al., 2011; Parameswaran et al., 2010) that often is associated with more robustness and functional stability, compared to less diverse microbial communities (Werner et al., 2011; Wittebolle et al., 2009). In particular, ARB rely on fermenting bacteria to break down complex organic compounds into simple substrates, such as acetate and H_2, which are the donor substrates for ARB.

Another factor that might significantly affect the performance of MXCs is the anode surface area. ARB use an anode as their terminal electron acceptor to perform their respiration and gain energy. Therefore, when the donor substrate is non-limiting, the respiration rate is usually limited by anode surface area, but non-ARB can compete with ARB for anode surface area.

Due to their unique respiration, ARB can have the highest substrate flux, expressed as electron fluxes (g COD/m^2), compared to other anaerobic or aerobic biofilm system (Torres et al., 2010), suggesting a practical advantage for MXCs in comparison with aerobic wastewater treatment technologies.

In environments where more than one electron acceptor is present, a common situation for an MXC anode, the half-maximum-rate concentration (K_s) and the maximum specific growth rate (μ_{max}) control this competition (Rittmann and McCarty, 2001). In mixed-culture MXCs, Lee et al. (2009) computed K_s and μ_{max} for ARB to be 119 mg COD/L and 3.2 d^{-1}, respectively. In another study, Pinto et al. (2010) estimated a comparable value of μ_{max} (2.0 d^{-1}) in an air-cathode MFC fed with acetate. These modestly high μ_{max} value imply that ARB are much faster growers than acetoclastic methanogens (0.3 d^{-1}) (Rittmann and McCarty, 2001) and homoacetogens (0.58 d^{-1}) (Peters et al., 1998). Those estimations were done for only one operating condition (i.e., a fixed anode potential of –0.13 V vs SHE (standard hydrogen electrode) (Lee et al., 2009) or using an external resistor (10 and 800 Ω)). More recently, Hamelers et al. (2011) studied the effect of anode potential on K_s. They observed that K_s depended on the anode potential, with the highest value (2.2 mM or 141 mg COD/L) reported at 0.2 V potential. In general, the specific growth rate of ARB may depend on reactor configuration and anode potential as well as other factors – such as substrate concentration, pH, biofilm thickness, and temperature (Sleutels et al., 2016; Picioreanu et al., 2010; Lee et al., 2009).

2.2.3 Methanogens. Over the past century, methanogens have been identified to be one the most important group of microorganisms in environmental biotechnology systems (Rittmann and McCarty, 2001). They consume H_2 and acetate to produce CH_4. They

establish syntrophic relationship with fermenters to consume the H_2 coming from fermentation, thereby making fermentation thermodynamically favorable (Stams and Plugge, 2009; McInerney et al., 2008; Angenent et al., 2004). Similar to other anaerobes, methanogens are known to be slow growers; Eqs. 2.1 and 2.2 illustrate that methanogens capture small amount of energy (Angenent et al., 2004; Thauer et al., 1977).

Aceticlastic methanogenesis ($\Delta G^\circ = -31$ kJ/mol or -3.88 kJ/e^- eq):

$$CH_3COO^- + H_2O \rightarrow CH_4 + HCO_3^- \quad \text{(Eq. 2.1)}$$

Hydrogenotrophic methanogenesis ($\Delta G^\circ = -131$ kJ/mol or -16.38 kJ/e$-$ eq):

$$4H_2 + HCO3^- + H^+ \rightarrow CH_4 + 3H_2O \quad \text{(Eq. 2.2)}$$

Despite their essential function in anaerobic digesters, methanogens are undesired competitors for ARB in MXCs, especially hydrogenotrophic methanogens (Siegert et al., 2015; Parameswaran et al., 2010; Lee and Rittmann, 2010; Parameswaran et al., 2009). ARB have kinetic and thermodynamic advantages over aceticlastic methanogens, since their K_s are several orders of magnitude lower than aceticlastic methanogens (0.64 mg COD/L versus 177–427 mg COD/L) (Parameswaran et al., 2010; Esteve-Nunéz et al., 2005); hence, they are not a real risk for ARB. However, ARB do not have the same growth advantage over hydrogenotrophic (or H_2-consuming) methanogens, leading to channel H_2 electrons quickly to methane generation instead of electric current production (Parameswaran et al., 2009).

Several strategies have been investigated to either eliminate or minimize the methane production in laboratory-scale MXCs. These attempts include the use of chemical inhibitors, thermal treatment, periodic exposure to oxygen (O_2), pH excursions, alamethicin exposure, and adjust the substrate supply (Zhu et al., 2015; Rago et al., 2015; Parameswaran, et al., 2010; Chae et al., 2010; Freguia et al., 2008). Sleutels et al. (2016) suggested that low substrate loading might play a key role in controlling the competition between methanogens and ARB in mixed-culture MXCs, giving a favorable growth advantage of ARB over methanogens. Periodic exposure to oxygen is another strategy to limit the methanogens activity, given that ARB are less tolerant to O_2. However, chemical inhibitors, such as BES, seem to be the most effective approach to completely inhibit the growth of methanogens. This is mainly due to the ability to inhibit the activity of methyl coenzyme M reductase A (*mcrA*) gene, which is a conserved gene in aceticlastic and hydrogenotrophic methanogens. Although this method is very efficient, it is not feasible for practical applications of MXCs due to the continuous need to supply the inhibitor, which is environmentally toxic and expensive.

2.2.4 Homoacetogens. Homoacetogens are facultative autotrophic bacteria that utilize H_2 as the main electron donor to produce acetate. Parameswaran, et al. (2010) shed the light on the syntrophic role that homoacetogens can play to increase CE in mixed-culture MXCs fed with fermentable substrate when the methanogenesis is entirely suppressed. Under standard conditions, homoacetogenesis is less thermodynamically favorable (ΔG° = – 95 kJ/mol or – 11.88 kJ/e^-eq) than hydrogenotrophic methanogenesis (Eq. 2.3 below) (Schuchmann and Müller, 2014). In addition, homoacetogens are less-efficient H_2-scavengers, based on their K_s values (Kotsyurbenko et al., 2001). Thus, hydrogenotrophic methanogenesis are expected to outcompete homoacetogens and be

the main H_2-scavengers in anaerobic digester and MXCs, except under exceptional conditions, such as low-temperature environments (Conrad and Wetter, 1990; Conrad et al., 1989) and slightly-acidic environments (i.e., ~pH 6.1) (Phelps and Zeikus, 1984).

$$4H_2 + 2\,CO_2 \rightarrow CH_3COO^- + H^+ + 2H_2O \qquad \text{(Eq. 2.3)}$$

Recently, Gao et al. (2014) showed that the use of an anode with a large surface area (i.e., 1600 m^2 of anode surface area/m^3 anode volume) provided an advantage for ARB and homoacetogens to grow and outcompete hydrogenotrophic methanogens. This probably was due to the relatively high local H_2 concentration and relatively acidic environment in biofilm systems, which would give kinetic advantages for homoacetogens to outcompete hydrogenotrophic methanogens. In another study, Xafenias and Mapelli (2014) revealed that low cathode potential played an important role to favor homoacetogens in dual-chamber MEC, as evidenced from the low CH_4 production and the dominance of homoacetogenic *Acetobacterium* spp. Despite the positive role of homoacetogens, they use some of donor's electrons for growth and maintenance purposes, thereby limiting *j* generation in general and net H_2 production in single-chamber MXCs. Thus, more research is needed to minimize the "H_2-detour" in the anode chamber away from anode respiration.

2.2.5 Sulfate-reducing bacteria (SRB). Sulfate reduction has gained less attention in MXCs studies, since most of the used synthetic media lack sulfate, although real wastewaters that have high sulfate content include those from pulp and paper, food-production, petrochemical, mining and tannery industries (Hao et al., 2014). An early study showed that addition of sulfate (up to 4000 μg/L) had a minimal effect on the

performance of MFCs in terms of current production (Kim et al., 2004). In another study, Lee et al. (2012) observed very low CE (6.7–17.5%), maximum power density (0.2–0.3 W/m^2), and *j* (< 0.6 A/m^2) in parallel with high sulfate reduction (from 248 mg/L to 39.3 mg/L) in MFCs. The role of sulfate reduction can be complicated, because reduction of sulfate by SRB yields sulfide, which can be oxidized by some ARB to generate *j* and a variety of compounds, such as elemental sulfur and sulfite (Lee et al., 2012; Rabaey et al., 2006). No comprehensive study definitively documents the effect of sulfate on MXC performance, but the most likely impact is negative on CE and *j*, as SRB compete with ARB for space (i.e., anode surface) and donor substrate (i.e., acetate).

2.2.6 Nitrate-reducing bacteria (NRB). Given that several pure-culture ARB, such as *Geobacter metallireducens* (Lovley et al., 1993), *Shewanella oneidensis* (Cruz-Garcia et al., 2007), and *Geoalkalibacter subterraneus* (Greene et al., 2009), have the ability to use nitrate as their electron acceptor – which is undesired for achieving high CE and *j* generation – the effect of nitrate reduction is of particular interest for anode respiration and MXC performance. For example, Sukkasem et al. (2008) studied the effect of nitrate reduction on the performance of mixed-culture MFCs. They observed a significant decrease in CE and maximum voltage upon adding 8 mM nitrate, most-likely due to competition between ARB and nitrate-reducing bacteria for space and donor substrate. Similarly, Kashima and Regan (2015) reported a significant decrease in CE (from ~78% to ~4%) as a result in increasing nitrate concentration (0 to 10 mM) in anode-respiring *Geobacter metallireducens* biofilm. They also observed that the anode potential had no effect on nitrate reduction, since it is controlled by the nitrate concentration. So far, no strategies have been developed to inhibit nitrate-reducing bacteria in MXC anodes.

2.3 Treatment efficiency of MXCs

Recently, many research studies have focused on: (1) defining the limiting factors for MXC scale-up (Logan, 2010), (2) developing new electrodes (Zhou et al., 2011) and reactor designs (Logan et al., 2015), (3) exploring the possibility to produce value-added products (Pant et al., 2012; Logan and Rabaey, 2012), (4) characterizing new ARB (Lusk et al., 2015; Badalamenti et al., 2013; Miceli et al., 2012), and (5) developing new cathode catalysts (Liew et al., 2014; Erable et al., 2012; Zhao et al., 2005). A common feature of these studies was the use of a simple donor substrate, such as acetate, for a good control on experiments, a fast utilization rate, and high electron recovery and *j* generation (Pant et al., 2010). However, MXC scale-up eventually has to use real wastewater. Table 2.1 summarizes real wastewaters that have been used in MXCs studies. High *j* and CE are often linked to the ability of an MXC's microbial consortia to utilize the organic matter and transfer the resulting electrons to the anode. Achieving high *j* and CE seems to be related to the complexity of the organic matter. For example, Heilmann and Logan (2006) showed that a simple protein compound (i.e., bovine serum albumin (BSA)) produced high power density in an MFC compared to more complex proteinaceous organic matter, such meat-processing wastewater.

Table 2.1 Real wastewater used in microbial electrochemical cells.

Substrate type	Reactor configuration	Substrate concentration [a]	HRT [b]	j_{max} [c]	CE (%)	Reference
Acetate	MEC	960	0.83 [d]	~8	NA [f]	Torres et al. (2009)
Propionate	MFC	~51	~3.1 [e]	0.31	50	Oh and Logan (2005)
Butyrate	MEC	2240	~25 [e]	~11	~70	Miceli et al. (2014)
Glucose	MFC	384	~24 [e]	< 1	49	Lee et al. (2008)
Ethanol	MEC	800	~30 [e]	< 2	60	Parameswaran et al. (2009)
Sucrose	MFC	2670	0.5 [d]	0.19	3.26	Behera and Ghangrekar (2009)
Brewery wastewater	MFC	1300	0.61 [d]	0.15	NA [f]	Wen et al. (2010)
Domestic wastewater	MFC	214	1 [e]	~1.8	14–22	Zhang et al. (2015)
Corn-stover biomass	MFC	NA [f]	~12 [e]	~1.4	22	Wang et al. (2009)
Landfill leachate	MEC	2590	0.74 [d]	0.11	1.8	Mahmoud et al. (2016)
Food-processing wastewater	MFC	892	~21 [e]	0.36	27.1	Oh and Logan (2005)
Primary sludge	MEC	1050	~3 [e]	1.3	10	Ki et al. (2015)

[a] Organic matter concentration has unit of mg COD/L; [b] HRT has unit of days; [c] maximum current density (j_{max}) has unit of A/m^2; [d] continuous-flow MXC; [e] batch MXC; [f] NA: not available in the original study.

In a review, Ge et al. (2014) revealed that the normalized energy recovery (NER) of MFCs was inversely related to substrate complexity. They showed that the highest NER was achieved with acetate (i.e., 0.25 kWh/m^3 or 0.40 kWh/kg of COD), which was much higher compared to domestic wastewater (0.04 kWh/m^3 or 0.17 kWh/kg of COD) and industrial wastewater (0.10 kWh/m^3 or 0.04 kWh/kg of COD). Another interesting finding is that MFCs were more suitable for treating low- or medium-strength wastewater than was anaerobic digestion (Ge et al., 2013; Rajeshwari et al., 2000). This trend is consistent with recent studies that revealed that the efficiency of MXCs – in terms of CE, PD, and j – was remarkably increased when integrated with prior anaerobic digestion when treating high-strength organic-waste streams (Escapa et al., 2016; Ki et al., 2015; Mahmoud et al., 2014; Gómez et al., 2011). Rozendal et al. (2008a) predicted that the wastewater treatment capacity of MXCs can reach 7 kg COD/m^3.day, but many technical challenges need to be addressed before moving the MXC technology to commercial scale.

2.4 Landfill leachate as a potential feedstock for MXCs

Landfill leachate presents a good option for either electric current or H_2 generation in MXCs. Leachate is the aqueous effluent generated from organic matter degradation in municipal landfills through a combination of physical, chemical, and biological processes. The liquid can be derived from percolating rainwater entering landfill cells, from the water in the incoming solid waste, or from release of H_2O from microbiological breakdown of the organic matter (Renou et al., 2008; Tchobanoglous and Kreith, 2002).

Leachate is a strongly polluted wastewater; it contains relatively large concentrations of biodegradable organic matter, ammonium-nitrogen, xenobiotic

organic compounds (XOCs), humic compounds, and inorganic salts, such as chloride. Landfill leachate represents a serious threat to groundwater and surface water, as well as soil. Historically, leachate generated from "old-fashioned" landfills that were built without engineered leachate collection systems and liners was a main cause of groundwater and soil contamination. The improper discharge of leachate into surface-water bodies has led to oxygen depletion and alteration in fauna and flora due to severe ammonia toxicity (Kjeldsen et al., 2002).

The leachate's quality and flow rate depend on many factors – including age of the landfill, the type of solid waste, and the seasonal weather variations (Renou et al., 2008). For example, young landfill leachate (landfill age < 5 years) is usually characterized by a high concentration of organic acids and a relatively high biodegradability ratio (based on the BOD_5/COD ratio) that tends to decrease with increasing landfill age, mainly due to anaerobic biodegradation of organic matter that takes place in the landfill cells. Consequently, leachate's organic matter becomes dominated by recalcitrant organic compounds, such as humic- and fulvic-acid-like organic compounds that causes a significant decrease in the BOD_5/COD ratio (Wiszniowski et al., 2006). Therefore, interest in energy recovery (i.e., CH_4) from young leachate in anaerobic-digestion reactors has been growing. For example, Timur and Özturk (1999) showed high CH_4 production (~83% of COD removed) in anaerobic reactors treating young landfill leachate, with BOD_5/COD ratios of 0.54 to 0.67.

Regardless of the relatively high BOD_5/COD ratio in young leachate, monoaromatic hydrocarbons (e.g., benzene, ethylbenzene, toluene, and xylenes) and halogenated hydrocarbons (e.g., trichloroethylene and tetrachloroethylene) are among the most abundant XOCs found in intermediate and mature landfill leachate samples, which are specified as priority containments by the U.S. Environmental Protection

Agency (EPA) (Kjeldsen et al., 2002). Those hydrocarbons are readily oxidized in aerobic conditions; however, their degradation in strictly anaerobic conditions often is very slow (Meckenstock et al., 2004; Kazumi et al., 1997; Ball and Reinhard, 1996). The absence of microorganisms that are capable of biodegrading those hydrocarbon compounds might be another factor that affects their metabolism under strict anaerobic conditions (Weiner and Lovley, 1998). Thus, the energy recovery from intermediate and mature landfill leachate samples in either MXCs and anaerobic digestion reactors are usually low.

Despite the large portion of poorly biodegradable organics in the leachate's COD, it has feature that may make it a good candidate for generation of different forms of renewable energy in an MXC: high electrical conductivity, substantial buffering capacity, and low solids content (Pant et al., 2010). However, previous studies on treatment of landfill leachate in MXCs shows that it is challenging compared to many other real wastewaters (Ganesh and Jambeck, 2013; Pant et al., 2010). In leachate treating MFCs where the anode surface was the only electron acceptor, Greenman et al. (2009) showed low j (3.2 to 3.8 mA/m^2) and BOD_5 removal efficiency (up to 47%) when MFCs operated in continuous-flow mode with hydraulic retention times ranged between 4.7 to 38 h (Greenman et al., 2009). However, introducing oxygen in an air-cathode MFC accelerated the fermentation kinetics, leading to up to 8.5 kg COD/m^3 d removal of biodegradable organics; however, the CE was extremely low (<2%). Higher CE (~7%) was observed when diluted landfill leachate used as a substrate for air–cathode, dual-chamber MFCs leachate (You et al., 2006).

Due to this recalcitrant nature of landfill leachate to biodegradation, pre-treatment technologies, such as advanced oxidation processes, chemical coagulation/flocculation, adsorption, and air stripping, are gaining interest (Renou et al.,

2008; Deng and Englehardt, 2006). Compared to other leachate pre-treatment options, hydroxyl radical-based advanced oxidation processes (AOPs), including the Fenton oxidation reaction (Fe^{2+}/H_2O_2), have proven to be effective pre-treatment technologies for removal of a variety of recalcitrant organic contaminants, mainly due to ability of hydroxyl radicals ($OH^{\cdot}$) to non-selectively oxidize recalcitrant organic contaminants (Buxton et al., 1988). This catalytic process relies on the electron transfer between H_2O_2 and Fe^{2+}, which acts as a homogenous catalyst, yielding $OH^{\cdot}$.

2.5 Polishing an MXC's effluent quality

Because one main goal of an MXC is to treat wastewater, the final effluent quality has to meet discharge limits (i.e., <30 mg BOD_5/L). However, the majority of MXC studies have focused on maximizing PD, *j*, or H_2 production rate, rather than treatment efficiency. Recent research revealed that high energy recovery and organic matter removal are not likely to occur simultaneously (Akman et al., 2013; Zhuang et al., 2012; Nam et al., 2010a). The reason is that decreasing the concentration of organic matter to a low level slows ARB metabolism, resulting in a minimal *j* (Zhang et al., 2015; Ren et al., 2014a). However, operating MXCs at relatively short HRTs – close to those of activated sludge – can achieve both goals simultaneously (Kim et al., 2015; Puig et al., 2011; Min and Logan, 2004).

A possible way to polish the MXC's effluent quality is to integrate the MXC with membrane-based post-treatment. Recently, Katuri et al. (2014) developed a novel anaerobic electrochemical membrane bioreactor (AnEMBR) for wastewater treatment. They observed up to 95% COD removal and ~71% of donor's electrons were recovered as methane-rich biogas (~83% of total biogas produced) with very low H_2 (<1%). They estimated that the net energy needed to operate the AnEMBR system (at an applied

voltage of 0.7 V) was 3.7- to 7.4-fold less than the energy needed for conventional aerobic membrane bioreactors (i.e., 0.27 kWh/m^3 versus 1–2 kWh/m^3). In another study, Ren et al. (2014b) evaluate the efficiency of two-stage microbial fuel cells— anaerobic fluidized bed membrane bioreactor (MFC-AFMBR) for domestic wastewater (COD = 210 mg/L) treatment. Despite the relatively-low HRT (i.e., 9 h) for the treatment system, they observed very high COD removal (92.5%) and total suspended solids (TSS; > 99%), with only residual COD and TSS of 16 and < 1 mg/L, respectively. The net energy needed to operate their system was 0.0186 kWh/m^3, which was slightly less than MFC's electric energy produced (i.e., 0.0197 kWh/m^3), meaning that the combined MFC-AFMBR system could polish the MXC's effluent with a low energy requirement.

Regardless of recent efforts to improve the MXC's effluent, we still lack complete understanding for how MXCs could not produce an effluent with low organic concentration, even though the MXCs were usually operated with very long HRTs (up to 30 days). A likely reason is the release of soluble microbial products (SMP) during normal biomass metabolism and decay (Ni et al., 2011a). A recent study showed that SMPs represent ~23% of influent COD in an MEC fed with acetate (An and Lee, 2013).

MXCs and anaerobic wastewater treatment processes, such as AnMBRs, anaerobic filters, and upflow anaerobic sludge blanket (UASB) reactors, are known to be an energy-saving technology compared to conventional activated sludge technology (McCarty et al., 2011). They have several other advantages over conventional activated sludge technology, such as less sludge production and the ability to treat medium- to high-strength wastewater (Li et al., 2014; Logan and Rabaey, 2012; McCarty et al., 2011). As shown in Figure 2.2, these advantages can lead to cost benefits.

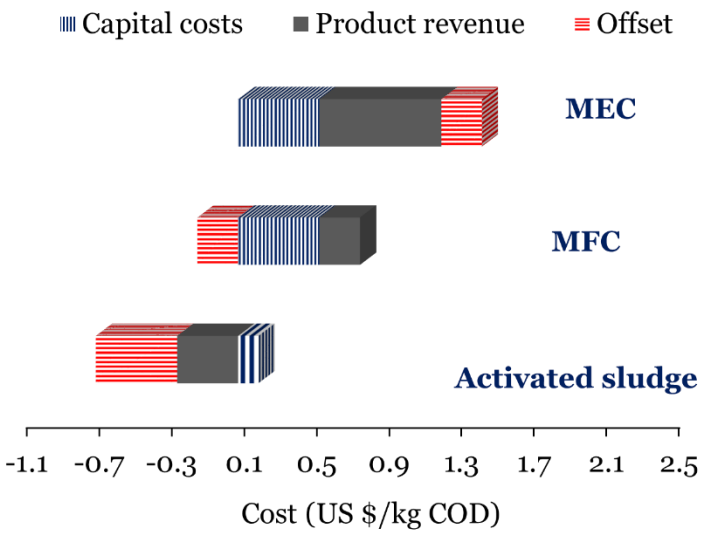

Figure 2.2 Comparison of estimated capital costs, product revenues, and offset (product revenue minus capital costs) among different wastewater treatment technologies (Source: Rozendal et al. (2008a)). The calculations for MFC and MEC are based on the predicted future capital costs using less expensive substitute materials. Exchange rate of € to US $ is 1.12 $/€.

CHAPTER 3

RELIEVING THE FERMENTATION INHIBITION ENABLES HIGH ELECTRON RECOVERY FROM LANDFILL LEACHATE IN A MICROBIAL ELECTROLYSIS CELL [1]

3.1 Introduction

The organic substrates fed to MXCs used for wastewater treatment usually are complex, which leads to a diverse microbial community (Logan and Rabaey, 2012; Rittmann et al., 2008). The biodegradation of these complex wastewater must take place through a cascade of anaerobic reactions, including hydrolysis, fermentation, homoacetogenesis, and anode respiration; undesired processes, such as methanogenesis, also can occur in parallel. Fermentation appears to be the rate-limiting step in an MXC utilizing complex, but mostly soluble organic substrates, such as in landfill leachate. In an MXC, the fermenters must first break down the complex organic matter into simple substrates that can be efficiently consumed by anode-respiring bacteria (ARB) (Kiely et al., 2011; Torres et al., 2010; Parameswaran et al., 2009; Freguia et al., 2008).

Although some of the fermentation can be carried out separately from anode respiration in a pre-fermentation reactor, other fermentations must occur along with anode respiration in the MXC due to the need for syntrophic relationships between fermenters and ARB. For example, syntrophic coupling of fermenters and ARB was required during the degradation of cellulose in a microbial fuel cell (MFC) (Ren et al., 2007). The maximum power density of 143 mW/m^2 (anode area) and Coulombic efficiency (CE) of 47% were obtained with a co-culture of *Clostridium cellulolyticum* and *Geobacter sulfurreducens*, whereas neither pure culture generated electric current. Likewise, a microbial electrolysis cell (MEC) fed with ethanol involved a three-way

[1] This Chapter was published in an altered format in *RSC Advances* (Mahmoud *et al.*, 2016. RSC Advances 6, 6658–6664).

syntrophic interaction among fermenters, homoacetogens, and ARB (Parameswaran et al., 2010; Parameswaran et al., 2009). So far, nothing is known about the syntrophic interactions among ARB and other microbial community members in MXCs fed with landfill leachate.

Over the past few years, current density (*j*), CE, and Coulombic recovery (CR) of MXCs fed with a variety of complex organic substrates have significantly improved (Pant et al., 2010). For example, early MXC experiments had CE < 3% and maximum current density (j_{max}) < 0.2 A/m^2 when real wastewaters were used as the sole electron donors (Zhang et al., 2008; You et al., 2006; Min and Logan, 2004). Subsequently, the performance has improved by applying pre-treatment technologies – such as pre-fermentation, microwave treatment, sonication, acid treatment, and alkaline treatment – that increase the bioavailability of the organic matter (Yusoff et al., 2013; Xiao et al., 2013; Yang et al, 2013; Min et al., 2005). Nevertheless, *j* values achieved so far with landfill leachate remain well below the target current density of ~140 A/m^3 needed to achieve an organic removal rate of ~1 kg 5-day biochemical oxygen demand (BOD_5)/m^3.d, as observed in anaerobic digesters treating landfill leachates (Mahmoud et al., 2014; Kennedy and Lentz, 2000). Better pre-treatment approaches are needed for landfill leachate.

Among pre-treatment options, advanced oxidation processes (AOPs), through the strong, but non-selective action of hydroxyl free radicals ($OH^{\cdot}$), have promise to transform a variety of recalcitrant organic contaminants into forms that are more readily biodegradable (Duesterberg and Waite, 2006; Deng and Englehardt, 2006). One common AOP is the Fenton reaction, which relies on electron transfer between hydrogen peroxide (H_2O_2), the initiating oxidant, and Fe^{2+}, a homogenous catalyst, to yield $OH^{\cdot}$,

which attacks the recalcitrant organic matter. The Fenton process occurs through a cascade of reactions that are summarized in Table A.1 in appendix A.

Here, I use the Fenton reaction as pre-treatment to improve the biodegradability of organic matter in landfill leachate that is subsequently fed to an MEC. Previous work with landfill leachate showed that, although the raw leachate had a relatively high absolute BOD_5 concentration, the *j*, CE, and CR values were very low, mainly due to toxicity in the influent organics (Ganesh and Jambeck, 2013; You et al., 2006). Thus, I evaluated the feasibility of the Fenton process to improve the biodegradability of leachate before energy capture in a downstream MEC. Specifically, I evaluated if partial oxidation of organic matter in landfill leachate increased the fermentation kinetics of the organics for downstream electron recovery by ARB at an MEC anode. For this proof-of-concept effort, I used fixed ratios of $[H_2O_2]$:$[Fe^{2+}]$ and H_2O_2:COD. I investigated: (1) the degree to which Fenton pre-treatment of leachate enhanced *j*, CE, CR, and organic-matter removal in an MEC; (2) what step of the biodegradation process that Fenton pre-treatment affected, and (3) how Fenton pre-treatment altered the microbial community in ways that explain the enhanced performance.

3.2 Materials and Methods

3.2.1 Landfill leachate

I collected landfill leachate from the Northwest Regional Landfill (Surprise, AZ) and kept it refrigerated at 4°C prior to use. The leachate samples had a dark brownish-black color, a relatively high concentration of organic matter (chemical oxygen demand (COD) = 2594±94 mg/L; BOD_5 = 802±10 mg/L; total organic carbon (TOC) = 663±15 mg/L; and volatile fatty acids (VFAs) = 283±73 mg/L), and good buffering strength (total alkalinity = 4068±464 mg as $CaCO_3$/L with a pH = 8.1±0.3). The leachate would be classified as a medium-age leachate based on its BOD_5/COD ratio of ~0.31 (Renou et al., 2008). The nitrogen content was relatively high, with most of nitrogen in inorganic forms (734±4 mg TN-N/L and 645±8 mg NH_3–N/L). Finally, the leachate had a high aromatic content, measured as absorbance at 254 nm normalized to TOC concentration (specific ultraviolet absorption at 254 nm ($SUVA_{254}$) = 1.23±0.06 L/mg TOC with 5-fold dilution), as well as to a high conductivity from the high concentration of chloride (3100±20 mg/L) and sulfate (74.6±1 mg/L). Throughout this study, I used the leachate samples without dilution.

3.2.2 Fenton reaction

I carried out batch Fenton-reaction experiments using 250-mL glass vessels mixed with a magnetic stir bar at a constant mixing speed of 150 rpm at ambient temperature (25±2 °C). I used a $[H_2O_2]$:$[Fe^{2+}]$ molar ratio of 4.0 and a H_2O_2:raw leachate's COD ratio of 1.1 (*w:w*) at an initial pH value of 3.5. First, I continuously and manually adjusted the reaction medium's pH to 3.5±0.1 using 10 N NaOH or 50% H_2SO_4. After initial pH adjustment, I added measured amounts of ferrous sulfate ($FeSO_4.7\ H_2O$) to reach the targeted ferrous ion (Fe^{2+}) concentration. Then, I added

H_2O_2 in one step to reach the designated H_2O_2 concentration. Just before the addition of H_2O_2 and Fe^{2+}, I collected a sample (set as reaction time = 0) to measure COD and TOC. Aliquots of treated leachate were taken every 30 min with a syringe, and the experiment was carried out for 3 hours. I split the samples into two portions. The first portion was used to measure residual H_2O_2 and COD after filtering the sample through a 0.22-μm filter membrane. The second portion was neutralized to ~pH 9.0 with 10 N NaOH and then mixed in a beaker for 30 min with a magnetic stirring bar. I centrifuged the second sample for 10 min at 4000 rpm to collect the supernatant to analyze COD, TOC, and H_2O_2. In order to eliminate any possibility of H_2O_2 interference with COD measurements, I corrected the COD by subtracting the COD value equivalent to residual H_2O_2 from the measured COD. I repeated this experiment 6 times.

3.2.3 Microbial electrolysis cells

I used two dual-chamber, H-type MECs with a liquid volume of 320 mL in each chamber. Anodes were two square graphite electrodes having a total surface area of 22 cm^2 (each 6.1 cm-long and 0.45 cm-width). I had treated the graphite-rod anodes by soaking them in 1 M H_2SO_4 for 12 h followed by soaking in 1N NaOH overnight. Following the treatments, I washed the graphite rod anodes 4 times with distilled water before placing them in the MEC. A 0.8-cm outer diameter (OD) graphite rod was the cathode, and the pH of the cathode was maintained at 12 by addition of 10 N NaOH. The cathode chamber was separated from the anode chamber by an anion exchange membrane (AMI 7001, Membranes International, Glen Rock, NJ). An Ag/AgCl reference electrode (BASI Electrochemistry, west Lafayette, IN) was placed about 0.5 cm away from the anode to control the anode potential at – 0.3 V vs. Ag/AgCl (– 0.046 V vs SHE) using a VMP3 digital potentiostat (Bio-Logic USA, Knoxville, TN). The

temperature was controlled at 30°C in a temperature-controlled room, and the liquid in both chambers was mixed at 220 rpm using a magnetic stirrer.

Prior to the MEC start-up, I seeded the anode chamber with a mixture of effluent of an MEC supplemented with acetate (150 mL) and anaerobic digester sludge (3 mL) as the inoculum. For the initial formation of biofilm on the anode, I fed each MEC with acetate as a sole substrate and operated MEC in batch mode for about 2 days. After achieving a stable current density, I changed the operation mode to continuous feeding (hydraulic retention time (HRT) = 17.8 h) with acetate and then with a mixture of volatile fatty acids (VFAs; acetate, 20.4 mM; propionate, 11.1 mM; and butyrate, 1.8 mM) for about 12 days. Following the start-up period, I fed both MECs with raw leachate (control MEC) and Fenton-treated leachate, neutralized with 10 N NaOH to pH ~7.6, in continuous mode with an HRT of 17.8 h to reflect the anode biofilm that can be used for real applications of MECs. I calculated CE and CR by normalizing the recovered electrons as measured current to the COD removal and to total influent COD, respectively.

In order to investigate whether fermentation or anode respiration was the main cause for poor organic-matter consumption and *j* generation with raw leachate, I performed acetate-spike experiments on the control MEC. Before performing the spike experiments, I stopped the continuous flow of raw leachate, and then acetate was introduced to the MEC's anode using a syringe to a final concentration of ~25 mM or ~21 mM. After the acetate spike, I operated the MEC in batch mode for about 10 days and monitored the *j* generation. I repeated these experiments twice.

3.2.4 Chemical analyses

COD, total nitrogen (Total–N), VFAs, ammonia, alkalinity, and sulfate were measured, in duplicate, using HACH kits (HACH, Ames, IA). BOD_5 was measured according Method 5210 in *Standard Methods* (APHA, 1998). I measured TOC using a TOC analyzer (TOC-VCSH, Shimadzu Scientific Instruments, Columbia, MD) equipped with combustion catalytic oxidation/non-dispersive infrared (NDIR) gas analyzer, the chloride concentration using ion chromatography (ICS 2000, Dionex Corporation, CA) after filtration through a 0.22-μm membrane filter, the Fe^{2+} concentration using the 5-sulfosalicylic acid (SSA) colorimetric method (Karamanev et al., 2002), and the H_2O_2 concentration using the starch-iodine colorimetric method, in which a mixture of potassium iodide, ammonium molybdate, and starch reacted with H_2O_2 in acidic medium forming a blue peroxo-complex (Graf and Penniston, 1980). I assessed the aromatic content by the $SUVA_{254}$, in which the absorbance reading at 254 nm is divided by the TOC concentration (Mrkva, 1983). All spectrophotometric analyses were carried out using either a UV-Vis spectrophotometer (Varian Cary 50 Bio, Varian Inc., Walnut Creek, CA) or a Genesys 20 spectrophotometer (Thermo Spectronic, MA).

I quantitatively estimated the biomass concentration, as mg/cm^2 of anode surface area, by harvesting the entire biofilm at the end of each run from the MEC anode and suspending it in sterilized deionized water. After centrifuging the entire content at 10000*g* (Eppendorf Centrifuge 5414 D, USA) for 10 min, I measured the dry-weight of the pellets gravimetrically and normalized it to the anode surface area.

3.2.5 Microbial community analyses

At the end of each experiment, I harvested the entire biofilm biomass from the MEC anode by scraping it off with a sterilized pipette tip and suspending the biomass

sample in sterilized deionized water. I extracted the DNA from a fraction of biomass (~0.125 g) using the MOBIO Powersoil DNA extraction kit according to manufacturer's instructions and determined the quality and quantity of the extracted DNA using a nanodrop spectrophotometer (ND 1000, Thermo Scientific) by measuring absorbance at 260 and 280 nm. The DNA samples were sent to the Microbiome Analysis Laboratory at Arizona State University (Arizona, USA) for amplicon pyrosequencing of the V4 region of the 16S rRNA gene with the barcoded primer set 515f/806r designed by Caporaso et al. (2012) and following the protocol by the Earth Microbiome Project (EMP) (http://www.earthmicrobiome.org/emp-standard-protocols/) for the library preparation. PCR amplifications for each biofilm sample were performed in triplicate, and sequencing was performed in a MiSeq Illumina sequencer (Illumina Inc., USA) using the chemistry version 2 (2 x 150 paired-end).

I analyzed data received from the Microbiome Analysis Laboratory using QIIME software version 1.8 (Caporaso et al., 2010) after discarding sequences shorter than 25 bp, longer than 450 bp, or labeled as chimeric sequences. The forward and reverse reads of each sequence were paired before downstream data analysis. After screening, primer sequences were trimmed off, and taxonomic classification was performed using the RDP classifier at the 80%-confidence threshold (Cole et al., 2009). The total number of sequence reads for each sample after screenings were: raw leachate biofilm = 69472 and treated leachate biofilm = 141650.

3.3 Results and Discussion

3.3.1 Effects of the Fenton reaction on the biodegradability of leachate organic matter

Table 3.1 summarizes the effects of the Fenton reaction. The most important trends are that the BOD_5/COD ratio and VFAs increased significantly, although the absolute concentrations of COD and TOC declined. The organic material in the leachate was partially oxidized: ~53% loss of COD and TOC. The treated leachate also had less aromatic organic content, as the $SUVA_{254}$ declined by about 30%. The BOD_5/COD ratio, VFAs, and $SUVA_{254}$ findings support that Fenton oxidation significantly improved the biodegradability of leachate organics by converting refractory organic matter into more biodegradable organic matter.

Table 3.1 Effects of Fenton oxidation of landfill leachate. Experimental conditions: $[H_2O_2]$:$[Fe^{2+}]$ molar ratio of 4.0, a H_2O_2:COD *w/w* ratio of 1.1, pH 3.5, and time = 3 h.

Parameter	Unit	Raw leachate	Fenton-treated leachate
COD	mg/L	2594±94	1227±93
BOD_5	mg/L	802±10	608±50
BOD_5/COD ratio	–	0.31±0.01	0.56±0.04
TOC	mg/L	663±15	317±4
VFAs	mg/L as CH_3COOH	283±73	340±4.6
$SUVA_{254}$	L/mgC.m	6.15±0.3	4.4±0.2

3.3.2 MEC performance

I operated two MECs – one of them fed with raw leachate (control) and the other fed with treated leachate in a continuous mode with an HRT of 17.8 h – to achieve quasi-

steady state conditions following an ~2-months start-up and acclimation period. The performance of each MEC was stable and reproducible over repeated HRTs. Figure A.1, in appendix A, reports the current density during the initial period of biofilm formation on the anode. Throughout the entire operating period, I maintained constant organic loading rates for the MECs fed with raw leachate and treated leachate, ~1.08±0.01 kg BOD_5/m^3.day (~3.5±0.11 kg COD/m^3.day) and ~0.82±0.06 kg BOD_5/m^3.day (~1.7±0.07 kg COD/m^3.day), respectively. The performance of both MECs was evaluated in terms of *j* at a fixed anode potential (– 0.3 V vs. Ag/AgCl or – 0.046 V vs. SHE), which led to the stable and clearly distinct performance patterns that can be seen in Figure 3.1A.

The MEC fed with the treated leachate had nearly 13-fold higher *j*, with an average value of 1.42±0.27 A/m^2 vs. 0.11±0.06 A/m^2 for the untreated leachate. This increase was much more dramatic than the increase in the BOD_5/COD ratio: to 0.56±0.04 from 0.31±0.01. Treated leachate also gave remarkably enhanced removals of COD, BOD_5, and TOC, as well as CE and CR values, all shown in Figure 3.1B. The higher MEC performance supports that significant organic matter removal is possible if toxic components in the influent are substantially reduced. Thus, while direct oxidation of leachate's organic compounds by ARB in MECs may not be feasible, pre-treatment has a positive impact on MEC performance in terms of *j*, CE, CR, and organic matter removal.

Approximately 5.9% of the influent COD ended up as biomass in the biofilm of the MEC fed treated leachate, corresponding to much higher total biofilm accumulation (i.e., ~0.70±0.01 mg/cm^2) compared to the control MEC (i.e., ~0.66% of influent COD and biofilm accumulation of ~0.16±0.02 mg/cm^2). The higher biofilm accumulation for the MEC fed treated leachate is consistent with its greater rate of organic-matter consumption.

The likely cause for the poor MEC performance and low biofilm accumulations with raw leachate was inhibition caused by the complexity and aromaticity of its organic matter. The Fenton reaction reduced the leachate's $SUVA_{254}$ value by ~30% and increased the VFA/COD ratio by ~1.6–fold, both consistent with the hypothesis that the Fenton reaction relieved inhibition related to aromatics. Zhang et al. (2008) detected leachate inhibition to anode respiration in a membraneless air-cathode microbial fuel cell (MFC) with even higher leachate biodegradability (BOD_5/COD ratio ~0.40). A recent study by Cheng et al. (2015) supports that eliminating aromatics relieved inhibition to fermentation and anode respiration in an MFC. They observed that anaerobic biodegradation of aniline, a typical recalcitrant aromatic organic matter, was sluggish compared to aerobic biodegradation. Air sparging of the biofilm anode caused an ~5-fold increase in power density and an ~6-fold increase in aniline removal, suggesting that aerobic biodegradation of aromatics relieved inhibition for fermentation and anode respiration.

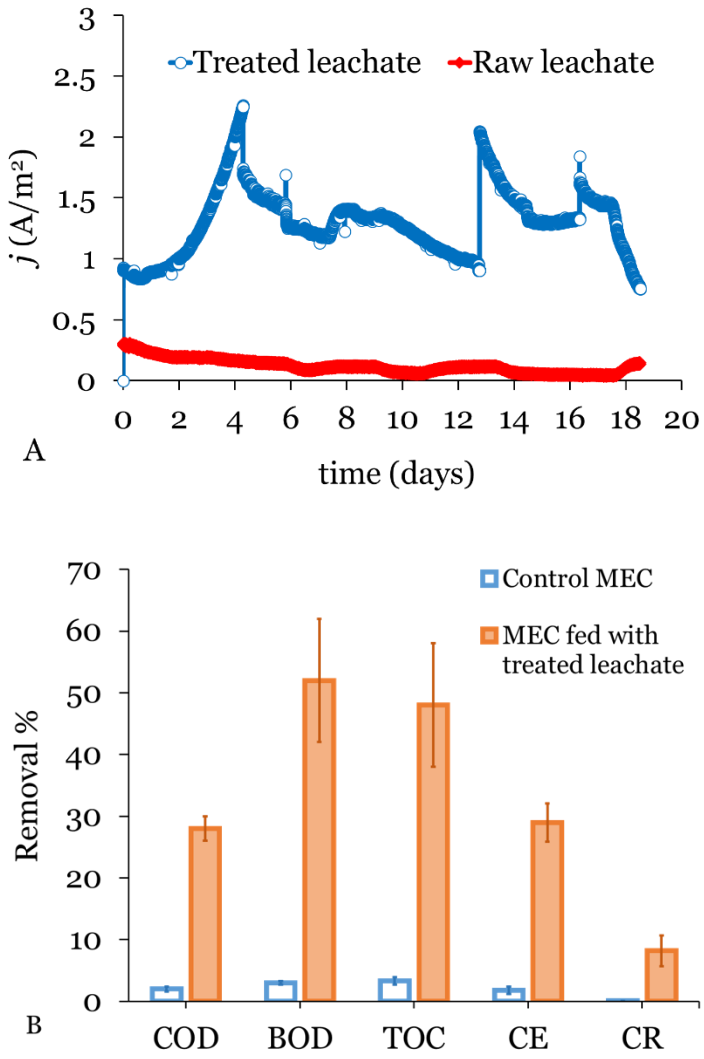

Figure 3.1 Performance of MECs fed treated and raw leachates during continuous operation at an HRT = 17.8 h. (A) Quasi-steady state current generation versus time. (B) Summary of MEC performance parameters.

To test whether fermentation or anode respiration was the inhibited step, I spiked the anode chamber of the control MEC with a known amount of 1-M acetate medium to yield a final acetate concentration in the anode-chamber of ~25 mM. Figure 3.2 shows a rapid increase in *j* upon addition of acetate, and the CE was ~80% based on the COD change. Given that acetate is the preferred electron donor for ARB (Kiely et al., 2011; Torres et al., 2010), the rapid response to acetate indicates that fermentation was

the inhibited step. After the added acetate was consumed, *j* decreased to less than 0.05 A/m² for 36 days, at which time I added a second acetate spike (~21 mM). The second spike gave trends consistent with the first spike experiment, again showing that the biofilm was capable of rapid anode respiration if a readily available donor were present.

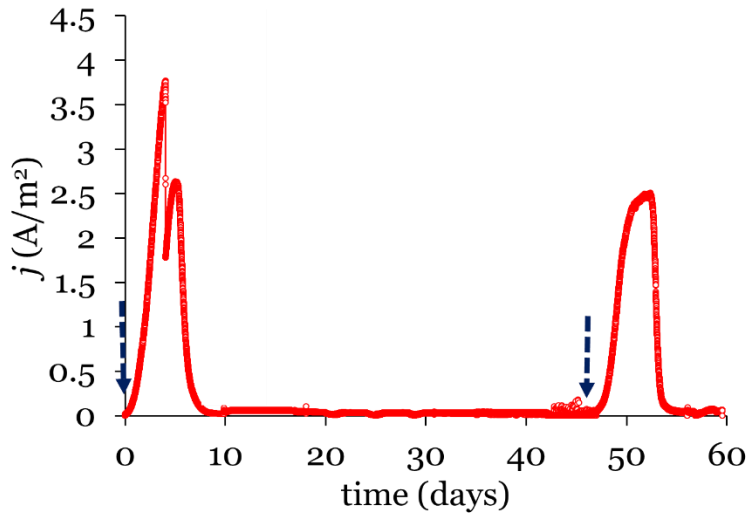

Figure 3.2 Current density in response to acetate spikes in the MEC fed with raw leachate. The dashed blue arrows indicate acetate spikes of 25 or 21 mM.

Since a goal of MXC technology is to treat wastewater, it is important to have a high removal efficiency for organic matter, along with maximizing *j,* CE, and CR. The BOD_5 concentration in the effluent of MEC fed with treated leachate was 270 mg/L, which represents ~70% BOD_5 reduction for the integrated treatment system (i.e., Fenton oxidation and MEC). This residual BOD_5 concentration is close to the discharge limits for landfill leachate (220 mg BOD_5/L) imposed by the USEPA (2000).

Thus, several pieces of evidence support that complexity of the biodegradable organic matter and the presence of inhibitors led to minimal fermentation and low *j* with the raw leachate. Pre-treating the leachate with the Fenton reaction overcame both

bottlenecks to fermentation, and this allowed the syntrophy of fermenters and ARB to function more robustly: higher organic-matter removal, CE, and *j*.

3.3.3 Microbial community analysis

Since I operated both MECs in continuous mode with a relatively short HRT (~17.8 h), which is shorter than the minimum solids retention time for fermenting bacteria (≥ 1.5 day) and acetoclastic methanogens (≥ 3 days) (Rittmann and McCarty, 2001), I performed microbial community analysis only on the biofilms, as most of microbial community was washed out from the suspended phase. Figure 3.3A presents the microbial community analyses at the phylum level, and Figure 3.3B gives the family-level information. At the phylum level, *Proteobacteria* dominated the microbial community with treated leachate (~66% of the sequences), followed by *Bacterioidetes* (~16% of the sequences) and *Firmicutes* (~12% of the sequences). Earlier studies revealed that *Bacteroidetes*, *Firmicutes*, and *Proteobacteria* were among the most abundant phyla in the anode of MXCs successfully treating different waste streams (Sanchez-Herrera et al., 2014; Yusoff et al., 2013; Shimoyama et al., 2009). *Bacteroidetes* and *Firmicutes* have members responsible for polysaccharide hydrolysis and fermentation, whereas many members of *Proteobacteria* are known to perform anode respiration (Ishii et al, 2012; Parameswaran et al, 2010). Predominance of *Proteobacteria* after Fenton treatment supports that the anode respiration was enhanced due to greater bioavailability of the partially oxidized recalcitrant organic matter into compounds that could readily be transformed into the simple substrates used by ARB (Parameswaran et al., 2009; Rittmann et al., 2008; Freguia et al., 2008). Since the Fenton reaction produced little or no acetate directly (data not shown), the Fenton products had to be fermented, which is why fermenters (*Bacteroidetes, Firmicutes,*

Spirochaetes, and *Actinobacteria*) had to be present along with ARB to create the necessary syntrophy.

In contrast for the biofilm anode fed raw leachate, *Deferribacteres* (~23% of the sequences) became the second abundant phylum after *Firmicutes* (~45% of the sequences), and *Proteobacteria* were only ~23%. *Deferribacteres*, which, like *Proteobacteria*, are Gram-negative and can respire iron, were among the most abundant phyla in anaerobic digesters treating complex organic wastes, such as brewery wastewater and leachate (Liu et al., 2011; Díaz et al., 2006), but previously have not been associated with anode respiration.

Figure 3.3C presents that community breakdowns at the genus level within the *Proteobacteria*. Notable is the dominance of *Geobacter* in both biofilms, which reflects that the metabolic core of the biofilm was anode respiration. For the treated leachate, *Arcobacter* and *Pseudomonas* also became important. This probably reflects the high diversity of organic substrates available to the community after Fenton pre-treatment. The low fraction of *Proteobacteria* in the biofilm fed raw leachate is consistent with a recent phylogenetic and metagenomic analysis (Zhang et al. 2014a) showing that introducing leachate to an acetate-fed MFC caused a significant decline (~10-fold) in the relative abundance of *Geobacter*-affiliated phylotypes that was accompanied by a 50% decrease in CE.

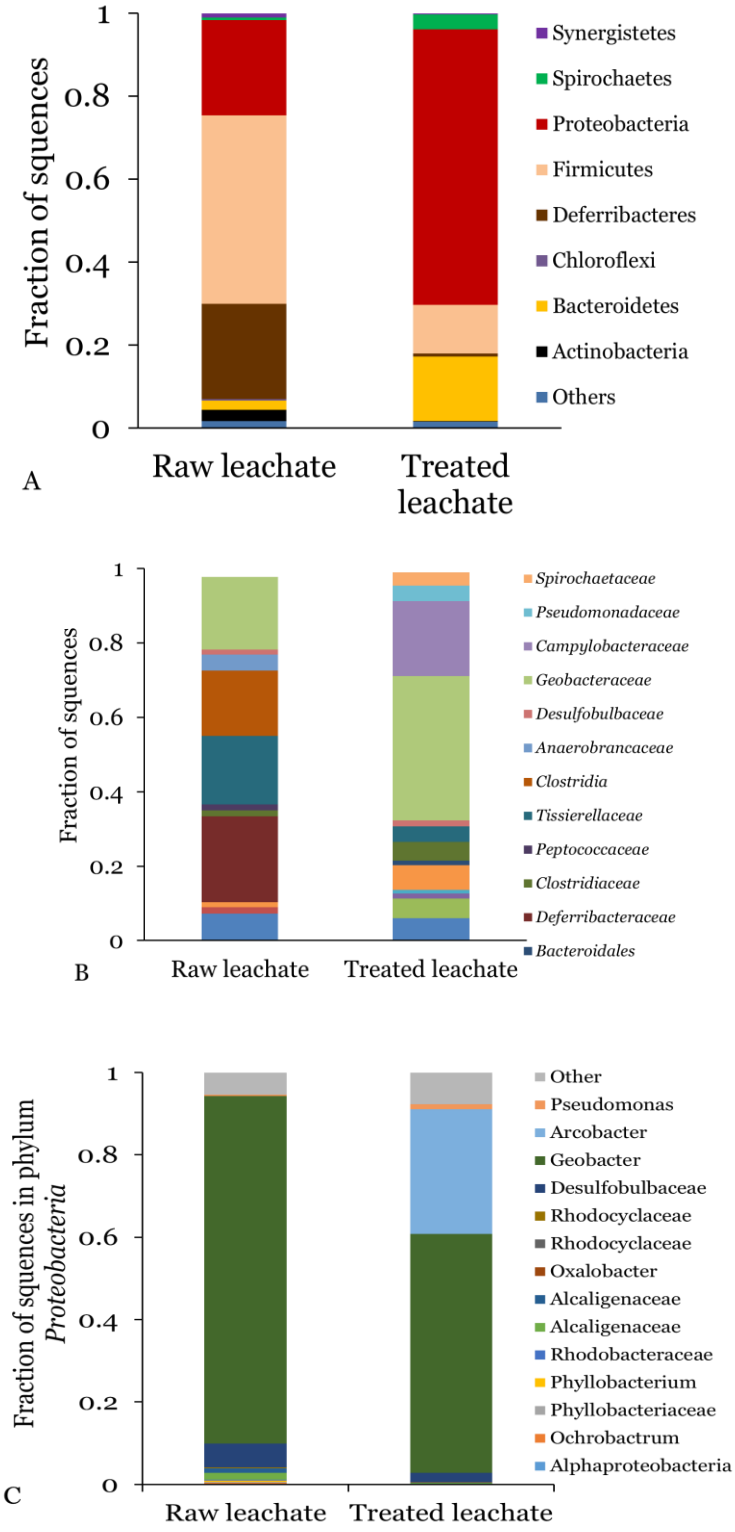

Figure 3.3 Microbial community distribution for MEC biofilms: (A) at phylum level, (B) at the family level, and (C) at the genus level within phylum *Proteobacteria*.

3.3.4 Evaluation of the MEC and the integrated treatment system

Table 3.2 summarizes results from a range of studies on treating landfill leachate in an MEC or MFC. It is obvious that landfill leachate without pre-treatment led to low *j,* CE, and CR in almost all the studies; a main cause was the low BOD_5 content due to the largely recalcitrant organic matter in the leachate's COD and the presence of inhibitory materials. An exception was with diluted leachate, which may have relieved inhibition You et al. (2006). The lack of microbial-community analysis in these studies makes it impossible to determine the relative impacts of recalcitrance versus inhibition. Our results after Fenton treatment gave the highest (and usually much higher) values of *j,* CE, and CR, confirming that Fenton pre-treatment of leachate was able to enhance the biodegradability of the organic material in the MXC setting. Here, our data suggest that relieving the fermentation inhibition may have been the more important factor.

This work establishes the fundamental proof-of-concept that pre-treatment by the Fenton's reaction can make recalcitrant organics in landfill leachate much more biodegradable in an MEC. This greatly enhanced *j*, CE, and CR, and final effluent quality. Further research is required to determine the optimal conditions of Fenton oxidation process to improve leachate biodegradability before energy capture in a downstream MEC. Optimization will be essential for making large-scale application economically feasible, since H_2O_2 might be costly. Recent studies by our team (and others) are showing that H_2O_2 can be produced sustainably in MXCs in high concentration (up to ~74 mM H_2O_2) via partial reduction of O_2 using inexpensive carbon cathode materials (Fu et al., 2010; Rozendal et al., 2009). Combining the possibility of energy capture from recalcitrant landfill leachate with H_2O_2 production in MXCs may offer a truly sustainable means of enhancing treatment and energy capture from recalcitrant landfill leachate.

Table 3.2 Summary of landfill-leachate treatment in microbial electrochemical cells.

Reactor configuration	Influent COD (influent BOD_5) [d]	Organic matter removal %	*j* (A/m^2)	CE (%)	CR (%)	Reference
MFC [a]	12,033 (898)	28.6 [e]	0.102	1.27	~0.36 [h]	Ganesh and Jambeck (2013)
MFC [a]	2386 (305)	16 [e]	0.07	17.4	~4.7 [h]	Damiano et al. (2014)
MFC [b]	1257–1612 (572)	12.5 [f]	3.79×10^{-3}	~0.3 [h]	~0.03 [h]	Greenman et al. (2009)
MFC [b]	1960 (823)	~ 70 [e]	~1	6.6	~4.6 [h]	You et al. (2006)
MFC [a]	3,400 (1,360)	60–90 [e]	~0.16–1.3	1.2–14.4	~0.7–13 [h]	Zhang et al. (2008)
MEC [a]	2594 (802)	2 [e] (3 [f])	0.11	1.8	0.04	This study
MEC [c]	1227 (608)	28 [e] (52 [f])	1.42	29	8.2	This study

[a] Experiment was performed with raw leachate; [b] Experiment was performed with diluted leachate; [c] Experiment was performed with Fenton-treated leachate; [d] Unit is mg/L; [e] COD removal %; [f] BOD removal %; [h] Not reported in the original study, but calculated based on their data.

3.4 Conclusions

While landfill leachate gave poor MEC performance – 3±0.3% BOD_5 removal, 1.8±0.5% CE, and 0.11±0.06 A/m^2 *j* – pre-treating the leachate with the Fenton reaction greatly improved all aspects of performance: 52±10% BOD_5 removal, 29±3 % CE, and 1.42±0.27 A/m^2 *j*. Inhibition of fermentation, not anode respiration, was the main cause of poor MEC performance when treating landfill leachate. Fenton pre-treatment of landfill leachate overcame fermentation bottlenecks by decreasing the complexity of the biodegradable-organic matter and the presence of inhibitors. Feeding the MEC with pre-treated leachate led to an ~5-fold increase in biofilm dry weight and to a microbial community enriched in phyla known to contain strains able to hydrolyze and ferment in complex organic matter – *Firmicutes*, *Bacterioidetes*, *Spirochaetes*, and *Actinobacteria* – along with known ARB within the *Proteobacteria*.

CHAPTER 4

FERMENTATION PRE-TREATMENT OF LANDFILL LEACHATE FOR ENHANCED ELECTRON RECOVERY IN A MICROBIAL ELECTROLYSIS CELL [2]

4.1 Introduction

As discussed in Chapter 2, recent reviews on MXCs highlight the growing interest in this technology as a means to gain value from organic waste streams (e.g., Logan and Rabaey, 2012; Pant et al., 2010; Rittmann, 2008). Most waste streams that are of interest for practical application of MXCs are comprised of complex organic substrates (Pant et al., 2010). Characteristics of the substrates influence MXC performance: organic matter removal, Coulombic efficiency (CE), Coulombic recovery (CR; the fraction of electrons recovered as electric current at the anode of an MXC compared to the total influent electrons in the substrate), and current density (j, A/m^2 or A/m^3, the current produced normalized to the active surface of anode or to the reactor volume, respectively).

Landfill leachate is a possible feedstock for MXCs (Ganesh and Jambeck, 2013; Zhang et al., 2008; You et al., 2006). Leachates are liquid discharges from landfills, which dispose of around 95% of municipal solid wastes (MSW) worldwide (Renou et al., 2008). Leachate typically is a strong wastewater that contains high concentrations of organic matter (usually measured as chemical oxygen demand, COD), ammonium-nitrogen (NH_4^+–N), heavy metals, xenobiotic organic compounds (XOCs), humic compounds (HCs), and inorganic salts. Many factors affect the quality of leachate: the type of waste, age of the landfill, and the seasonal variations in the weather (Renou et al., 2008). Leachate composition changes as a landfill progresses through successive

[2] This Chapter was published in an altered format in Bioresource Technology (Mahmoud *et al.,* 2014. *Bioresource Technology* 151, 151 – 158).

aerobic, acetogenic, methanogenic, and stabilization stages (Renou et al., 2008), and leachate can be classified into 3 groups based on the landfill age, i.e., young, intermediate, and mature. Table 4.1 summarizes typical characteristics of each group. Young leachate has significantly higher COD and biodegradability (based on the BOD_5/COD ratio, where BOD_5 is the 5-day biochemical oxygen demand), but the BOD_5/COD ratio for young leachates often is relatively low (~0.3).

Table 4.1 Landfill leachate classification according to age and typical characteristics (Source: Renou et al., 2008).

	Young	**Intermediate**	**Mature**
Age (years)	< 5	5 – 10	> 10
pH-value	6.5	6.5 – 7.5	> 7.5
COD (g/L)	> 10	4 – 10	< 4
BOD_5/COD ratio	> 0.3	0.1 – 0.3	< 0.1
Organic composition	80% VFA [a]	5 – 30% VFA + HCs and FCs [b]	HCs and FCs

[a] VFA: volatile fatty acids; [b] HCs and FCs: humic and fulvic acids, respectively.

Although leachate might be considered a good feedstock for MXCs because of its relatively high conductivity, buffering capacity, and BOD_5, as well as minimal solids, my results as discussed in Chapter 3 (and others) show that *j*, CE, and CR are relatively low (Mahmoud et al., 2016; Zhang et al., 2008; You et al., 2006), probably due to the large portion of poorly-biodegradable organics in the leachate's COD. Previous research has shown that only 8–43% of the BOD_5 was removed in an MFC fed with diluted leachate (Greenman et al, 2009), while only 7% of the COD was converted to electricity in dual chamber, air-cathode MFCs fed with young landfill leachate (You et al, 2006). Recently, Ganesh and Jambeck (2013) investigated the performance of a single chamber air–

cathode, semi-continuously-fed MFC for electricity generation from landfill leachate. They reported an average COD removal of 28% and current density of 26.8 mA/m^2. Moreover, CE was very low ranging from 1 to 14% with an average value of 6.9%. Li et al (2013) demonstrated the feasibility of treating food-waste leachate with 87% VFA removal, although with CE in the range of 14–20%.

MXC biodegradation of complex organic compounds, like those present in a landfill leachate, must occur through a series of anaerobic reactions. Anode-respiring bacteria (ARB), the key microorganisms that colonize the anode of MXCs, are known to use only a few simple compounds as electron donors, in particular acetate and H_2 (Pant et al., 2010; Lee et al., 2008; Torres et al., 2007). Thus, fermentation reactions are necessary to produce the mixture of simple products that ARB can oxidize. However, fermentation products depend upon the organic sources, the microbial community, and operating conditions, such as pH and temperature (Lee et al., 2008; Ren et al., 2007).

As discussed in Chapter 3, Fenton oxidation of landfill leachate enhanced MEC performance by accelerating fermentation, allowing more biofilm accumulation, and establishing a syntrophic relationship between fermenters and ARB. Although fermentation and anode respiration can occur together in the anode of an MXC (Parameswaran et al, 2009; Ren et al, 2007), it may be advantageous to have some or most of the fermentation reactions occur in an independent reactor that precedes the MXC. In this case, the MXC receives simpler organic compounds that can be oxidized more directly by ARB, thereby simplifying the structure and function of the ARB community in the biofilm anode and helping bring about higher current density (Torres et al., 2007). Separate fermentation reactors whose effluent is then fed to an MXC anode were evaluated for primary sludge (Yang et al, 2012), cellulose (Wang et al, 2011), and

primary municipal wastewater (Nam et al, 2010a). These studies showed increased performance compared to direct addition of raw complex substrate to the MXC anode.

Pre-fermentation treatment also might help to remove xenobiotic compounds that may be toxic to the ARB. Phenolics are a good example, and past studies have shown that phenolic compounds can be removed in anaerobic environments through syntrophic activities of phenol metabolizers, hydrogen-utilizers, and acetoclastic methanogens. For example, Tay et al. (2001) investigated the anaerobic biodegradation of phenol with different initial phenolic concentrations (105–1,260 mg phenol/L). They were able to achieve 88–98% phenol removal even at a high phenol loading rate (6 kg phenol-COD/L.day).

My main goal of this study was to evaluate whether or not fermenting landfill leachate in a separate reactor improved the performance of an MEC. I first characterized the performance of the first-stage fermenter, and then experimentally evaluated electron flow in biofilm anodes for MECs treating raw leachate versus fermented leachate.

4.2 Materials and Methods

4.2.1 Landfill leachate

I collected leachate from the Northwest Regional Landfill (Surprise, AZ) and kept it refrigerated at 4°C prior to use. The leachate was used as is for all experiments: without pH adjustments, addition of nutrients/trace metals, or dilution. I added a specific methanogen inhibitor, 2-bromoethanesulfonate (BES), at 50 mM (Parameswaran et al., 2010) in certain experiments, as explained below.

4.2.2 Anaerobic fermentation experiments

I carried out batch anaerobic fermentation assays using serum bottles with a working volume of 100 mL and a total volume of 160 mL. Anaerobic digester sludge from the Mesa Northwest Water Reclamation Plant (Mesa, AZ) was the inoculum and had total suspended solids (TSS) and volatile suspended solids (VSS) concentrations of 27±10 and 23.2±8 g/L, respectively. I inhibited methanogenesis by adding 50 mM BES. Once the inoculum (final concentration of ~5 g VSS/L) and leachate were added into the serum bottles, I capped the bottles with rubber serum stoppers and aluminum caps, purged them with N_2/CO_2 (80%:20%) gas for 30 min to remove O_2, placed them in a 37°C incubator shaker (175 rpm, C25KC, New Brunswick Scientific), and followed the batch biochemical methane potential (BMP) protocol (Parameswaran and Rittmann, 2012) in triplicate. I measured the volume of gas produced with a friction-free glass syringe of 10 or 50 mL volume (Popper & Sons, Inc., New Hyde Park, NY, USA).

In order to confirm the results from the batch fermentation experiments and produce enough fermented leachate for MEC experiments, I evaluated fermentation under semi-continuous operation. The reactor was operated in a 37°C incubator shaker, and leachate (with 50 mM BES) was fed in a semi-continuous mode once every 2 days.

At the end of each HRT, I allowed the solids in the fermentation reactors to settle for 2 h and then centrifuged the supernatant at 2000 rpm for about 10 min. Although the hydraulic retention time (HRT) was 2 days, the solids retention time (SRT) was controlled at 44 to 50 days by regularly discharging a specified amount of sludge according to the definition of SRT (Rittmann and McCarty, 2001).

4.2.3 Microbial electrolysis cells

I used dual-chamber, H-type MECs with a liquid volume of 320 mL in each chamber (Parameswaran et al., 2010; Lee et al., 2008; Torres et al., 2007). For anodes, I cut ~270,000 graphite fibers (~8 cm length) and mounted them on a stainless steel rod using plastic ties. I had treated the graphite-fiber anode by soaking them in 0.1 M HNO_3 for 4 h and then soaked them in pure acetone overnight, followed by ethanol (95%) for 3 h. Following the treatments, I washed the graphite fiber anode three times with distilled water before placing them in the MEC. I used a 0.8-cm outer diameter (OD) graphite rod as a cathode, and I maintained a cathode pH of 12 by addition of 10 N NaOH. I separated the cathode chamber from the anode chamber using an anion exchange membrane (AMI 7001, Membranes International, Glen Rock, NJ), and placed an Ag/AgCl reference electrode (BASI Electrochemistry, West Lafayette, IN) about 0.5 cm away from the anode to control the anode potential at – 0.3 V vs. Ag/AgCl using a potentiostat (Bio-Logic USA, Knoxville, TN). The temperature was controlled at 30°C in a temperature-controlled room, and the liquid in both chambers was mixed at 150 rpm using a magnetic stirrer.

I estimated the areal current density (A/m^2) for our system with the following estimate for the maximum anode surface area: 270,000 fibers x 3.14 x 7 μm (circumference) x 8 cm (length) = 0.47 m^2. I also computed current density normalized

to the reactor volume (A/m^3). Due to mass-transport limitations within the bundle of graphite fibers, the A/m^2 current densities I report are very low compared to what can be achieved with a simple geometry, such as a graphite rod. Thus, the A/m^2 values I report should not be compared directly to values from different configurations. Since I used the same MEC for both leachates, I can make direct comparisons to gauge the effect of pre-treatment on performance using either current density.

Prior to the MEC start-up, I seeded the anode chamber with 3 mL of the digester-sludge inoculum. For the initial formation of biofilm on the anode, I fed the MEC with a mixture of VFAs (acetate, 20.4 mM; propionate, 11.1 mM; and butyrate, 1.8 mM) in batch mode until a stable current density was achieved (~1.5 days). At this point, I fed the MEC with raw leachate in batch mode, which continued for 2 consecutive cycles (~15 days). After the experiments with raw leachate were complete, I carried out another new acclimation cycle with the same composition of mixed VFAs medium and new inoculum and cell components (electrodes and membrane). Then, I performed two successive batch cycles in which the MEC anode was fed the effluent of a semi-continuous fermentation test with BES (i.e., the fermented leachate as described above). Since I had a limited volume of fermented leachate, I collected the effluent of the semi-continuous fermentation reactor for several days prior to introducing it into the MEC. All batch MEC experiments were performed in duplicate.

4.2.4 Analyses

I measured total and soluble COD, total nitrogen (Total–N), ammonium-nitrogen (NH_4^+), total alkalinity, and total phosphorus (Total-P) in duplicate using HACH kits (HACH, Ames, IA). Soluble COD was quantified after filtration through a 0.22-µm membrane filter (PVDF GD/X, Whatman, GE Healthcare, Ann Arbor, MI). Total BOD_5

was measured according to *Standard Methods* (APHA, 1998). I measured total organic carbon (TOC) using a TOC analyzer (TOC-VCSH, Shimadzu Scientific Instruments, Columbia, MD) equipped with combustion catalytic oxidation/non-dispersive infrared (NDIR) gas analyzer. I also measured nitrite, nitrate, chloride, and sulfate concentrations using ion chromatography (ICS 2000, Dionex Corporation, CA) after filtration through a 0.22-μm membrane filter. I analyzed liquid samples for organic fermentation products using high-performance liquid chromatography (HPLC; Model LC-20AT, Shimadzu, Columbia, MD) equipped with an Aminex HPX-87H (Bio-Rad Laboratories, Hercules, CA) column after filtration through a 0.22-μm membrane filter. I used 2.5 mM sulfuric acid as an eluent fed at a flow rate of 0.6 mL/min, and chromatographic peaks were detected using photo-diode array (210 nm) and refractive index detectors. The total elution time was 60 min, and the oven temperature was constant at 50°C. I developed a calibration curve for every set of analyses, performed duplicate assays, and report the average concentrations.

I analyzed carbohydrate and protein by a colorimetric method (DuBois et al., 1956) and the bicinchoninic acid method using the BCA protein-assay kit (Sigma–Aldrich, St. Louis, MO) (Lee et al., 2008), respectively. For analyzing carbohydrate, I added 2 mL of sample into a 15-mL culture tube containing 80% phenol solution (wt/wt), followed by 5 mL of sulfuric acid (95.5%). For both analyses, I developed standard calibration curves with glucose and bovine serum albumin, and measured the absorbance at wavelengths of 485 and 562 nm for carbohydrate and protein, respectively, using UV-Vis spectrophotometer (Varian Cary 50 Bio, Varian Inc., Walnut Creek, CA). I measured the lipid content gravimetrically by a procedure adapted from Bligh and Dyer (1959) using a mixture of chloroform and methanol as an extraction solvent (1:1 v/v). Briefly, I placed 10 mL of sample into 50 mL culture tube containing 5

mL of chloroform and 10 mL of methanol, and shook the mixture overnight at 180 rpm. The next day, I added an additional 5 mL of chloroform to make the final ratio of chloroform:methanol to be 1:1 (*v/v*), vortex mixed them for 1 minute, and centrifuged them at 4000 rpm for 10 minutes. The lipid content was soluble in the solvent, which formed a dense layer at the bottom of the centrifuge tube. I analyzed the total phenolic compounds by the Prussian blue assay (Budini et al., 1980).

I measured gas percentages of H_2, CH_4, and CO_2 in samples taken with a gas-tight syringe (SGE 500 µL, Switzerland) using a gas chromatograph (GC 2010, Shimadzu Corporation, Columbia, MD) equipped with a thermal conductivity detector and a packed column (ShinCarbon ST 100/120 mesh, Restek Corp., Bellefonte, PA). N_2 was the carrier gas at a constant flow rate of 10 mL/min and pressure of 5.4 atm. Temperature conditions for column, injection, and detector were 140, 110, and 160 °C, respectively. I employed analytical grade H_2, CH_4, and CO_2 gases for standard curves, carried out gas analyses in duplicate, and averaged the two values.

4.2.5 Calculations

The percentages of COD represented by carbohydrate, protein, and lipids were calculated using stoichiometric conversion factors of 1.067, 1.56, and 2.875 g COD/g organic type, respectively, based on typical formulae for carbohydrate (CH_2O), protein ($C_{16}H_{24}O_5N_4$), and lipids ($C_8H_{16}O$) (Rittmann and McCarty, 2001).

I express all electron equivalents as total COD (1 e^- equivalent = 8 g COD) to establish mass balance according to equation (4.1):

$$COD_{influent} = COD_{current} + COD_{suspended\ biomass} + COD_{gases} + COD_{effluent} + COD_{unaccounted} \quad \text{(Eq. 4.1)}$$

where $COD_{influent}$ is the input COD in the anode chamber (mg COD/L), $COD_{current}$ is the COD equivalent of the current over the operation time (mg COD/L), $COD_{suspended\ biomass}$ is the COD equivalent of the suspended biomass over the operation time in the anode chamber (mg COD/L), COD_{gases} is the COD equivalent of the cumulative gasses (CH_4 and H_2) over the operation time in the anode chamber (mg COD/L), $COD_{effluent}$ is the soluble COD in anode chamber at the end of current generation (mg COD/L), and $COD_{unaccounted}$ is the unaccounted for COD in the liquid of the anode chamber at the end of current generation (mg COD/L). I converted units with the following relationships (Lee et al., 2008):

1 C of current =

$$\frac{1\ e^- eq}{96485\ C} \times \frac{8\ g\ TCOD}{e^- eq} \times \frac{1000 mg}{g} = 0.083\ mg\ COD \quad \text{(Eq. 4.2)}$$

$$1\ mL\ CH_4 = \frac{1\ mmol\ CH_4}{22.4\ mL} \times \frac{273.15\ K}{303.15\ K} \times \frac{8\ me^- eq}{mmol\ CH_4} \times \frac{8\ mg\ TCOD}{me^- eq} = 2.57\ mg\ COD \quad \text{(Eq. 4.3)}$$

$$1\ \text{mL}\ H_2 = \frac{1\text{mmol}\ CH_4}{22.4\ \text{mL}} \times \frac{273.15\ \text{K}}{303.15\ \text{K}} \times \frac{2\ \text{me}^{-}\text{eq}}{\text{mmol}\ CH_4} \times \frac{8\ \text{mg TCOD}}{\text{me}^{-}\text{eq}} = 0.64\ \text{mg COD} \qquad \text{(Eq. 4.4)}$$

I calculated *j* by normalizing the current produced to the active surface of anode (0.47 m^2) or to the reactor volume (320 mL). I estimated CE by dividing cumulative electron equivalents collected at the anode by the electron equivalents of total COD consumed by ARB (the difference between COD in the MEC's influent and effluent). I also computed CR by dividing cumulative electron equivalents collected at the anode by the electron equivalents of influent COD.

I used the carbon oxidation state (COS) as an indicator for change in the reduction status of organic matter during anaerobic fermentation of the leachate. I computed COS with the following relationship, which is based on the change in COD and TOC concentrations (Amat et al., 2007):

$$\text{COS} = 4 - \left(1.5 \times \frac{\text{COD}}{\text{TOC}_{\text{influent}}}\right) \qquad \text{(Eq. 4.5)}$$

where $TOC_{influent}$ is the total organic carbon and COD is the total COD for the same sample.

4.3 Results and Discussion

4.3.1 Landfill leachate characterization

The chemical characteristics of the leachate are summarized in Table B.1 in appendix B. The leachate contained relatively low concentrations of organics compared to leachate characteristics presented in the literature (Renou et al., 2008). Average values of COD and BOD_5 were 2630 and 830 mg/L, respectively. Most of the organics were present in the soluble form, since the suspended solids were only 67 mg/L. The BOD_5/COD ratio of 0.32 indicates a medium-age leachate (5–6 years old) and biodegradability large enough to justify biological treatment (Metcalf and Eddy, 2003). The leachate also had a COD:TN:TP ratio = 194:43:1 in grams, alkalinity of 3900 mg/L as $CaCO_3$, and a near-neutral pH, all of which support anaerobic biological treatment (Metcalf and Eddy, 2003). The sample also contained low concentrations of nitrate (0.42 mg N/L) and modest sulfate levels (37 mg SO_4^{2-}/L), which could support competing anaerobic microbial processes to anode respiration, albeit to a small extent.

4.3.2 Batch fermentation

Figure 4.1 shows that the VFA concentration increased from 114 mg VFA–COD/L to 495 mg VFA–COD/L at the end of batch fermentation experiments. Succinate was the most abundant species and had the highest accumulation, acetate increased to be the second largest, and formate had a very low concentration. Succinate accumulation has been observed for anaerobic conditions with different microbial species: e.g., *Anaerobiospirillum succiniciproducens* (Werf et al. 1997), *Bacteroides fragilis* (Macfarlane and Macfarlane, 2003), and *Escherichia coli* (McKinlayet al., 2007), all of which are typically detected in anaerobic digesters (Nakasaki et al., 2009). Fermentation

studies using pure cultures of *Bacteroides fragilis* showed that acetate and succinate were the major fermentation products when substrate was abundant, while succinate was decarboxylated to produce propionate when substrate was limiting (Macfarlane and Macfarlane, 2003).

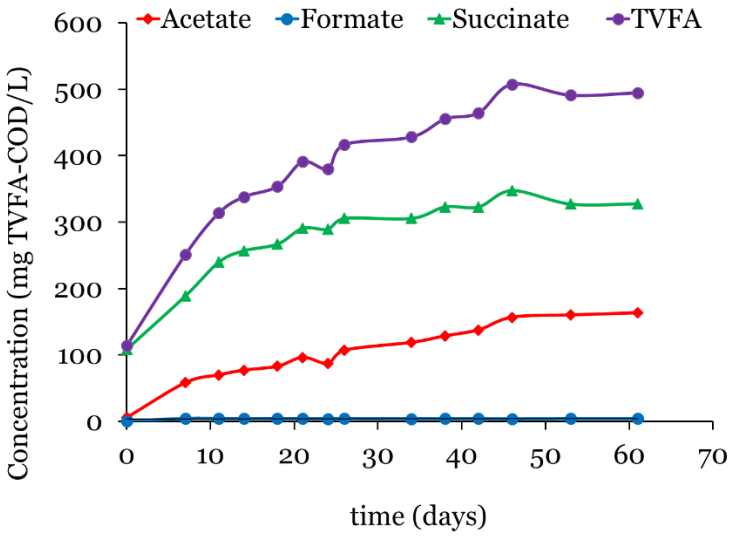

Figure 4.1 Detected VFAs (as COD) during the batch anaerobic fermentation of landfill leachate.

Figure 4.2 presents the alkalinity and pH results that correspond to Figure 4.1. As a result of VFAs accumulation, total and bicarbonate alkalinities decreased by 25% and 33%, respectively (Figure 4.2A), and the VFA-to-total alkalinity ratio increased from 0.03 to 0.17 mg COD-VFA/mg $CaCO_3$. This led to decrease in the pH from 8.4 at the start of the experiment to 7.45 at the end of the 60-day experiment (Figure 4.2B).

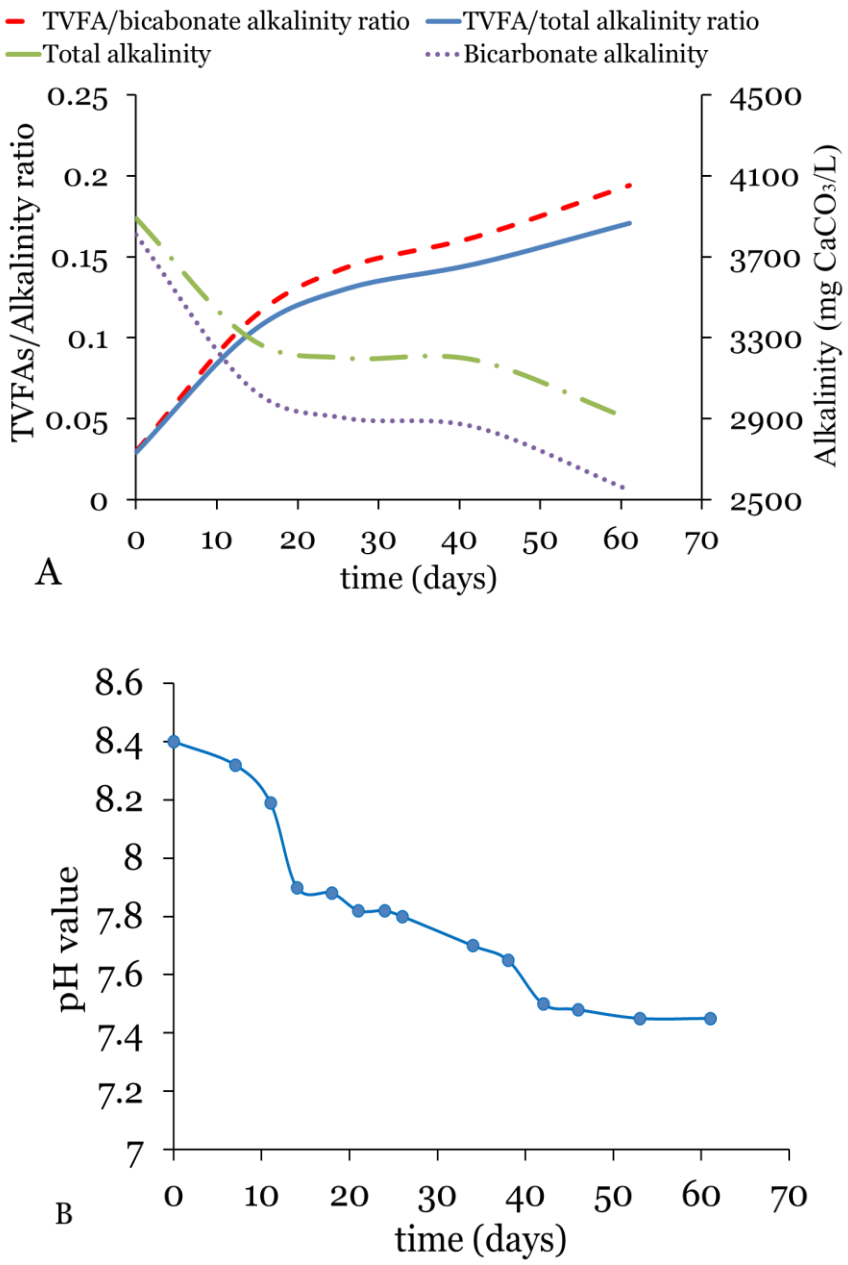

Figure 4.2 Performance of batch anaerobic fermentation of landfill leachate. (A) Total and bicarbonate alkalinity and VFA/total and bicarbonate alkalinity ratio. (B) pH values.

The performance of a fermentation process can be evaluated by the degree to which the initial COD is converted to VFAs. I used Eq. 4.6 to calculate the degree of VFA conversion:

$$\text{VFA conversion} = \frac{S_{VFA}}{S_{influent}} \times 100 \qquad \text{(Eq. 4.6)}$$

where S_{VFA} is the COD equivalent of the produced VFAs (mg VFA-COD/L), and $S_{influent}$ is initial substrate concentration (mg (COD or BOD_5)/L).

Figure 4.3A plots the VFA conversions based on the influent COD and BOD_5. The VFA conversion was up to 19% based on COD and 60% based on BOD_5. The final concentrations of carbohydrate, protein, and lipids were 76±10, 754±152, and 72±10 mg/L, respectively. These represent 60% removal for carbohydrate, but only 18% and 1% removals for protein and lipid, respectively. My results agree with other studies that show that carbohydrate degradation is faster than for protein and lipids (Liu et al., 2003; Rittmann and McCarty, 2001). The very low removal of lipids suggests that lipids degradation may be the ultimate rate-limiting step for full conversion of COD to VFAs. The COS, shown in Figure 4.3B, became less negative during the fermentation of leachate due to the partial oxidation of complex organics (carbohydrate and protein) into more oxidized by-products i.e., VFAs. The TCOD also declined, and this is analyzed below through a COD mass balance.

I also observed a 33% removal of total phenolic compounds during fermentation, from 110 mg/L in the raw leachate to 74 mg/L in the final fermentation effluent. My results were less dramatic than those obtained by Gonçalves et al. (2012), who investigated the degradation of phenolic compounds in olive-mill wastewater for batch

anaerobic conditions. They achieved 60–81% reduction in phenolics concentration. My relatively low removal was probably due to the non-acclimated sludge inoculum, a more recalcitrant phenolic fraction in leachate than olive-mill wastewater, or both.

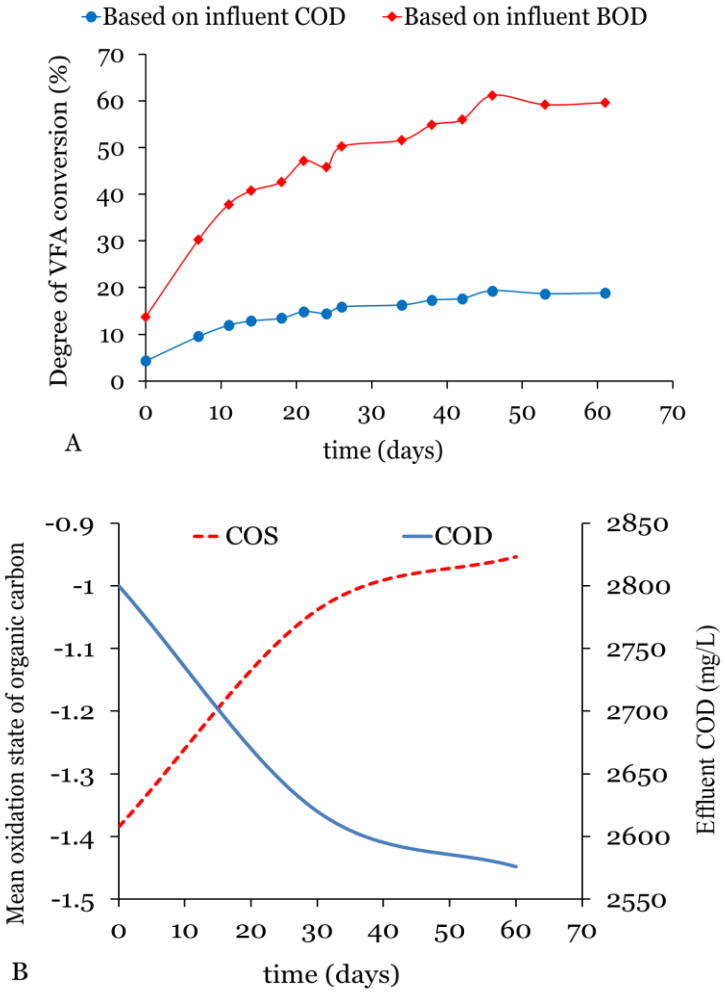

Figure 4.3 Landfill leachate organic matter oxidation during batch anaerobic fermentation assays: (A) VFA conversion degree. (B) COS and TCOD.

Table 4.2 distributes COD and BOD_5 from the leachate to the possible sinks at the end of the batch fermentation. CH_4 and H_2 were not detected, only 4% and 0.6% of the initial COD were associated with biomass and sulfate reduction, respectively, and about 92% of influent total COD was measured as soluble COD. At the end of fermentation

experiment, VFAs and protein were the major components in the soluble COD, and their concentrations reached 495 and 1180 mg COD/L (20.3% and 48.2% of effluent COD), respectively. Carbohydrate and lipids had low concentrations, 3.3% and 7%, respectively. Unidentified components (3% of the influent COD) might be nucleic acids, humic-like substances, and other soluble microbial products (SMPs) (Argelier et al., 1998; Rittmann and McCarty, 2001). 86% of influent BOD_5 ended up as soluble BOD_5, and approximately 10.2% and 1.8% of BOD_5 was associated with biomass synthesis and sulfate reduction, respectively, with only 1.2% of the original BOD_5 unaccounted.

Table 4.2 Summary of COD mass balance for batch anaerobic fermentation of leachate.

	COD [a]	**Fraction of COD (%)**	**BOD_5** [a]	**Fraction of BOD_5 (%)**
Initial leachate TCOD	2640±210	100	835±62	100
Final liquor SCOD	2440±140	92.4±5.2	725±54	86.8±6.2
Sulfate reduction	15±4	0.6±0.1	15±4	1.8±0.84
Biomass	85±23	4±0.9	85±23	10.2±2.4
CH_4 gas	ND [b]	–	ND [b]	–
H_2 gas	ND [b]	–	ND [b]	–
Unaccounted electron sinks	95±18	3±0.9	10±3	1.2±0.69

[a] COD and BOD_5 have unit of mg/L; [b] ND: not detected.

4.3.3 Semi-continuous fermentation

I also investigated anaerobic fermentation of leachate using semi-continuous operation: HRT = 2 days, SRT = 44–50 days, and organic loading rate = 1.13±0.25 kg COD/m^3.day. I chose a short HRT with a long SRT to make acetate the dominant product in our fermentation reactor effluent (Elefsiniotis and Oldham 1994), since acetate is the most readily utilized substrate by ARB (Pant et al., 2010; Torres et al., 2007).

Similar to batch fermentation and as expected, organics removal was low: ~3.6% for COD and ~5% for BOD_5. Acetate was the only acid metabolite detected in the reactor effluent, due to the high SRT, and its BOD_5 concentration was about 10% of the input BOD_5. Carbohydrate had the highest fermentation efficiency (21%), followed by protein fermentation (9%) and negligible fermentation of lipids. In addition, I detected a 24% reduction in total phenolic compounds (from 120 mg/L in the influent to 91 mg/L in the fermentation effluent), which was similar to the 33% removal obtained in the batch fermentation. The effluent from this semi-continuous fermentation was collected and used for the MEC experiments reported next.

4.3.4 MEC performance with fermented and raw leachate

The performance of the MEC during the startup period was evaluated by monitoring the current density over time during batch operation for two batch cycles. The current density stabilized at 41 mA/m^2 (60 A/m^3) after 6 days of batch operation with a mixture of VFAs. At this point, I fed the MEC with raw leachate and operated the MEC in batch mode for two successive cycles. After the experiment with raw leachate was completed, I carried out a new re-acclimation cycle, achieving the same current

density (41 mA/m^2 or 60 A/m^3). Then, I performed two successive batch cycles in which the MEC anode was fed the effluent of a semi-continuous fermentation test.

Figure 4.4A displays the current density for the batch MEC fed with raw leachate. The current density rose rapidly up to 1.7 mA/m^2 (2.5 A/m^3), had a period of near constant current density, and then fell relatively sharply. The decrease in current density probably was due to the depletion of readily available substrate. The second batch gave trends consistent with the first batch.

For the fermented leachate (Figure 4.4B), I observed a rapid increase in the current generation to reach its maximum value at around 16 mA/m^2 (23 A/m^3) for about 4 hours. After that, the current density declined significantly; this might have been due to the decrease in the availability of substrate in the form of metabolic intermediates that can act as electron donor for ARB. Similar to the raw leachate MEC batch experiments, the second batch of fermented leachate repeated the pattern of a rapid rise in current density, a stable period of near constant current density, and then a relatively sharp fall.

Figure 4.4C shows 83±6% BOD_5 and 26±7% COD removals for the MEC fed with fermented leachate, but only 5.6±0.8% BOD_5 and 3±0.9% of COD removals with raw leachate. Likewise, the final CEs for the first and second batch experiments were 67 and 68%, respectively, for the fermented leachate, but 55 and 56% for the raw leachate. The reported CEs are the highest reported among all published data using landfill leachate. In summary, fermented leachate led to consistently better MEC performance in terms of COD and BOD_5 removals, *j*, and CE.

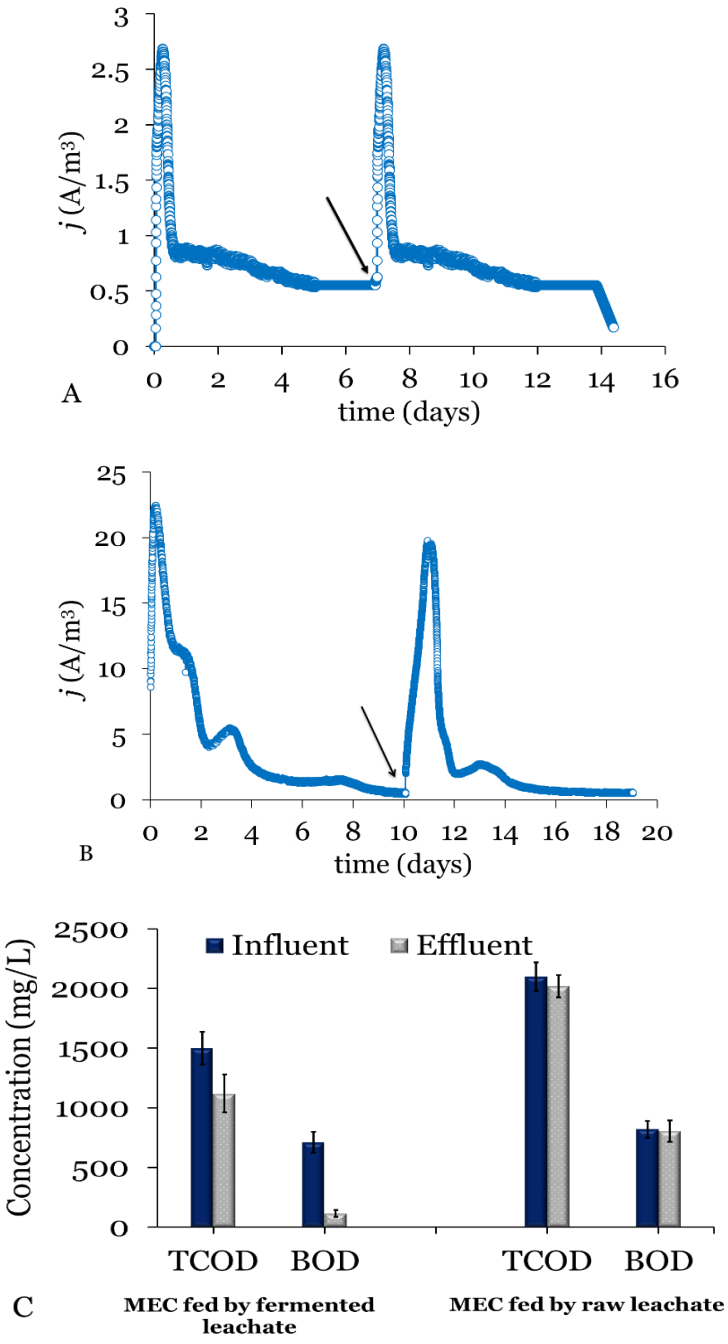

Figure 4.4 Performance of MECs fed with raw and fermented leachate: (A) Current generation versus time in a batch MEC fed with raw leachate, (B) Current generation versus time in a batch MEC fed with fermented leachate, and (C) Average concentrations of total COD and BOD5 for MECs fed by fermented or raw leachate. The arrows in panels A and B indicate substrate feeding for the second batch.

4.3.4 Electron flow distribution for the batch MECs with fermented and raw leachate

Table 4.3 shows the distribution of electrons from fermented and raw leachate to the various electron sinks at the end of batch operation and based on influent BOD_5. About 17% and 94% of the influent BOD_5 ended up as soluble BOD_5 in the final liquor for fermented and raw leachates, respectively. Corresponding coulombic recoveries were 17.3% and 2.1% for fermented leachate and raw leachate, respectively. Approximately 8.4% and 1.7 % of the electrons in the original BOD_5, ended up in suspended biomass. This is smaller than 10% and 5% suspended biomass obtained in acetate and glucose fed batch MFC, respectively (Lee et al., 2008), supporting that biomass synthesis is very low in MXCs fed with a complex electron donor. I also found no H_2 or CH_4 in the headspace gas of the anode chamber. The lack of CH_4 was related to our use of BES, which inhibited methanogens. Because H_2 did not accumulate, any H_2 produced by fermentation was channeled to ARB and current production. The most likely fate of H_2 was its conversion to acetate through homoacetogenesis, with subsequent oxidation by ARB (Parameswaran et al., 2010). However, I cannot rule out that H_2 was oxidized directly by ARB, since H_2 was a good electron donor for a pure culture of *Geobacter sulfurreducens* (Bond and Lovley, 2003), and active H_2 metabolism was observed at an anode fed with 100% hydrogen gas (Rozendal et al., 2008b). Overall, the electron balance reinforces the benefit of fermentation for greatly increasing the electron recovery to current.

Table 4.3 Summary of BOD_5 mass balance for batch MECs.

	Raw leachate		Fermented leachate	
	BOD_5 [a]	**Fraction of BOD_5 (%)**	**BOD_5 [a]**	**Fraction of BOD_5 (%)**
Initial leachate total BOD_5	835±98	100	820±80	100
Final liquor soluble BOD_5	788±250	94.4±5.2	142±41	17.3±8.0
Current	17±5	2.0±0.6	469±95	57.2±10.2
Suspended biomass	14±2	1.7±0.2	69±20	8.4±3.4
CH_4 gas	ND [b]	–	ND [b]	–
H_2 gas	ND [b]	–	ND [b]	–
Unaccounted electron sinks	16±8	1.9±1.2	140±85	17.1±4.0

[a] COD and BOD_5 have unit of mg/L; [b] ND: not detected.

4.4 Conclusions

Pre-fermentation of leachate improved MEC performance by converting complex organics to readily biodegradable substrates for ARB. Batch fermentation generated primarily acetate and succinate, but mostly acetate in semi-continuous studies. Feeding the semi-continuously fermented leachate to the anode of an MEC significantly improved its performance: 83% BOD_5 removal, 68% CE, 17.3% CR, and *j* of 23 A/m^3 ($16mA/m^2$), compared to 5.6% BOD_5 removal, 56% CE, 2.1% CR, and 2.5 A/m^3 (1.7 mA/m^2) *j* for the raw leachate. All differences support the value of pre-fermentation before an MEC for BOD_5 stabilization and enhanced electron recovery as current when treating a recalcitrant wastewater like leachate.

CHAPTER 5

ALTERATIONS IN THE FERMENTATION RATE AS A RESPONSE TO CHANGES IN ORGANIC MATTER COMPOSITION OF LANDFILL LEACHATE [3]

5.1 Introduction

Over the past 2 centuries, the accelerating use of fossil fuels has led to a buildup of greenhouse gases, particularly carbon dioxide. One way to slow and eventually reverse this trend is to develop technologies that convert organic waste streams into high-quality energy-value products (Rittmann, 2008). Landfill leachate is one example of such a feedstock for renewable energy production (Mahmoud et al., 2014; Hafez et al., 2010; Greenman et al., 2009; Renou et al., 2008).

The microbiological conversion of complex organic compounds to useful energy products occurs through a cascade of biochemical reactions that occur under anaerobic conditions (Rittmann and McCarty, 2001). Fermentation is an essential step whether the final product is methane gas (Gunaseelan, 1997), electric current, or hydrogen gas (Lee et al., 2008; Torres et al., 2007). Fermenting bacteria transfer electrons that originate in a variety of complex biodegradable organics, such as carbohydrate and protein, to short-chain organic acids, alcohols, and hydrogen gas (H_2) (Rodríguez et al. 2006). Fermentation is influenced by many factors, including the nature of organic matter used, the operating pH, the inoculum, the presence of inhibitory compounds, and temperature (Metcalf and Eddy, 2003; Rittmann and McCarty, 2001). For example, the distribution of fermentation products (i.e., organic acids and H_2) is strongly affected by the carbohydrate-to-protein ratio of the organic feed, and the distribution corresponds to changes in the microbial community structure (Alibardi and Cossu, 2016; Lai et al., 2016; Palatsi et al., 2011; Supaphol et al., 2011; Feng et al., 2009).

[3] This Chapter will be submitted for publication.

Although leachate is known for its poorly biodegradable organic matter, it is in other ways a good candidate for use on environmental biotechnology systems, such as microbial electrochemical cells and anaerobic digester, due to its high electrical conductivity and buffering capacity, along with its low solids content. Therefore, the overarching goal of this research is to overcome the main cause of poor fermentation rate of landfill leachate. I use Fenton oxidation with different initial molar ratios of hydrogen peroxide (H_2O_2) to ferrous ion (Fe^{2+}) as pre-treatment technology to obtain different organic matter compositions of leachate's organic matter. I inhibit methanogenesis by performing my experiments in batch fermentation reactors with 50-mM 2-bromoethanesulfonate (BES) and with a previously adapted anaerobic digester sludge to landfill leachate. Then, I experimentally evaluate electron flow in fermenters treating raw leachate versus treated leachate samples. Using these results, I was able to evaluate whether complexity of the biodegradable-organic matter in leachate, the presence of inhibitors, or both is the main cause for low fermentation rate of leachate and how best to overcome the limiting factor(s) by using Fenton oxidation as a pre-treatment.

5.2 Materials and Methods

5.2.1 Landfill leachate

I collected leachate from the Northwest Regional Landfill (Surprise, AZ) in August 2015 and kept it refrigerated at 4°C prior to use. The leachate samples were classified as medium-age leachates based on their 5-day biochemical oxygen demand (BOD_5)/chemical oxygen demand (COD) ratio (= 0.31±0.03) (Mahmoud et al., 2014; Renou et al., 2008). The concentrations of COD, BOD_5, and Total organic carbon (TOC) of leachate samples had average values of 2730±279 mg/L, 800±17 mg/L, and 663±15 mg/L, respectively. In addition, they had a good buffering strength (pH = 8.0±0.3 and total alkalinity as $CaCO_3$ = 4068±464 mg/L). Throughout this study, the leachate samples were used as is for all experiments without addition of nutrients/trace metals, or dilution.

5.2.2 Fenton experiment

I carried out batch Fenton oxidation experiments using 100 mL or 250 mL glass vessels at a constant mixing speed of 150 rpm using a magnetic stir bar at ambient temperature (25±2 °C) as described in Mahmoud et al. (2016). I evaluated the effect of the following operational parameters for the Fenton process: (1) pH (i.e., from 2.5 to 7.0), (2) molar ratios of H_2O_2 to Fe^{2+} (i.e., from 1 to 10; *w:w*), and (3) ratios of H_2O_2 to COD (i.e., from 0.5 to 2.8; *w:w*). All experiments were repeated 4 times.

5.2.3 Anaerobic fermentation experiments

I carried out batch anaerobic fermentation assays using serum bottles with a working volume of 200 mL and a total volume of ~255 mL. I used anaerobic digester sludge from the Mesa Northwest Water Reclamation Plant (Mesa, AZ) as the inoculum.

Prior to start-up the experiment, I conducted 2 consecutive transfers (i.e., ~3 months) for adaptation of inoculum with raw leachate as the sole carbon and energy source. In order to remove all residual organics, I centrifuged the sludge twice at 4000 rpm for 20 min and re-suspended it in basal medium with no substrate, which I used later to inoculate my fermentation reactors. I inhibited methanogenesis by adding 50 mM 2-BES. Once the inoculum (final concentration of ~5 g VSS/L) and leachate (with 50 mM BES) were supplied to the fermentation reactors, I capped them with rubber serum stoppers and aluminum caps, purge them with N_2/CO_2 (80%:20%) gas for 30 min to remove O_2, place them in a shaker (~140 rpm, Thermo Scientific), and followed the batch biochemical methane potential (BMP) protocol in duplicate as outlined in Parameswaran and Rittmann (2012). The temperature was kept constant at 30°C in a temperature-controlled room.

5.2.4 Chemical analyses

I measured, in duplicate, COD, ammonium-nitrogen (NH_4^+), and total alkalinity using HACH kits (HACH, Ames, IA). BOD_5 was measured according to *Standard Methods* (APHA, 1998). I measured total organic carbon (TOC) using a TOC analyzer (TOC-VCSH, Shimadzu Scientific Instruments, Columbia, MD) equipped with combustion catalytic oxidation/non-dispersive infrared (NDIR) gas analyzer. I analyzed the fermentation-product organic acids using high-performance liquid chromatography (HPLC; Model LC-20AT, Shimadzu, Columbia, MD) equipped with an Aminex HPX-87H (Bio-Rad Laboratories, Hercules, CA) column after filtration through a 0.22-μm membrane filter according the method described in Mahmoud et al. (2014). Briefly, I used 2.5 mM sulfuric acid as an eluent fed at a flow rate of 0.6 mL/min, total elution time was 50 min, and the oven temperature was constant at 50°C. I developed a

calibration curve for every set of analyses, performed duplicate assays, and report the average concentrations.

I measured the volume of gas produced from the fermentation reactors with a friction-free glass syringe of 10 or 50 mL volume (Popper & Sons, Inc., New Hyde Park, NY, USA). Then, I quantified the gas composition using a gas chromatograph (GC 2010, Shimadzu Corporation, Columbia, MD) equipped with a thermal conductivity detector and a packed column (Carboxen™ 1010 PLOT Capillary Column, Supleco, Inc.). Helium was used as the carrier gas at constant flow rate and pressure of 10 mL/ min and 42.3 kPa, respectively. Temperature conditions for column, injection, and detector will be 80, 150, and 220 °C, respectively. I employed analytical grade H_2, CH_4, and CO_2 gases for standard curves, carried out gas analyses in duplicate, and average the two values.

I analyzed carbohydrate and protein by the phenol–sulfuric acid colorimetric method (DuBois et al., 1956) and the bicinchoninic acid method using the BCA protein-assay kit (Sigma–Aldrich, St. Louis, MO), respectively. For both tests, standard calibration curves were developed with glucose and bovine serum albumin, and the absorbance was measured at wavelengths of 485 and 562 nm, respectively, using UV-Vis spectrophotometer (Varian Cary 50 Bio, Varian Inc., Walnut Creek, CA).

5.2.5 Mass balance and calculations

I established mass balances, based on COD measurements, by estimating the COD equivalents of experimentally measured carbohydrate and protein using stoichiometric conversion factors of 1.067 and 1.56 mg COD/mg organic type, respectively, based on typical formulae for carbohydrate (CH_2O) and protein ($C_{16}H_{24}O_5N_4$) (Mahmoud et al., 2014). The COD conversion units for organic acids were adapted from Rittmann and McCarty (2001) as follows: 16 mg COD per mM formate, 64

mg COD per mM acetate, 112 mg COD per mg propionate, and 112 mg COD per mg succinate.

5.2.6 Statistical analysis

I performed the Spearman's rank-order correlation analysis using the IBM SPSS Statistics for Windows, Version 24.0 (Armonk, NY: IBM Corp). P-values < 0.01 were considered statistically significant.

5.3 Results and Discussion

5.3.1 Fenton oxidation of landfill leachate

Since my target is to carry out partial oxidation of organic matter and to improve the biodegradability of leachate for downstream electron recovery, I first evaluated how different operational parameters influencing the Fenton process by varying the following parameters: pH, H_2O_2 to Fe^{2+} molar ratio, and ratios of H_2O_2 to COD (*w:w*). Figure 5.1A shows the effect of pH on the efficiency of Fenton oxidation when the pH changed between 2.5 and 7.0 at a constant molar H_2O_2:Fe^{2+} ratio of 5.0. I saw the highest COD removal (~61%) at pH 3.0 and 3.5 (Figure 5.1A). Increases or decreases in pH led to lower COD removal efficiencies. My results are consistent with previous studies showing that pH 3.0–3.5 are the optimum pH values for Fenton oxidation (Deng and Englehardt, 2006; Pignatello et al., 2006; Zhang et al., 2005; Gogate and Pandit, 2004). I used pH 3.5 as initial pH for Fenton oxidation process in this study.

Figure 5.1B shows the effect of the change in H_2O_2:Fe^{2+} molar ratio (R) on COD removal from the landfill leachate sample under study. COD removal plateaued at 55–60% at a molar H_2O_2:Fe^{2+} ratio ranging between 1.0 and 4.0 and remained relatively constant with further increase of the molar ratios. This trend has been observed before by others (see Table 5.1), probably due to that the reaction order is second order at relatively low H_2O_2:Fe^{2+} molar ratios, but approaches zero order at high molar ratios (Hermosillo et al., 2009).

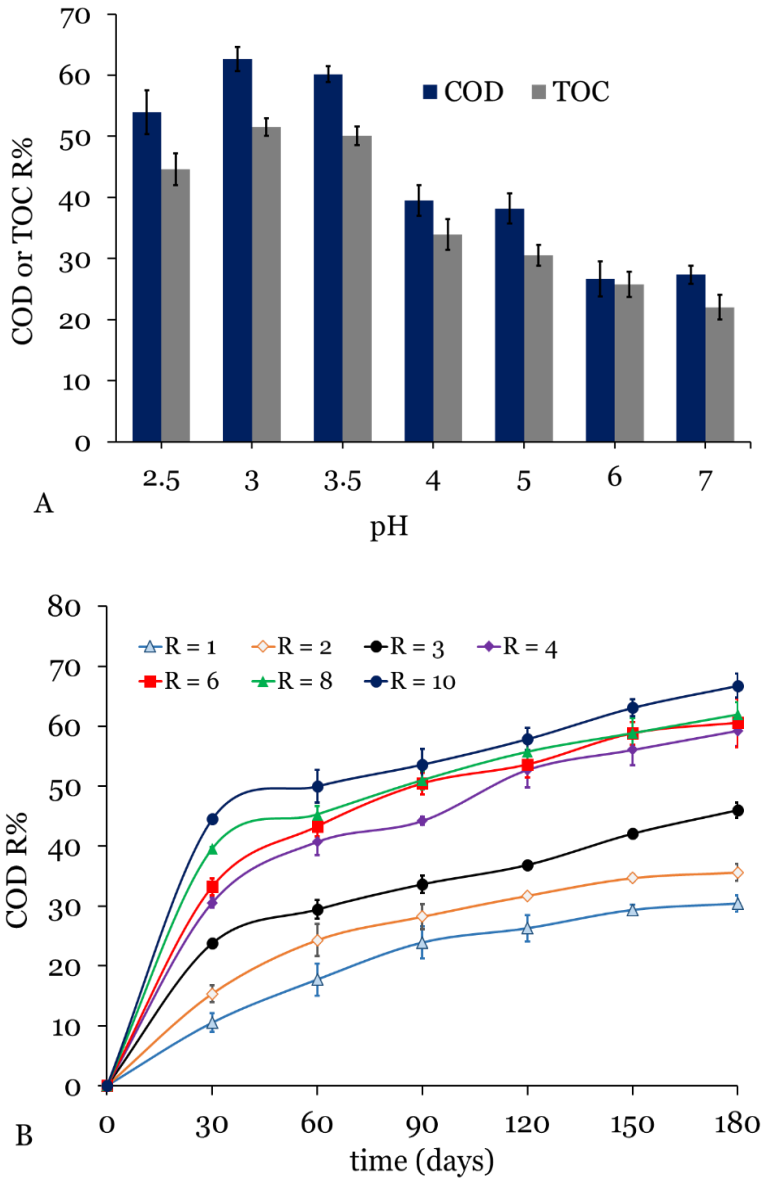

Figure 5.1 The efficiency of Fenton oxidation of landfill leachate. (A) Effect of pH value on COD and TOC removal. Values are average ± std. deviation (n = 6). (B) Effect of molar ratio (R) of H_2O_2:Fe^{2+} on COD removal. Values are average ± std. deviation (n = 4).

Table 5.1 Summary of Fenton oxidation process for treatment of landfill leachate from literature.

COD [a]	COD/BOD ratio	pH	H_2O_2 [a]	Fe^{2+} [a]	Molar H_2O_2:Fe^{2+}	COD removal (%)	References
1800	0.125	3.0	1500	2000	1.23	52	Kim et al. (2001)
2000	0.044	3.5	1500	120	20.5	69	Kim and Huh (1997)
3000	N/A [b]	2.5	2550	2792	1.32	37.5	Zhang et al. (2005)
1500	0.02	3.5	1650	645	4.20	75	Kang and Hwang (2000)
1100–1300	< 0.05	3.0	8160	3351	4.00	61	Deng (2007)

[a] unit is mg/L; [b] N/A: not available.

I also evaluated the change in oxidation degree and the efficiency of the oxidative process of leachate by calculating the carbon oxidation state (COS) according to equation 5.1:

$$COS = 4 - \left(1.5\, x\, \frac{COD}{TOC_0}\right) \qquad \text{(Eq. 5.1)}$$

where TOC_0 is the initial total organic carbon and COD is total chemical oxygen demand at time *t*.

Figure 5.2 shows the change in COS values as a function of H_2O_2:Fe^{2+} molar ratios. The COS values are consistently increased from its initial value of ~ –1.8 into values that ranged between – 0.2 to + 1.8, indicating a strong net oxidation of the leachate's organic matter to more oxidized organic products.

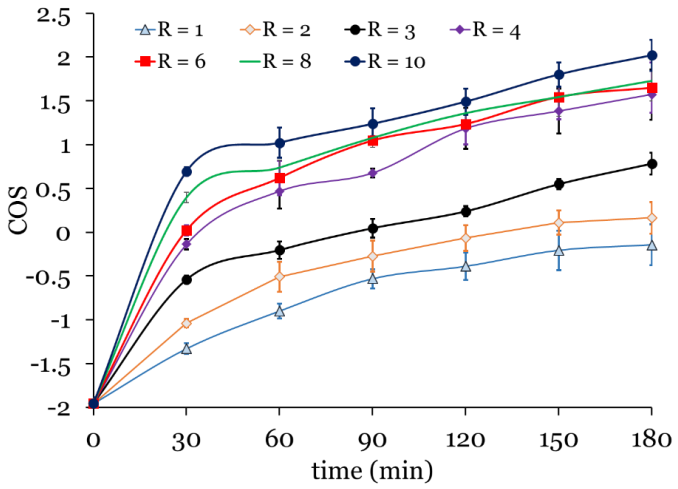

Figure 5.2 Change in COS as a function of H_2O_2:Fe^{2+} molar ratios. Values are average ± std. deviation (n = 4).

Second, I chose to test the effect of relatively low H_2O_2:COD ratios (0.5 to 2.8; *w:w*) on the oxidation process efficiency. I observed only a slight enhancement in the oxidation efficiency by increasing the H_2O_2:COD ratio in this range (Figure 5.3A), implying that an even smaller ratio may be workable and even preferable.

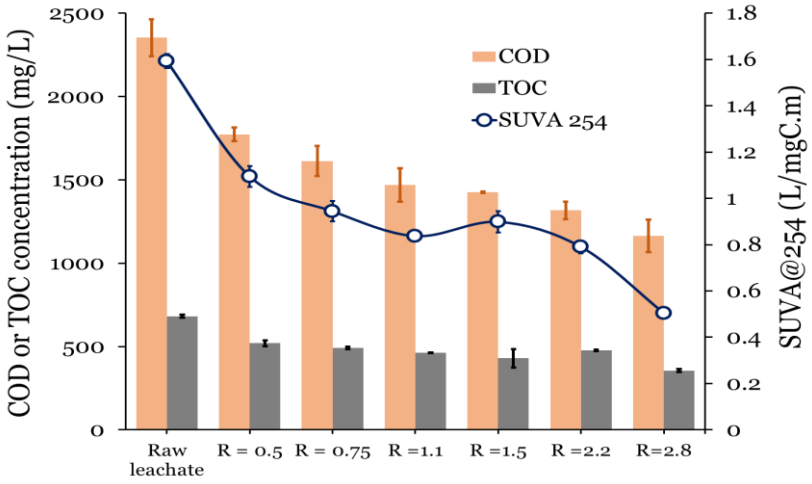

Figure 5.3 Effect of ratio of H_2O_2:initial COD ratio (R) on COD removal, TOC removal, specific ultraviolet absorption (SUVA) at 254 nm. Experimental conditions: pH = 3.5, initial average COD = 2353±111 mg/L, temperature = 25 °C, and reaction time = 3 h.

Based on the results presented in the previous sections and in order to change the composition of organic matter of the leachate, I performed 2 sets of Fenton oxidation experiments with leachate at two different molar ratio of H_2O_2 and Fe^{2+}: case I ($[H_2O_2]:[Fe^{2+}] = 4$) and case II ($[H_2O_2]:[Fe^{2+}] = 15$) (Figure 5.4).

For the lower ratio, which had Fe^{2+} = 28.5 mM, I observed consumption of H_2O_2 within the first 90 min, and concomitantly the COD was reduced from 2620 to 1400 mg/L, where it remained until the end of experiment with a residual concentration of H_2O_2 of ~5 mM. Fe^{2+} was fully oxidized as early as 90 min for the lower molar ratio (i.e., 4:1).

In contrast, the higher ratio (with Fe^{2+} = 7.6 mM) had a significant H_2O_2 residual (~18 mM) up to 180 min, and the simultaneous reduction in COD was 37% (i.e., from 2620 to 1651 mg/L). Fe^{2+} drastically diminished during the first 90 minutes for the higher molar ratio and remained constant at a detectable level (~0.45 mM).

TOC removal with the higher Fe^{2+} concentration (case I; TOC removal was 46%, from 669 to 359 mg/L) was ~1.5-fold higher than case (II) (Figure 5.4B); however, TOC removal reached a plateau after 1 hour of treatment. This trend has been observed before by others (Sarria et al., 2002), where the chemical nature of the organic by-products produced did not change significantly over the long term.

These results show that the kinetics of Fenton oxidation followed 2 major steps. Initially, Fe^{2+} ions reacted with H_2O_2 (reaction 1 below) yielding $OH^{\cdot}$ that had the ability to reduce the COD concentration. In parallel, the produced Fe^{3+} ions reacted with the residual H_2O_2 to produce $HO_2^{\cdot}$ and regenerate Fe^{2+} (reaction 2), but with a much slower reaction rate unless the H_2O_2 concentration is high (Deng and Englehardt, 2006). The degree of oxidation of the recalcitrant organics depended on having Fe^{2+} to produce $OH^{\cdot}$.

With a high Fe^{2+} concentration (case I), COD removal was faster, compared to case II, in which the low Fe^{2+} concentration was low due to reaction 2.

Reaction 1: $Fe^{2+} + H_2O_2 \rightarrow Fe^{3+} + OH^- + OH^{\cdot}$

Reaction 2: $Fe^{3+} + H_2O_2 \rightarrow Fe^{2+} + HO_2^{\cdot} + H^+$

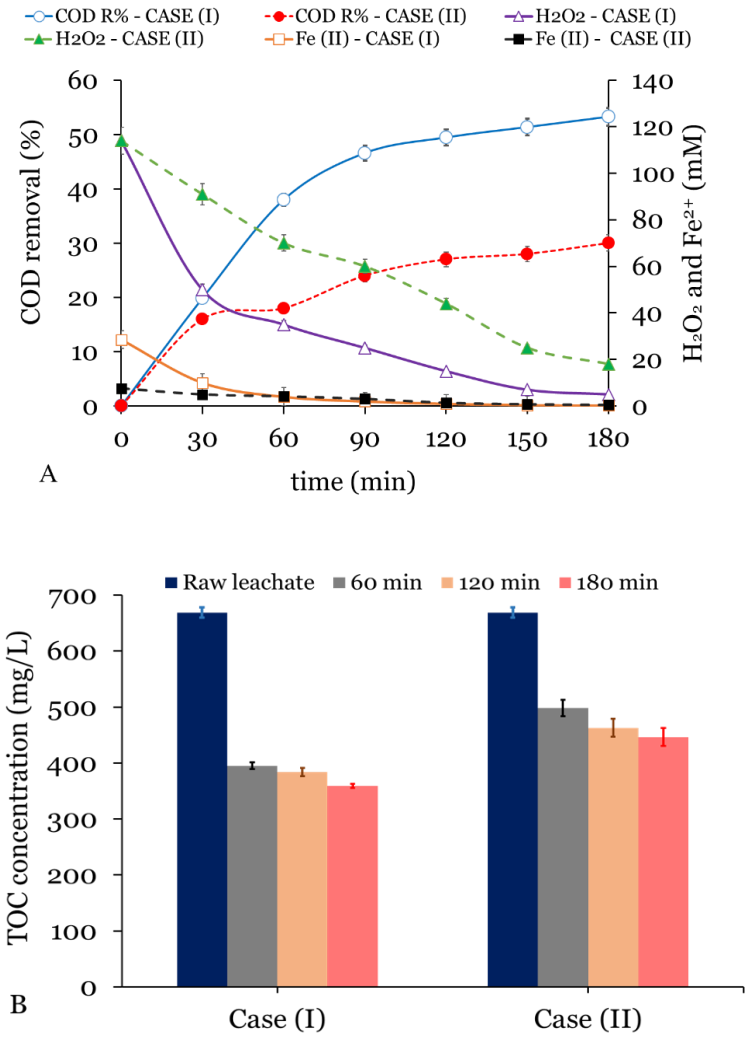

Figure 5.4 Effect of Fe^{2+} dosage on the efficiency of Fenton oxidation of leachate. (A) COD removal and change in $[H_2O_2]$ as a function of time in the treatment of landfill leachate by conventional Fenton. (B) TOC concentration corresponding to Figure 5.4A.

Due to change in the initial Fe^{2+} concentration and molar H_2O_2 and Fe^{2+} ratio, the BOD_5/COD ratio and carbohydrate-to-protein ratio (C/P) ratio were highly altered (i.e., 0.61±0.1 and 1.44±0.3 for case (I) effluent, and 0.55±0.08 and 1.09±0.06 for case (II) effluent, respectively) compared to raw leachate (0.31±0.03 and 0.57±0.1, respectively). These results confirm that Fenton oxidation significantly changed the leachate's organic make up by oxidizing recalcitrant organics into more-biodegradable products. Since organics removal reached a plateau after 1 hour, I performed 1 h treatment at different molar H_2O_2 and Fe^{2+} ratios (i.e., 4 (case I) and 15 (case II), which were used later as influent for fermentation reactors.

5.3.2 Batch fermentation of leachate

Figures 5.5 report the fermentation results of leachate samples. The fermentation efficiency, defined as ratio of organic acids produced from fermentation to initial COD, was significantly changed in response to change in biodegrability ratio (based on BOD_5/COD ratio) and C/P ratio of leachate samples. The lowest fermentation was observed with raw leachate (18.4±0.3%), which had the lowest BOD_5/COD ratio (0.31±0.03). The concentration of organic acids increased from its initial value of 56±8 mg VFA–COD/L to 480±7 mg VFA–COD/L at the end of fermentation assays. Formate became the most abundant fermentation products with a final concentration of 235±15 mg VFA–COD/L, which represents ~49±4% of total organic acids. Acetate increased to be the second largest (~217±23 mg VFA–COD/L), whereas succinate had much lower concentration (~29±1 mg VFA–COD/L) (Figure 5.6A). I detected no H_2 or CH_4 in the headspace gas. The trend is different than my previous findings (Mahmoud et al., 2014), showing that succinate was the most abundant product in the leachate fermentation.

This discrepancy was likely caused by the use of pre-acclimated inoculum to leachate that had the ability to ferment the organic matter in leachate to acetate and formate.

Compared to the raw leachate, case (II) experiment exhibited much higher fermentation efficiency, most probably due to the higher BOD_5/COD ratio, the higher C/P ratio, or both. The fermentation efficiency was ~65±2%, with acetate being the largest fermentation product (1030±42 mg VFA–COD/L), followed by propionate (292±3 mg VFA–COD/L), formate (39±5 mg VFA–COD/L), and succinate (27±1 mg VFA–COD/L) (Figure 5.6B). Similar to raw leachate fermentation, I did not detect any H_2 in the headspace gas.

A further increase in the biodegrability ratio yielded a slight improvement of fermentation, which achieved its largest efficiency (76±0.5%). During the first 10 days, the fermentation rate was much higher compared to case (II) experiment, in which acetate and propionate accumulated to ~88% of total organic acids. Later, acetate and propionate dominated the fermentation products and stabilized at ~1069±5 mg VFA–COD/L and 282±11 mg VFA–COD/L, respectively, with a very low level of formate (44±7 mg VFA–COD/L) and (25±1 mg VFA–COD/L) (Figure 5.6C). These results suggest that the lowest molar ratio of $[H_2O_2]$:$[Fe^{2+}]$ (i.e., = 4 or Fe^{2+} = 28.5 mM) accelerated the fermentation kinetics compared to a $[H_2O_2]$:$[Fe^{2+}]$ molar ratio of 15, although the accumulated organic acids at the end of fermentation assays reached comparable levels.

For all fermentation assays and as a result of the accumulation of organic-acids accumulation, the pH decreased from its initial value (i.e., 8.1) to comparable pH range (i.e., 6.85–7.10), owing to the high buffering strength of leachate.

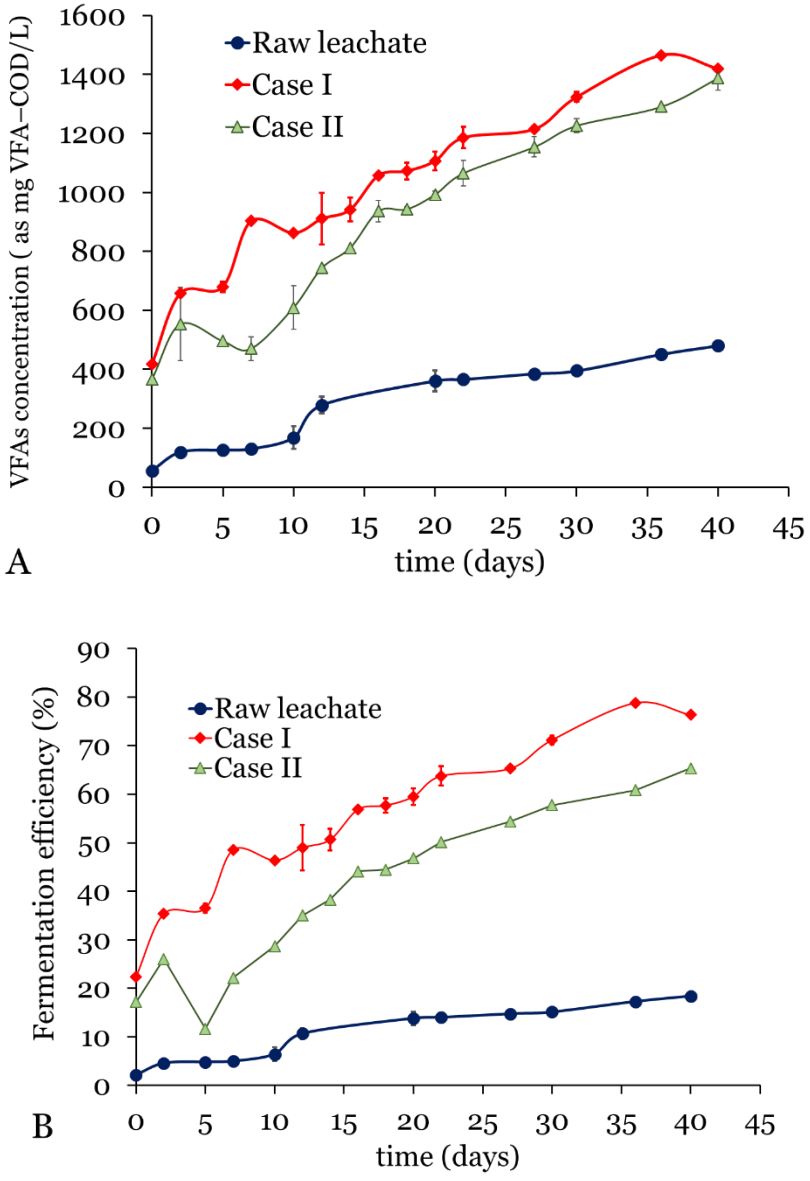

Figure 5.5 The results of batch anaerobic fermentation of landfill leachate. (A) Detected organic acids (as COD). (B) The fermentation efficiency (based on the ratio of organic acids (as COD) to influent total COD).

Figure 5.6 shows the effect of C/P ratio on the fermentation efficiency and organic acids distribution. The ratio had a minimal effect on overall fermentation efficiency for pre-treated leachate samples; however, it strongly altered the distribution of organic acids. At a high C/P content, acetate and propionate were the most abundant species of fermentation products, whereas formate and acetate dominated at high protein content, which is consistent with literature data (Alibardi and Cossu, 2016). Regardless the fermentation efficiency, the final of carbohydrate and protein concentrations were reduced by 63±10% and 31±6%, 66±7% and 38±8%, and 65±10% and 16±3% for raw leachate, case I experiment, and case II experiment, respectively.

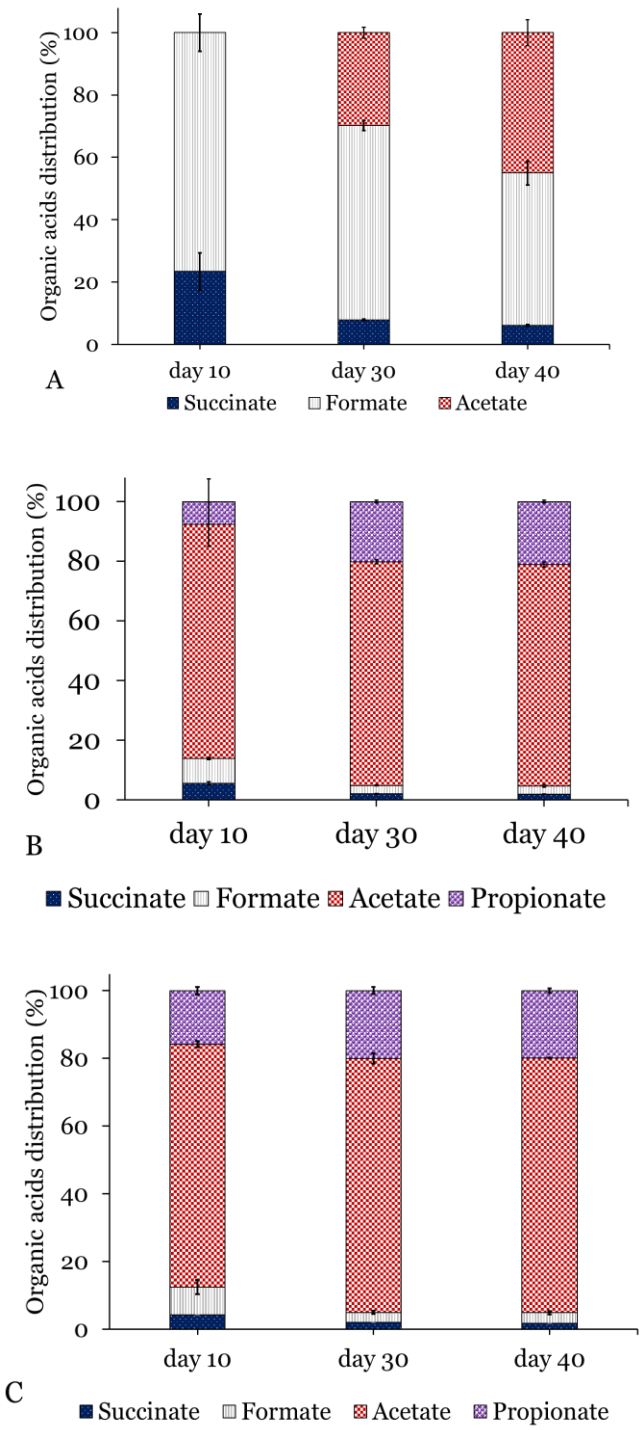

Figure 5.6 The effect of carbohydrate-to-protein ratio on the fermentation efficiency and organic acids distribution. (A) Raw leachate (carbohydrate-to-protein = 0.6 mg carbohydrate–COD/mg protein–COD). (B) Case II (carbohydrate-to-protein = 1.08 carbohydrate–COD/mg protein–COD). (C) Case I (carbohydrate-to-protein = 1.44 carbohydrate–COD/mg protein–COD).

Table 5.2 reports the Spearman rank order correlation coefficients between organic acids, BOD_5/COD ratio, and carbohydrate-to-protein ratio in raw leachate and treated-leachate samples. The BOD_5/COD and carbohydrate-to-protein ratios together influenced the leachate fermentation and distribution of organic acids. For example, BOD_5/COD and carbohydrate-to-protein ratios had strong negative correlations with succinate and formate, whereas they were directly correlated to propionate.

Table 5.2 Spearman's correlation coefficients between organic acids, BOD_5/COD ratio, and carbohydrate-to-protein ratio in raw and treated leachate samples (p-value < 0.01).

		C/P ratio	Succinate	Formate	Acetate	Propionate	BOD_5/COD ratio
C/P ratio	Correlation Coefficient	1 **	-1 **	-1 **	0.500	1 **	1 **
	Sig. (2-tailed)	–	–	–	0.667	–	–
Succinate	Correlation Coefficient	-1 **	1 **	1 **	-0.500	-1 **	-1 **
	Sig. (2-tailed)	–	–	–	0.667	–	–
Formate	Correlation Coefficient	-1 **	1 **	1 **	-0.500	-1 **	-1 **
	Sig. (2-tailed)	–	–	–	0.667	–	–
Acetate	Correlation Coefficient	0.500	-0.500	-0.500	1 **	0.500	0.500
	Sig. (2-tailed)	0.667	0.667	0.667	–	0.667	0.667
Propionate	Correlation Coefficient	1 **	-1 **	-1 **	0.500	1 **	1 **
	Sig. (2-tailed)	–	–	–	0.667	–	–
BOD_5/COD ratio	Correlation Coefficient	1 **	-1 **	-1 **	0.500	1 **	1 **
	Sig. (2-tailed)	–	–	–	0.667	–	–

** Correlation is significant at the 0.01 level (2-tailed).

5.3.3 COD mass balance during batch fermentation of leachate

Figure 5.7 presents the COD mass balance at the end of batch fermentation based on experimentally measured electron sinks. During the fermentation assays, I observed high COD conservation, with only 5–7% of initial COD being unaccounted by

carbohydrate, protein, organic acids, and other soluble COD. The missing COD probably was present in biomass. I did not detect any CH_4 and H_2, and sulfate reduction was negligible. The lack of H_2 occurred because it was channeled quickly into acetate through homoacetogenesis (Schuchmann and Müller, 2014). The lack of CH_4 is mainly due to the use of BES to inhibit the methanogens. Sulfate reduction was negligible because the sulfate concentrations in leachate samples were quite low (< 40 mg/L).

At the end of fermentations, organic acids represented the largest electron sink for case I (76%) and case II (65%); thus, fermentation for cases I and II led to a predominance of the most desired end products and about 4-fold more than with fermentation of raw leachate.

The fractions of electrons ending up as carbohydrate and protein were 8.9% and 11.4% for case I and 8.1% and 17.9% for case II. The carbohydrate values were well below those with raw leachate, but the protein values were about the same. These results are consistent with previous studies (Alibardi and Cossu, 2016; Lai et al., 2016; Mahmoud et al., 2014) in that carbohydrate had a faster fermentation rate than protein.

Approximately ~3% of the initial COD was unidentified other COD for cases I and II, but this was much lower of the other COD obtained with fermentation of the raw leachate. These unidentified components might be soluble microbial products (SMPs), lipids, nucleic acids, and other fermentation products not measured by HPLC (Mahmoud et al., 2014; Rittmann and McCarty, 2001; Argelier et al., 1998).

Overall, the electron balance reinforces the positive benefit of Fenton oxidation of recalcitrant organic matter in leachate for greatly increasing the fermentation efficiency.

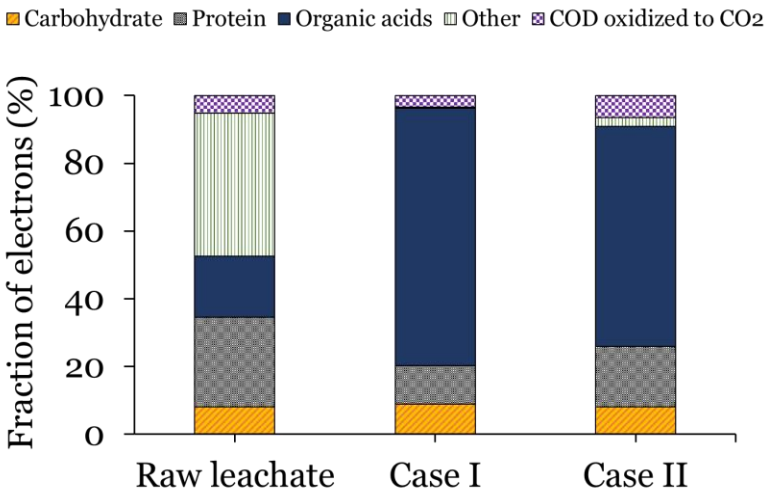

Figure 5.7 Total COD mass balance at the end of batch fermentation assays. 100% represents the COD of the starting leachate.

5.4 Conclusion

Although landfill leachate represents an excellent candidate for renewable-energy generation via different environmental biotechnologies, such as microbial electrochemical cells and anaerobic digesters, it often yields very low energy recovery. This is attributed mainly to low BOD_5/COD ratio and the complexity of its biodegradable organic matter. Here, using different Fenton oxidation conditions to alter the makeup of the leachate, I evaluated the fermentation efficiency of leachate samples with different BOD_5/COD and carbohydrate/protein ratios obtained by different types of Fenton treatment.

Fenton oxidation partially oxidized recalcitrant organic matter to more biodegradable organic products, leading to 1.8- to 2-fold increase in the BOD_5/COD ratio (i.e., 0.55—0.61 for treated leachate compared to 0.31 for raw leachate) and 1.9- to 2.5-fold increase in C/P ratio (i.e., 1.44–1.09 for treated leachate compared to 0.57 for raw leachate). These increases in BOD_5/COD and C/P ratios correlated to a significant increase in fermentation efficiency for Fenton pre-treated leachate: fermentation efficiency of 65–76% and organic acids concentrations of 1387–1419 mg VFA–COD/L, compared to 18.4% and 480 mg VFA–COD/L for raw leachate.

Although the two different Fenton treatments did not have a large impact of the overall fermentation efficiency or the total residual organic acids concentrations at the end of fermentations, the fermentation rates for treated leachate were faster during the first 10 days. Furthermore, the two Fenton pre-treatments led to different distributions of organic acids other than acetate. Spearman rank-order correlation revealed that the BOD_5/COD and carbohydrate/protein ratios together affected the fermentation rate and organic acids distribution. For example, producing less propionate and more formate can be achieved by increasing protein content and decreasing the BOD_5/COD ratio.

CHAPTER 6

ELECTROCHEMICAL TECHNIQUES REVEAL THAT TOTAL AMMONIUM STRESS INCREASES ELECTRON FLOW TO ANODE RESPIRATION IN MIXED-SPECIES BACTERIAL ANODE BIOFILMS [4]

6.1 Introduction

The microbial electrochemical cell (MXC) is a nascent technology that converts renewable energy contained in an organic waste stream into useful forms, such as electric current, hydrogen gas (H_2), hydrogen peroxide, caustic soda, and organic chemicals (Logan and Rabaey, 2012; Rittmann, 2008). The foundation of MXCs is the unique ability of anode-respiring bacteria (ARB) to oxidize organic matter and then transport the electrons beyond their outer membranes to a solid anode (Torres et al., 2010; Lovley, 2008; Lovley, 2006).

The true yield of ARB biomass depends on the potential difference between the electron donor, such as acetate, and the anode surface, which is the ARB's electron acceptor, since this difference translates into the energy available for bacterial growth (Torres et al., 2010). Compared to aerobic heterotrophs, ARB are known to be slow growers, since the anode potential often is only a few tenths of a volt higher than the potential of acetate (Bird et al., 2011; Torres et al., 2009; Mahadevan et al., 2006; Esteve-Nuñez et al., 2005). While this situation is beneficial for generating the output, it means that the ARB have to have a high ratio of electrons used for respiration (f_e) compared to electrons used for biomass synthesis (f_s) in order to gain enough energy to grow and maintain themselves (Torres et al., 2010; Rittmann and McCarty, 2001). For example, oxidation of one mole of acetate yields enough free energy to generate 3 moles of adenosine triphosphate (ATP) when the potential difference between the electron

[4] This Chapter has been submitted in an altered format for publication.

donor and acceptor is ~0.25 V, given that $\Delta G^{o'}$ for ATP synthesis is −60 kJ/mol (Rittmann and McCarty, 2001; Lehninger et al., 1993). If the ARB can harvest only about 0.1 V, then they can generate only around 1 mole of ATP per mole of acetate oxidized. Experimental evidence supports that *Geobacteraceae* – well-known ARB that found often in MXCs producing high current densities (*j*), which is crucial for scaling-up – have a low biomass true yield (i.e., 0.05 – 0.14 g volatile suspended solids (VSS) per g chemical oxygen demand (COD)) that is consistent with capturing only ~1 mole of ATP per mole of acetate oxidized (Marsili et al., 2010; Lee et al., 2009; Mahadevan et al., 2006; Esteve-Nuñez et al., 2005).

Additional evidence for low energy capture is provided by Rimboud et al. (2015) and Yoho et al. (2014), who documented that the midpoint potentials of the electron-transfer pathways of *Geobacter* species ranged from −0.22 to −0.05 V vs. standard hydrogen electrode (SHE). These midpoint potentials provide at most 0.24 V of harvested energy (compared to the potential of acetate, −0.29 V vs. SHE), and some were far less.

Certain environmental conditions create stresses for microorganisms. Many microbes can cope with modest stress by various acclimation mechanisms, but extreme stress can lead to a serious inhibition and even cessation of metabolic activity (Schimel et al., 2007). A high concentration of ammonium−nitrogen (NH_4^+) is a well-known stressor for many types of microorganisms (Li et al., 2016; Werner et al., 2014; Zhang et al., 2014; Kato et al., 2014; Lü et al., 2013; Baolan et al., 2012). Inhibition due to high NH_4^+ concentration can be caused by one or a combination of the following factors (Rajagopal et al., 2013; Yenigün and Demirel, 2013): (1) An increase in the maintenance-energy requirement, such as an increase in the energy cost required to manage the ammonia transport through the cytoplasm membrane, to repair other

damage, or to compensate for uncoupling. The fact that anaerobes, including methanogens and ARB, exist on a small energy budget makes them especially sensitive to an increased maintenance load (Müller et al., 2006). (2) A change in intracellular pH, which induces an efflux of cytoplasmic potassium ions (K^+) through an ammonium/K^+ exchange reaction. Cytoplasmic K^+ loss could lead to bacterial death or to increased endogenous respiration (Sprott and Patel, 1986). (3) Inhibition of specific catabolic reactions, which is usually indicated by low maximum-specific-substrate-utilization-rate (q_{max}) and high half-maximum-rate concentration (K_s) due to catabolic deactivation (Rittmann and McCarty, 2001; Kovárová-Kovar and Egli, 1998). When ammonium stress is associated with diverting electrons away from biomass synthesis (f_s) towards more respiration (f_e), it leads to a low biomass yield; this trend is consistent with stress responses 1 and 2.

The literature does not yield a consensus about the threshold stress or inhibition level of total ammonia nitrogen (TAN) – which is the sum of free ammonia nitrogen (FAN; NH_3) and ionic NH_4^+ – for ARB. Clauwaert et al. (2008) reported that a TAN concentration up to 5 g TAN/L did not affect the acetate consumption rate by ARB in a microbial fuel cell (MFC), since the Coulombic efficiency (CE) and current density (j) were not altered. In contrast, Nam et al. (2010b) showed a serious inhibition of ARB, measured as j and power density, at TAN concentrations over 500 mg TAN/L. This discrepancy likely was caused by factors that hampered having an accurate evaluation of TAN (or FAN) influence on ARB metabolism. The first factor was the lack of a controlled anode potential, which might have fostered a highly diverse microbial community not dominated by *Geobacteraceae* (Kiely et al., 2011; Torres et al., 2009). Second, the penetration of oxygen into the anode chamber could have led to a loss of TAN through nitrification that relieved TAN inhibition, as evidenced by low CE and by nitrate

accumulation (Tice and Kim, 2014; Nam et al., 2010b). Third, the use of a Nafion or cation-exchange membrane (CEM) could have led to loss of TAN from the anode due to NH_4^+ ion transport across the separator (Kuntke et al., 2012).

I designed experimental conditions to eliminate all the factors that can confound experiments to evaluate the effect of TAN and FAN on ARB. First, I minimized TAN losses and eliminated impacts of the cathode reaction by controlling the anode potential with a potentiostat; by using a half-cell microbial electrolysis cell (MEC), which has no oxygen in the cathode chamber; and by using an anion-exchange membranes (AEM), which prevent transport of NH_4^+ to the cathode. I also used continuous flow to the anode to minimize the effect of any minor TAN-loss mechanism, such as biomass synthesis. Second, I inoculated the MECs with biofilm from an MEC producing high current density; this enabled a fast start-up and a biofilm dominated with *Geobacteraceae*. Third, I used acetate as the sole electron-donor substrate and a 100-mM phosphate medium to minimize pH changes that might affect TAN speciation. By combining these factors, I had a highly enriched *Geobacteraceae* biofilm and stable and controlled concentrations of TAN and FAN. This setup allowed us to reliably measure inhibitory effects of TAN and FAN on *Geobacteraceae*.

6.2 Materials and Methods

6.2.1 MEC design and operation

For my fundamental experiments, I used MECs with an anode potential controlled by a potentiostat. This system allowed me to focus only on the anode reactions, excluding any interference from potential losses at cathode or potential losses due to large diffusion distance between anode and cathode (Mahmoud et al., 2014; Torres et al., 2009; Lee et al., 2009). The MECs held ~320 mL in each chamber. The anode was a graphite square having a surface area of ~12 cm^2. The cathode was a 0.8-cm OD graphite rod, and the pH of the cathode chamber was maintained at 12 by addition of 10 N NaOH. The anode chamber was separated from the cathode chamber by an AEM (AMI 7001, Membranes International, Glen Rock, NJ), which prevented transporting of NH_4^+ from the anode to the cathode, and I verified this by measuring the TAN concentration in the anode chamber. An Ag/AgCl reference electrode (BASI Electrochemistry, West Lafayette, IN) was located about 0.5 cm away from the anode, and the anode potential was controlled at – 0.3 V vs. Ag/AgCl, which equals –0.03 V vs. SHE (Torres et al., 2009), using a VMP3 digital potentiostat (Bio-Logic USA, Knoxville, TN). I mixed the liquid in the anode and cathode chambers using a magnetic stirrer and stir bar rotating at 220 rpm. Replicate experiments were performed with two independent MECs, operated in parallel, at a fixed temperature of 30°C. Since I used the same MEC configuration, anode material, and anode surface area, direct comparisons can be used to gauge the effect of TAN or FAN on MEC performance.

I inoculated the MEC anode with effluent (150 mL) from a continuous-flow MEC that had been operated for three months with acetate medium and had attained a current density of ~6.5 A/m^2. After sparging the MEC with N_2 gas (99.9%) for ~45 min, I fed the MEC with autoclaved (for 90 min at 121°C) acetate medium containing: 15 mM

acetate, 0.2 g TAN/L (NH_4Cl), 100 mM phosphate buffer (KH_2PO_4/Na_2HPO_4; pH = 7.35±0.1), and trace minerals (Parameswaran et al., 2009).

I operated the anode in batch mode for a few days until the current density was 6–7 A/m^2. I then continuously fed the anode chamber for ~80 days with acetate medium at a flow rate of 0.3 mL/min (~18-h HRT) using a peristaltic pump (Masterflex L/S®, Cole-Parmer, USA). Over the 80 days, I evaluated ARB inhibition for a series of TAN concentrations ranging from 0.2 to 4.4 g TAN/L (corresponding to FAN of ~2–78 mg FAN/L) in the continuous-flow MEC at a fixed pH of 7.35±0.1 and influent acetate concentration of 15 mM.

Later, I studied the effect of pH and FAN concentration on ARB in a continuous-flow MEC at a flow rate of 2 mL/min (~3-h HRT) with a non-inhibiting TAN condition (i.e., 2.2 g TAN/L) by varying the initial pH value in the range of 7.0 to 8.1. I used a shorter HRT in this experiment to minimize proton accumulation and pH depression in the anode chamber.

6.2.2 Chemical analyses

I measured the acetate concentration, after filtration through a 0.22-µm membrane filter (PVDF GD/X, Whatman, GE Healthcare, Ann Arbor, MI), using high-performance liquid chromatography (HPLC; Model LC-20AT, Shimadzu, Columbia, MD) with an Aminex HPX-87H column (Bio-Rad Laboratories, Hercules, CA), according to the procedure described in Mahmoud et al. (2014).

I measured TAN, in duplicate, using HACH kits (HACH, Ames, IA) after filtration through a 0.22-μm membrane filter. I estimated FAN from TAN and the pH (Hansen et al., 1998):

$$FAN = \frac{TAN}{1 + 10^{-pH+0.09+(2730/T)}} \quad \text{(Eq. 6.1)}$$

6.2.3 Electrochemical analyses

I performed low-scan-rate cyclic voltammetry (CV) on the anode at a scan rate of 1 mV/s between –0.43 to 0.17 V vs SHE, normalizing the current to the anode surface area. I performed CV experiments in duplicate; because the two CV curves were similar, I present only one curve. To eliminate any effect of conductivity due to increase the added amount of ammonium chloride, which I used as the sole N-source in our study, I corrected the CVs for Ohmic loss (iR drop) between the working and Ag/AgCl electrodes using electrochemical impedance spectroscopy (EIS) immediately after performing the CV (Yoho et al., 2014). Unless noted, all potentials are reported versus SHE. I computed CE by dividing cumulative electron equivalents collected at the anode by the electron equivalents of acetate consumed by the ARB (measured with the difference between acetate in the MEC's influent and effluent).

6.2.4 Inhibition recovery experiments

To test the nature of the TAN inhibition for ARB, I investigated the capability of ARB to recover their initial activity. I shifted the TAN feed from 3 or 4.4 g TAN/L to 0.2 g TAN/L. I performed 2 independent continuous-flow MEC experiments using conditions similar to those described previously: HRT = ~18 h, pH = 7.35±0.1, influent acetate concentration = 15 mM, and phosphate buffer concentration = 100 mM.

6.2.5 Growth-rate experiments

To estimate the doubling times and growth rate of ARB at the different TAN concentrations (i.e., 0.2, 2.2, and 4.4 g TAN/L), I performed 2 independent batch MEC experiments using conditions similar to those described in the previous section, except for using a smaller anode surface area (2–5 cm^2). From one of the MECs fed with acetate (15 mM) medium having 0.2 g TAN/L, I harvested all biofilm from the anode and suspended the biomass in 6 mL of basal medium. I then inoculated each MEC with 1 mL of this suspension for the growth-rate experiments. A small inoculum concentration and anode surface area usually are needed for reliably evaluating the growth rate of ARB, as they preclude the current generation due to the initial colonization of large number of metabolically active bacterial cells and minimize the background current due to large anode surface area (Parameswaran et al., 2013; Marsili et al., 2010). After the initial colonization phase (i.e., a lag phase), I estimated doubling times and growth rate of ARB based on the exponential increase in j, since the j is directly proportional to biofilm concentration under non-limiting substrate conditions (Parameswaran et al., 2013). The increase in j is a direct gauge of the increase in biofilm accumulation as long as biofilm detachment is small compared to biomass synthesis, which was the case for my experiments.

I also harvested the entire biofilm after j reached a plateau and quantified the biomass concentration by measuring the protein content using the bicinchoninic-acid (BCA) protein assay kit (Sigma, St. Louis, MO), in which I measured absorbance at a wavelength of 562 nm using a UV-Vis spectrophotometer (Varian Cary 50 Bio, Varian Inc., Walnut Creek, CA). I extracted the protein of each biofilm according to the method described in Ishii et al. (2008b). Briefly, I immersed the entire graphite electrode in a test tube containing 0.2 N NaOH solution (2 mL) and incubated it at 4°C for 1 h with

vortexing every 15 min for 30 s. Then, I harvested the entire extracted liquid and rinsed the electrode with another 2 mL of deionized water to reach a final concentration of 0.1 N NaOH. The extracted liquid was further subjected to 3 freeze–thaw cycles (i.e., frozen at – 20 °C and thawed at 90 °C). Finally, 0.1 mL of the extracted liquid was used for protein analysis. I developed a standard calibration curve with bovine serum albumin.

Based on the increase in biofilm protein and loss of acetate in the liquid, I estimated the net biomass yield (Y_{net}; expressed as g VSS per g COD) according to equation 6.2:

$$Y_{net}\left(\frac{\text{g VSS}}{\text{g COD}}\right) = \frac{C_{protein}\left(\frac{\text{g protein}}{\text{L}}\right)}{\Delta S_{acetate}\left(\frac{\text{mole}}{\text{L}}\right)} \text{ x} \frac{\text{2 g VSS}}{\text{g protein}} \text{ x} \frac{\text{1 mole}}{\text{64 g COD}} \qquad \text{(Eq. 6.2)}$$

where $C_{protein}$ is the protein concentration at the end of batch experiment (in g/L), assuming that 50% of the dry weight biomass is protein (Rittmann and McCarty, 2001), and ΔS acetate is the difference between influent and effluent acetate concentration (in mol/L).

I also computed f_s, which is proportional to Y_{net}, according to equation 6.3:

$$f_s = \frac{Y\left(\frac{\text{g VSS}}{\text{g COD}}\right) \text{ x } \frac{\text{mol}_{acetate}}{8\ e^{-}\text{eq}} \text{ x } \frac{64\ \text{g COD}}{\text{mol}_{acetate}}}{113\left(\frac{\text{g VSS}}{\text{mol}_{cells}}\right) \text{ x } \frac{1}{20}\left(\frac{\text{mol}_{cells}}{e^{-}\text{eq}}\right)} = 1.42\ Y_{net} \qquad \text{(Eq. 6.3)}$$

where 113 (g cells/mol cells), 20 (e^{-}eq/mol cells), 8 (e^{-}eq/ mol acetate), and 64 (g COD/mol acetate) are the molecular weight for bacterial cells according to the empirical formula of $C_5H_7O_2N$, number of electron equivalents in a mole of biomass (with NH_4^+ as

the N source), number of electron equivalents in a mole of acetate, and COD conversion factor for acetate, respectively (Rittmann and McCarty, 2001).

Finally, I estimated the maximum specific growth rate (μ_{max}) of ARB by plotting the natural logarithm of j versus time, according to equation 6.4, and performing linear regression for the initial growth phase (Parameswaran et al., 2013; Marsili et al., 2008):

$$\ln\left(\frac{j}{j_0}\right) = \mu_{max}\, t \qquad \text{(Eq. 6.4)}$$

where μ_{max} is the slope of the regression line, and j and j_0 represent current densities produced at time t and t = 0, respectively.

6.3 Results and Discussion

6.3.1 The rate of anode-respiration depended on the TAN concentration

I first performed chronoamperometry to investigate the effect of TAN (and FAN) levels on ARB respiration rates, measured as *j*. I performed all experiments with two independent mature biofilms following an acclimation period (60 days), at which time both biofilms had stable *j* at ~6.5 A/m^2 and were visibly thick (evident from the photograph in Figure C.1 in appendix C). Both MECs showed similar trends, and I present one set of results in Figure 6.1A, with the replicate data shown in Figure C.2. Because losses of TAN, attributable to biomass synthesis, were small, ≤ 10% (Figure C.3), I report the influent and effluent TAN concentrations.

The rate of anode respiration was stable between 5.5 and 7 A/m^2 over the influent TAN range of 0.2 to 1 g TAN/L (corresponding to 2 to 18 mg FAN/L) (Figure 6.1A). However, an increase in influent TAN to 2.2 g TAN/L led first to a decrease in *j* (from 7.0±0.4 A/m^2 to 4.6±0.5 A/m^2), but then *j* increased within 4 days to 8.2±0.8 A/m^2. Increasing the influent TAN concentration to 3 and then to 4.4 g TAN/L (giving FAN of 53 to 78 mg/L) nearly stopped anode respiration.

These results appear to be inconsistent with previous studies in which high influent TAN concentration, up to 4 g TAN/L, resulted only in a slight decrease in *j* (Kuntke et al., 2012; Kuntke et al., 2011; Kim et al., 2011b). However, those studies had much lower TAN concentrations in the anode chamber, since TAN loss was up to 63% due to either NH_4^+ oxidation in the anode chamber (Tice and Kim, 2014; Nam et al., 2010b) or transport into the cathode chamber (Kuntke et al., 2012). My experimental design eliminated these confounding factors.

Acetate removal was hardly affected by TAN concentration ≤ 2.2 g TAN/L (p-value < 0.5) (Figure 6.1B): approximately 60% of removed electrons were channeled

from acetate to *j*, achieving a CE comparable with that of an acetate-fed mixed-culture biofilm (An and Lee, 2013).

The CE results for 2.2 g TAN/L were complex and appeared to illustrate inhibition and acclimation responses. At first, when *j* decreased to 4.6 A/m^2, CE also decreased to 40%, both relative declines of about one-third compared to 0.2 g TAN/L biofilm. The initial declines in *j* and CE probably mean that TAN stress caused the ARB to divert electron flow to the generation of intracellular storage polymers (ISP), soluble microbial products (SMPs), and/or extracellular polymeric substances (EPS) (Laspidou and Rittmann, 2002; Ni et al., 2010). This diversion would have simultaneously decreased respiration (assayed as *j*) and CE, since *j* is the numerator in the CE and acetate removal (the denominator for CE) was not changed. After 4 days, *j* and CE increased steadily up to 8.2 A/m^2 and 73%, relative increments of 17% and 22% over the values with 1 g TAN/L, while acetate utilization (the denominator in CE) was relatively constant (i.e., 4.2 – 5.1 mM) (Figure C.4). The increases represent a multi-faceted acclimation response by the ARB, and the net impact was more anode respiration for the same acetate removal.

Further increasing TAN to 3 and 4.4 g TAN/L led to a substantial decrease in acetate removal, *j*, and CE. For example, when the influent TAN was 4.4 g TAN/L, acetate removal declined to ~1%, *j* was less than 0.2 A/m^2, and CE was only 28%. A likely explanation for the substantial decrease in acetate removal and CE is that ARB in the biofilm were inhibited in a way that most seriously impaired respiration (measured as *j*, the numerator in CE), although acetate catabolism (in the denominator in CE) probably also was inhibited, since the bulk-solution acetate concentration was ~15 mM.

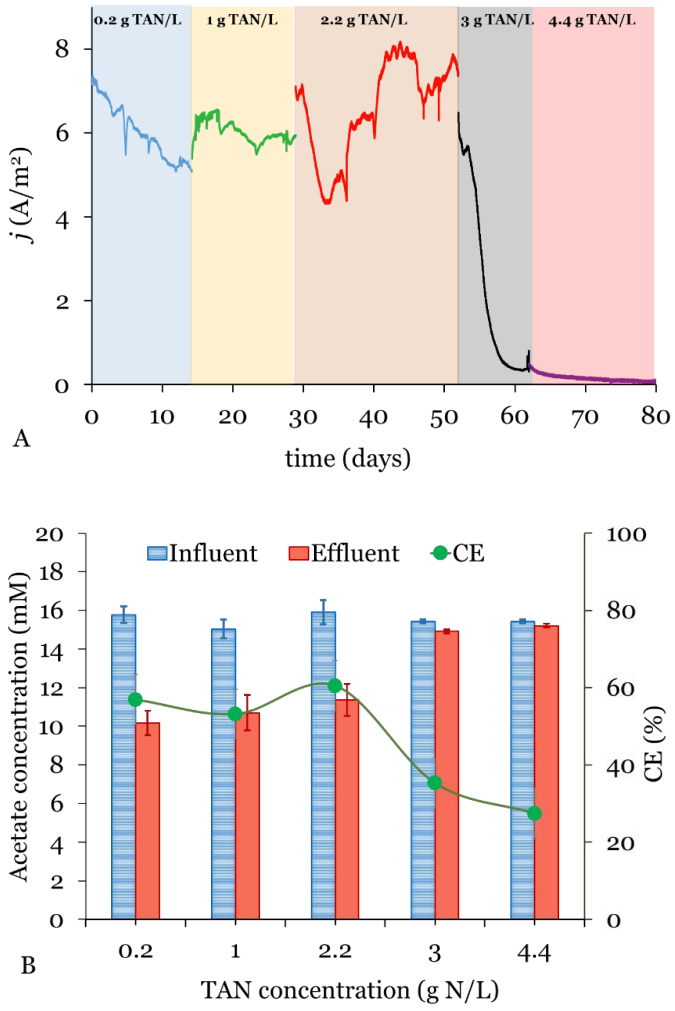

Figure 6.1 Performance of MECs fed with different influent TAN concentrations. (A) Steady-state current generation versus time for MECs during continuous operation at an HRT = ~18 h. (B) Summary of average acetate concentrations and CE.

6.3.2 Electrochemical analysis reveals that TAN stress stimulated a high respiration rate

I performed low-rate-scan CV once the chronoamperometric-polarization experiments reached steady-state. Figure 6.2A presents CVs of MEC anodes fed with TAN up to 2.2 g TAN/L. The CVs show the classic Nernstian (sigmoidal-shape) response characteristic of a biofilm dominated by *Geobacteraceae* (Torres et al., 2009). Current

appeared with an anode potential of around −0.26 V, a value only slightly above the formal potential of acetate (i.e., $E^{\circ\prime}_{acetate}$ = −0.29 V), and it saturated at around −0.05 V. Thus, the ARB were able to respire and grow with a potential harvest of 0.03 to 0.24 V. Since the Nernstian responses were similar for each biofilm, I normalized each CV in Figure 6.2A to its maximum j (j_{max}) (Figure 6.2B). The normalized CV of the MEC anode fed with 1 g TAN/L acetate medium had a slightly smaller slope than MECs fed with higher TAN concentrations, but the difference was very small and probably not meaningful. The apparent E_{KA} values based on j/j_{max} = 0.5 are almost the same, ~ −0.17 V vs SHE.

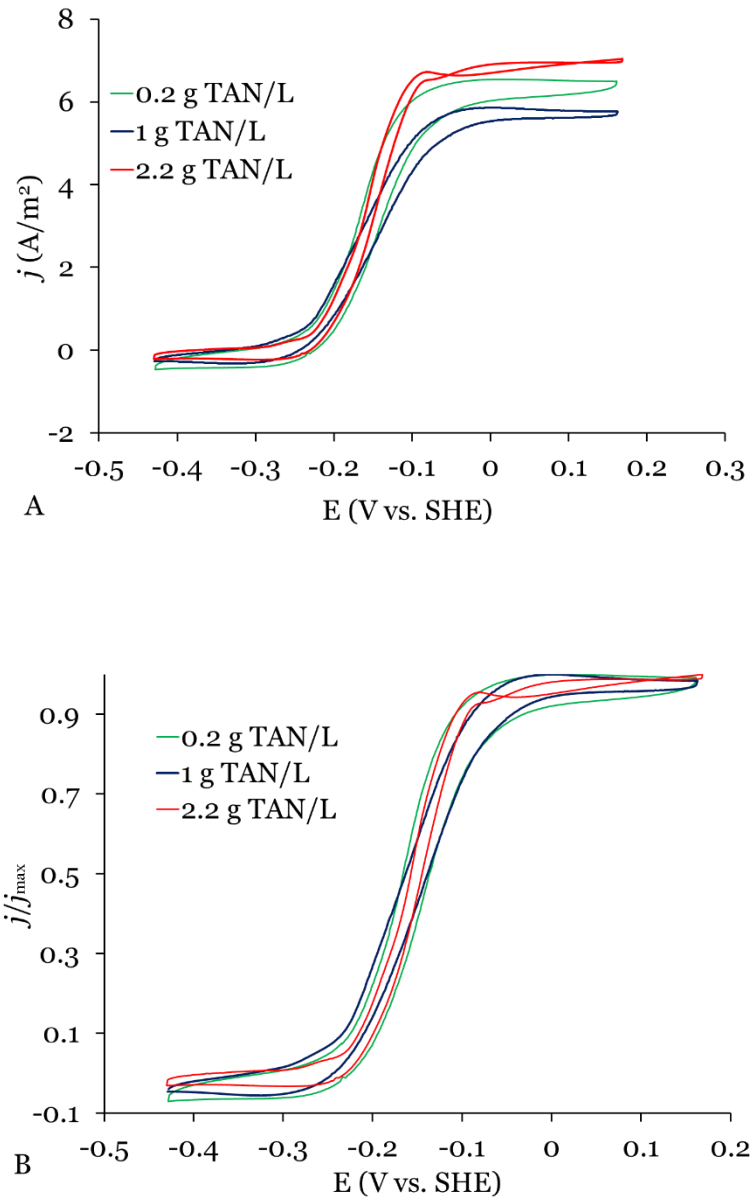

Figure 6.2 Cyclic Voltammograms of MECs having influent TAN concentration up to 2.2 g TAN/L. (A) Scan rate of 1 mV/sec. (B) CVs from (A) normalized to the maximum *j*.

Although Figure 6.2B suggests one apparent E_{KA} value, the first derivatives of the results in Figure 6.2A shows at least 2 inflection points, indicated as E_1 and E_2 in Figure 6.3, with redox potentials centered at −0.15 V and −0.19 V, respectively. These bracket the apparent E_{KA} value in Figure 6.3 (−0.17 V). A similar two-peak behavior is evident

for the ARB biofilm fed with 0.2, 1, or 2.2 g TAN/L, but with different peak magnitudes. Similar two-peak behavior was observed for *G. sulfurreducens* using acetate as an electron donor: first-derivative peaks from –0.25 to –0.19 V (Yoho et al., 2014; Katuri et al., 2010; Srikanth et al., 2008). Two peaks indicate that two redox proteins were involved in the EET process (Levar et al., 2014), one protein was capable of performing EET at two different formal potentials, or both. The emergence of the two-peak behavior in Figure 6.3 suggests that relatively high TAN concentration has some interaction with the EET chain of the ARB biofilm.

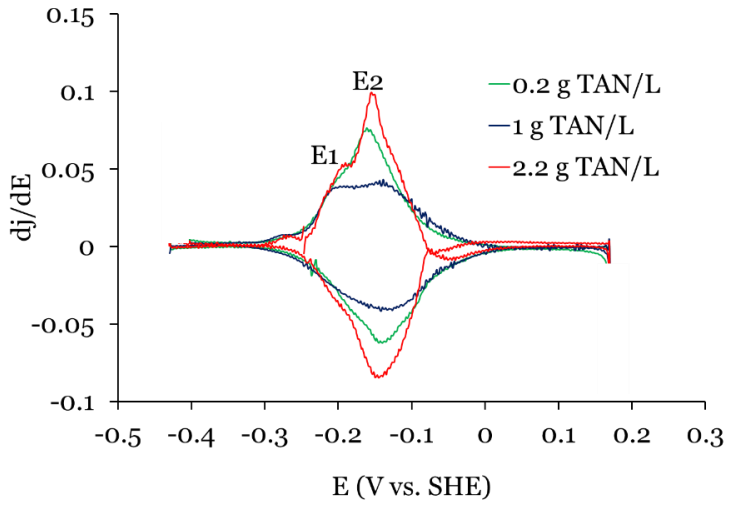

Figure 6.3 The first derivative of CVs shown in Figure 6.2A for the MEC fed with TAN concentration ≤ 2.2 g TAN/L (scan rate of 1 mV/sec).

The CVs for the MEC anodes fed media with 3 and 4.4 g TAN/L, shown in Figure 6.4, had very different responses from those presented in Figure 6.2. The CVs in Figure 6.4 are similar to the response of *G. sulfurreducens* under so-called non-turnover conditions (i.e., when an exogenous electron donor is absent so that current is generated only through endogenous respiration) (Katuri et al., 2012; Katuri et al., 2010; Marsili et al., 2008). The amorphous shapes of CVs and low values of *j* suggest that donor

catabolism by the ARB was severely inhibited. The effect was more severe for 4.4 g TAN/L: the MEC fed with 4.4 g TAN/L generated one-third of the cumulative coulombs, and acetate consumption was only 40% of that for 3 g TAN/L. It is not possible to distinguish if the primary impact of TAN inhibition was on catabolism or anode respiration, because a large-scale loss in one function necessarily causes a loss in the other. However, the amorphous shape for 4.4 g TAN/L supports inhibition of acetate catabolism.

Figure C.5 shows the derivative value for the data in Figure 6.4. The derivative for 3 g TAN/L shows a small and broad peak at from around –0.15 to –0.10 V vs SHE. This may correspond to one of the peaks in Figure 6.3. However, the derivative for 4.4 g TAN/L has only a very small peak around –0.15 V. The loss of clear peaks for both curves in Figure C.5 provides further support that TAN ≥ 3 g/L impaired anode respiration.

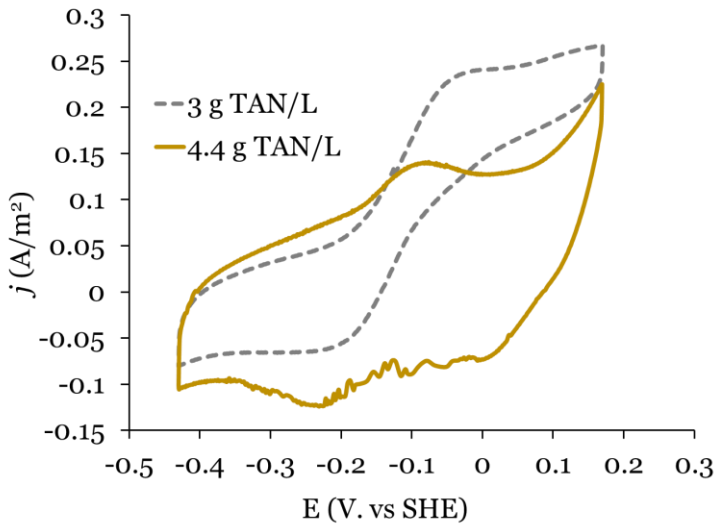

Figure 6.4 CVs of MEC fed with influent TAN concentrations of 3 and 4.4 g TAN/L (scan rate of 1 mV/sec). Note the low maximum j and the non-sigmoidal pattern.

6.3.3 ARB could recover from TAN inhibition

To test the reversibility of TAN inhibition for ARB, I shifted the TAN feed from 3 or 4.4 to 0.2 g TAN/L. The results in Figure 6.5A show that severe inhibition was almost completely reversed, although a longer lag time before the onset of recovery was required with 4.4 g TAN/L. Figure 6.5B plots the theoretical washout relationship of TAN concentration over time for the biofilms exposed to 3 and 4.4 g N/L. The effluent TAN concentration decreased to ~0.2 g TAN/L in both conditions within 3 days. For the biofilm starting at 3 g TAN/L, *j* significantly increased at ~0.8 day, when the bulk-solution TAN concentration was ~1.2 g TAN/L. This response is consistent with chronoamperometric and acetate-consumption data shown in Figure 6.1, in which respiration was hardly influenced by TAN concentration < 2.2 g TAN/L. However, the lag phase before the rapid rise in *j* was much longer (~3.8 days) for the biofilm starting at 4.4 g TAN/L. The strong increase in *j* began after the TAN concentration has been stable at close to 0.2 g TAN/L. This longer lag phase for 4.4 g TAN/L probably was caused by more severe inhibition that demanded more substantial (and lengthy) repair of damage to the ARB's catabolism or respiration mechanisms. It also is possible that new ARB had to grow to replace ARB killed by the high TAN concentration.

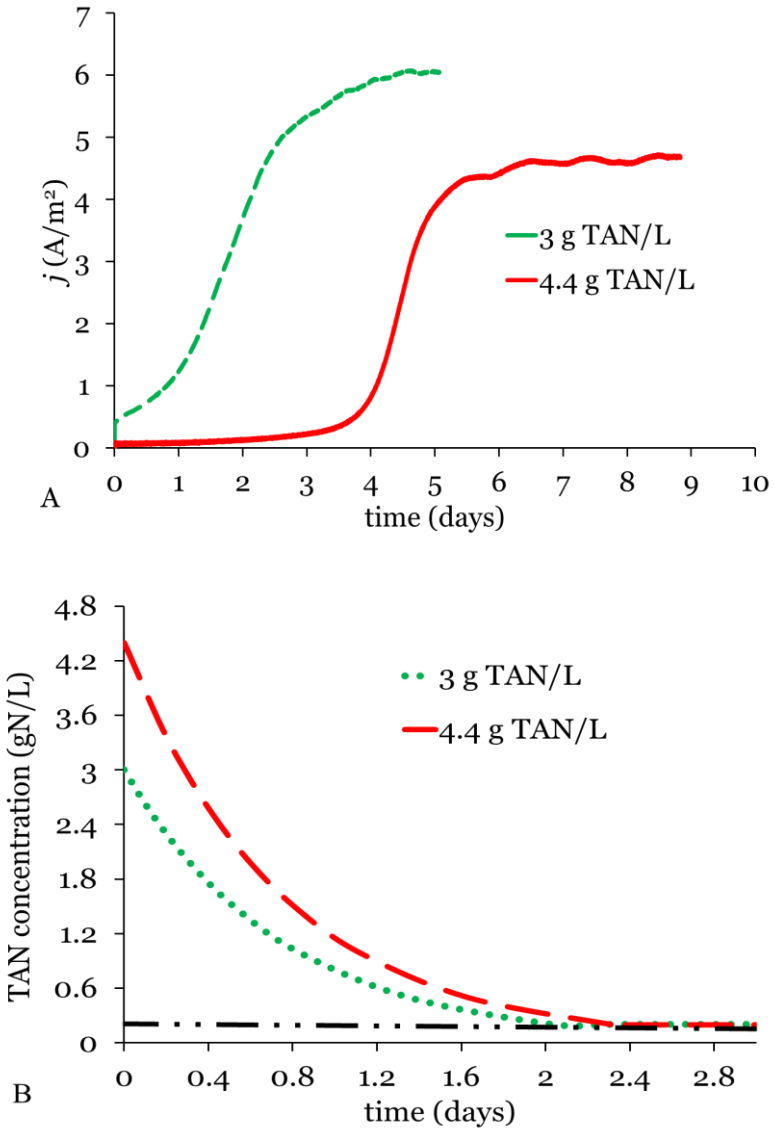

Figure 6.5 Performance of MECs during recovery experiments following TAN inhibition at 3 or 4.4 g TAN/L. (A) current density profile. The MECs were shifted to a feed of 0.2 g TAN/L at time 0. (B) Theoretical washout relationship of TAN over time during recovery experiments. The horizontal line indicates 0.2 g TAN/L.

6.3.4 ARB are resistant to high FAN, but sensitive to TAN

Figure 6.6 reveals how *j* depended on the medium pH in the range of 7.0 to 8.1 at a fixed non-inhibiting TAN concentration (i.e., 2.2 g TAN/L), giving FAN concentrations from 18 to 202 mg FAN/L. Anode respiration occurred over the entire pH range, and the

highest *j* occurred at the highest pH (Figure 6.6A). Thus, ARB were not adversely affected by relatively high FAN concentrations, up to at least 202 mg/L for pH 8.1, although they were sensitive to TAN concentrations > 2.2 g TAN/L (Figure 6.1). Figure 6.6B and Figure C.6 illustrate that pH and FAN had little impact on the electrochemical characteristics of EET. This lack of response to FAN is quite different from the response of methanogens to high FAN concentration, where FAN (not TAN) is the active component causing microbial inhibition (Angelidaki and Ahring, 1993). In fact, the highest *j* values occurred for the highest pH values, probably because a higher bulk pH was associated with higher alkalinity that enabled faster transport of protons out of the biofilm (Torres et al., 2008). Since ARB seem to have a metabolic advantage at slightly-alkaline pH compared to other anaerobic microorganisms, such as methanogens with whom they may compete, this relatively-high threshold for FAN toxicity by ARB may be a tool for managing microbial communities to favor ARB and high electron recovery in MECs fed with fermentable substrates, as long as TAN is not too high.

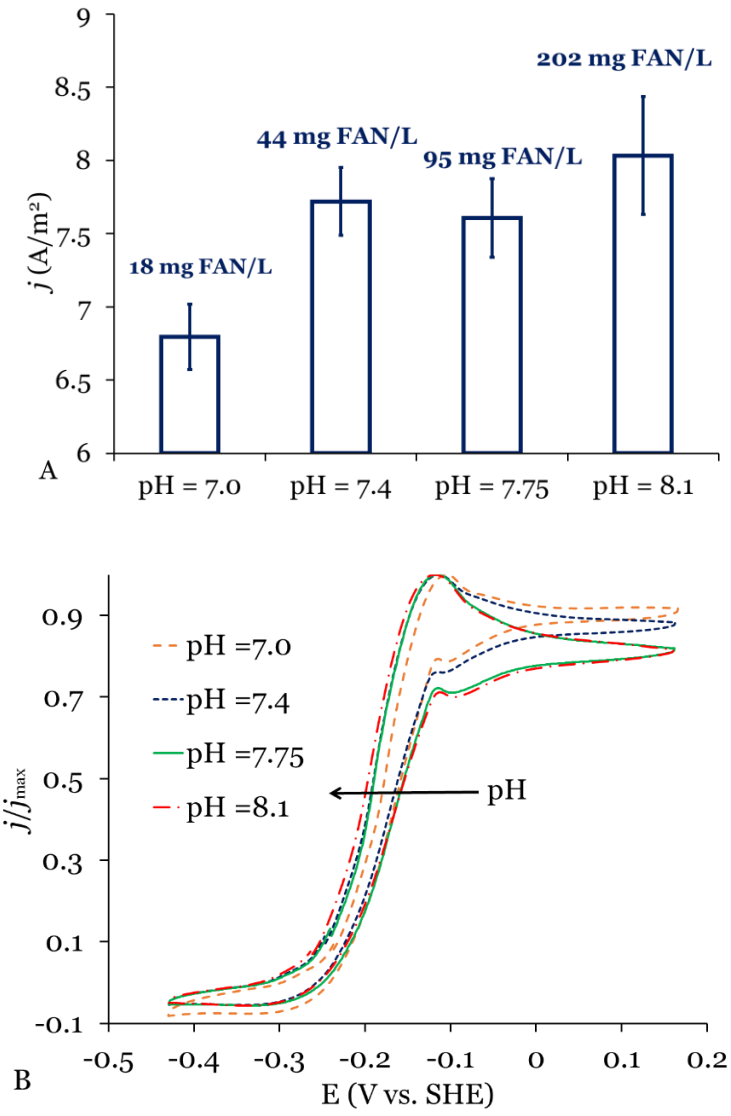

Figure 6.6 Effect of pH on performance of MEC fed with TAN concentration of 2.2 g TAN/L: (A) Average current density. (B) CVs normalized to the maximum current density.

6.3.5 Effect of TAN concentration on biofilm growth

To evaluate if TAN stress slowed the growth and accumulation of the ARB biofilm, I performed non-steady-state experiments at different TAN concentrations (0.2, 2.2, and 4.4 g TAN/L), as described in the Methods section. Both MECs showed similar trends, and I present one set of results in Figure 6.7, with the replicate data shown in

Figure C.7. I observed a much shorter lag phase for 0.2-g TAN–N/L biofilm (~70 h) than for 2.2-g TAN/L biofilm (~192 h), and biofilm accumulation was insignificant for the highest TAN condition (4.4 g TAN/L). Given that *j* is a gauge of biofilm accumulation as long as biofilm detachment is small, I estimated μ_{max} for each anode biofilm by plotting natural logarithm of *j* versus time during the first few hours of exponential growth. The highest μ_{max} value, 2.7±0.5 d^{-1}, occurred with 0.2 g TAN/L, compared to 0.84±0.2 d^{-1} for anode biofilm fed with 2.2 g TAN/L medium. These μ_{max} values correspond to doubling times of 9 and 29 h, respectively, values higher than the 6- to 8-h doubling time reported for *Geobacteraceae*-respiring electrodes (Levar et al., 2014; Marsili et al., 2010; Lee et al., 2009).

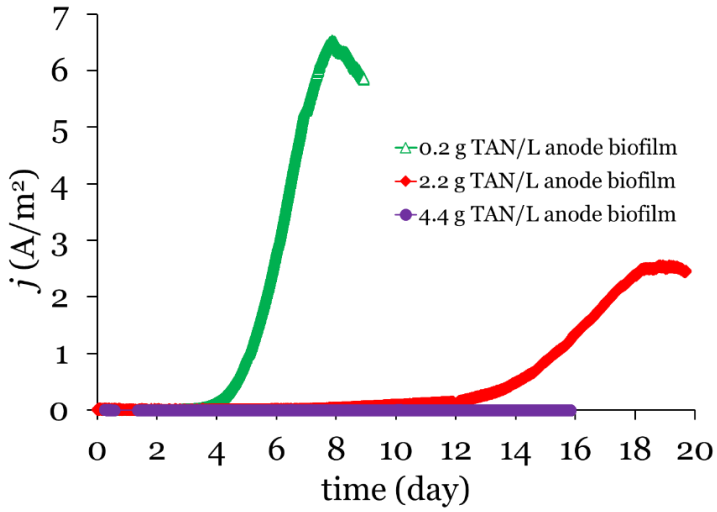

Figure 6.7 Growth-experiment data for MECs fed with different TAN concentrations.

Once *j* reached a plateau (i.e., ~6 and ~2.2 A/m² for biofilms grown with 0.2 g TAN/L and 2.2 g TAN/L, respectively), I harvested the entire biofilm for protein measurement. The 0.2 g TAN/L biofilm, grown for 214 h, achieved a biofilm accumulation of 520±80 μg of protein/cm², a value 1.5-fold higher than for the anode biofilm exposed to 2.2 g TAN/L (340±8 μg of protein/cm²). Assuming that a monolayer

of *G. sulfurreducens* contained about 20 μg/cm² of protein (Marsili et al., 2010; Marsili et al., 2008), the biofilms grown with either 0.2 or 2.2 g TAN/L medium formed multi-layer biofilm on the anode surface: ~26 and ~17 μm thick, respectively. Clearly, the ARB were carrying out extensive EET.

Based on cumulative Coulombs, protein measurement, and acetate consumption, the estimated CE, Y_{net}, and f_s values were 66±8%, 0.062±0.003 g VSS/g COD, and 0.09 e^- eq of biomass/e^- eq of donor consumed, and 50±6 %, 0.026±0.004 g VSS/g COD, and 0.04 e^- eq to biomass/e^- eq of donor consumed for 0.2 and 2.2 g TAN/L anode biofilms, respectively (Table 6.1). The estimated Y_{net} and f_s values decreased by ~58% in the presence of the higher TAN concentration. This trend confirms that electrons were diverted away from biomass synthesis with higher TAN up to 2.2 g TAN/L. However, I cannot distinguish whether the low values of Y_{net} and f_s were due to the need for the ARB to route more electron equivalents to compensate for a loss of energy capture in respiration (e.g., by uncoupling) or by more endogenous decay. The longer growth duration for 2.2 g TAN/L biofilm (~18 days vs. ~8 days for 0.2 g TAN/L biofilm) would have given more weight to endogenous decay. In any case, 2.2 g TAN/L resulted in more acetate-derived electrons being routed to anode respiration.

Table 6.1 Summary of kinetic, chemical, and electrochemical parameters at different TAN concentration.

Parameter (unit)	0.2 g TAN/L anode biofilm	2.2 g TAN/L anode biofilm
j_{max} (A/m^2)	5.9–6.4	1.6–2.5
Acetate consumption (mM)	4.9±0.1	3.8±0.1
CE (%)	66±8	50±6
μ_{max} (day^{-1})	2.7±0.5	0.84±0.2
Protein (μg/cm^2)	520±80	340±8
Biomass concentration (mg VSS/cm^2)	1.04±0.2	0.68±0.1
Y_{net} (g VSS/g COD)	0.06±0.002	0.03±0.007
f_s (e$^-$ eq biomass/e$^-$ eq acetate)	0.09±0.003	0.04±0.001

6.4 Conclusions

Two goals of MXCs are to achieve a high oxidation rate of organic matter and a high electron recovery. Here, I show that relatively high TAN concentration imposed a significant stress on the ARB biofilm. When exposed to a relatively high ammonium concentration (i.e., 2.2 g TAN/L), the anode biofilm diverted greater electron flow toward current generation and consequently lowered net biomass yield. As a result, the doubling times for the anode biofilm and from 9.0 h to 28.6 h and protein accumulation decreased from 520 mg/cm^2 to 340 mg/cm^2 in the presence of 2.2 g TAN/L, compared to 0.2 g TAN/L, respectively, although acetate consumption was comparable (i.e., 4.9 mM for 0.2 g TAN/L biofilm versus 3.8 mM for 2.2 g TAN/L biofilm). Further increases in TAN concentration (i.e., to 3 and 4.4 g TAN/L) almost completely inhibited ARB, although the TAN inhibition was reversible. Finally, the ARB were resistant to relatively high FAN concentrations, up to at least 200 mg FAN/L, even though they were sensitive to TAN concentrations > 2.2 g TAN/L.

CHAPTER 7

CHANGES IN GLUCOSE FERMENTATION PATHWAYS AS A RESPONSE TO THE FREE AMMONIA CONCENTRATION IN MICROBIAL ELECTROLYSIS CELLS: THE ROLE OF INTERSPECIES H_2 [5]

7.1 Introduction

Microbial electrolysis cells (MECs) represent one of the newest environmental biotechnologies for wastewater treatment coupled with the production of renewable energy in the form of electrical power, hydrogen gas (H_2), or valuable chemicals (Logan and Rabaey, 2012; Rittmann, 2008). Biodegradation of the organic compounds that are the "fuel" for the anode requires cooperation among different trophic guilds: fermenters, homoacetogens, methanogens, and anode-respiring bacteria (ARB) (Schink and Stams, 2013; Lovley, 2008; Angenent et al., 2004). Generally, an MEC's microbial community has a high complexity in terms of community structure and diversity, but key microbial populations have been identified (Borole et al., 2011; Kiely et al., 2011; Logan and Regan, 2006).

The defining guild in an MEC is the ARB, which perform a unique type of respiration. Typical anaerobes transfer electrons intracellularly to a terminal electron acceptor, such as sulfate, nitrate, or carbon dioxide (Muyzer and Stams, 2008; Lovley and Coates, 2000; Thauer et al., 1977). ARB oxidize organic matter internally, but transfer the resulting electrons outside their membrane to a solid electron acceptor, i.e., the anode (Borole et al., 2011; Franks and Nevin, 2010; Logan and Regan, 2006). Another feature of majority of ARB in mixed community is that their electron donors are limited to only simple substrates, such as acetate and H_2 (Lee et al., 2009; Freguia et al., 2008).

[5] This Chapter has been submitted in an altered format for publication.

In environments lacking electron acceptors, complex organic compounds, such as glucose, are fermented into a variety of organic acids and H_2. Acetate is the most prevalent organic acid, and Table 7.1 presents a number of reactions in which acetate and H_2 are formed or consumed. H_2-consumers include hydrogenotrophic methanogens, which use H_2 as the main electron donor and produce methane (reaction 3 in Table 7.1) (Stams and Plugge, 2009; Thauer et al., 2008; Liu and Whitman, 2008; Rittmann and McCarty, 2001; Zinder, 1993). Homoacetogens also scavenge H_2 to yield acetate. Homoacetogenesis and hydrogenotrophic methanogenesis have very low energy yields (Schuchmann and Müller, 2014). H_2 must be kept at low level to allow fermentation to be thermodynamically possible (Hatti-Kaul and Mattiasson, 2016; Hallenbeck, 2009; Stams and Plugge, 2009; McInerney et al., 2008; Angenent et al. 2004). When H_2 builds up, the fermentation stoichiometry changes such that higher organic acids, such as lactate, butyrate, propionate, and ethanol, are produced rather than acetate and H_2 (Hallenbeck, 2009; Angenent et al. 2004).

When the MEC's anode is the only respiratory electron acceptor, ARB can out-compete methanogens for acetate; due to their thermodynamic and kinetic advantages over the acetate-consuming methanogens (reaction 5 in Table 7.1) (Parameswaran et al., 2009). However, ARB do not have similar advantages for H_2 consumption, and the electrons in H_2 often are channeled to methane (CH_4) via hydrogenotrophic methanogens, which are able to grown in suspension, as well as in the anode's biofilm (Lee and Rittmann, 2010; Parameswaran et al., 2009). Thus, it is a challenge to minimize production of CH_4 from the H_2 generated via fermentation in the presence of hydrogenotrophic methanogens (Parameswaran et al., 2010; Lee and Rittmann, 2010; Freguia et al., 2008).

Table 7.1 Overview of reactions involving acetate and H_2.

Process	ΔG°_{rxn} (kJ/e⁻ eq) [a]
(1) Glucose fermentation: $C_6H_{12}O_6 + 2H_2O \rightarrow 2\ CH_3COO^- + 4H_2 + 2CO_2 + 2H^+$	– 8.59
(2) Acetoclastic methanogenesis: $CH_3COO^- + H_2O \rightarrow CH_4 + HCO_3^-$	– 3.88
(3) Hydrogenotrophic methanogenesis: $HCO_3^- + 4H_2 + H^+ \rightarrow CH_4 + 3H_2O$	–16.38
(4) Homoacetogenesis: $2\ CO_2 + 4H_2 \rightarrow CH_3COO^- + H^+ + 2H_2O$	– 11.88
(5) Acetoclastic anode respiration [b]: $CH_3COO^- + 2H_2O \rightarrow 2CO_2 + 8H^+ + 9e^-$	– 19.30
(6) Hydrogenotrophic anode respiration [b]: $2H_2 \rightarrow 2H^+ + 2e^-$	– 9.65
(7) Acetate oxidation to H_2: $CH_3COO^- + 4H_2O \rightarrow 2HCO_3^- + 4H_2 + H^+$	+13.10

[a] I calculated ΔG°_{rxn} at standard conditions (i.e., 298 K, 1 atm for gases, pH 7, and 1 M for soluble reactants) based on the thermodynamic data provided in Lever (2012) and Thauer et al. (1977); [b] Near-optimum anode potential = +0.2 V versus SHE (Freguia et al., 2008)

Previous researchers proposed different strategies to inhibit methanogenesis in laboratory-scale MECs, including thermal treatment, periodic exposure to oxygen (O_2), pH excursions, alamethicin exposure, and use of chemical inhibitors such as 2-bromoethanesulfonate (BES) (Zhu et al., 2015; Rago et al., 2015; Parameswaran, et al., 2010; Chae et al., 2010). Among the proposed strategies, chemical inhibitors seem to be the most effective approach, due to their selectivity for inhibiting the activity of methyl coenzyme-A (*mcr*A) in acetoclastic and hydrogenotrophic methanogens. For example, Parameswaran et al. (2009) inhibited methanogens in an ethanol-fed MEC with 50 mM BES, which boosted the coulombic efficiency (CE) by ~40%, as electrons from H_2 were

rerouted to anode respiration instead of to CH_4 production. Although BES is an effective way to inhibit methanogens (Rago et al., 2015; Parameswaran et al., 2010), it is not practical for field applications.

I recently revealed that ARB are resistant to relatively-high free-ammonia nitrogen (FAN) concentrations, up to at least 200 mg/L, but sensitive to total-ammonia nitrogen (TAN) concentrations > 2.2 g/L (Chapter 6). The relatively-high threshold for FAN toxicity by ARB may be a tool for managing microbial communities to favor ARB and high electron recovery in MECs fed with fermentable substrates, as long as TAN is not too high.

Therefore, I hypothesize that high-enough FAN can promote the desired syntrophy in MECs fed with fermentable substrate by inhibiting hydrogenotrophic methanogens. Suppressing methanogenesis should promote homoacetogens, which convert H_2 and CO_2 into acetate, the ideal substrate for ARB. This hypothesis requires that a FAN concentration high enough to suppress methanogens not have a strong inhibitory effect on ARB and fermenters. This strategy is highly relevant to MECs treating real wastewater that are characterized by high FAN concentrations, including landfill leachate and animal wastewater (Mahmoud et al., 2014; Yenigün and Demirel, 2013).

A high FAN concentration also might promote a new pathway for acetate consumption to produce CH_4 at very low H_2 partial pressure: syntrophic acetate oxidation (SAO) (alternatively known as reverse acetogenesis) (Zinder and Koch, 1984). SAO is a two-step process in which acetate is utilized by syntrophic acetate oxidizing bacteria (SAOB) (reaction 7 in Table 7.1) with the generation of reducing equivalents, often in the form of H_2. This step is a highly energy-demanding reaction that requires syntrophy with H_2-consuming bacteria (e.g., hydrogenotrophic methanogens or

hydrogenotrophic ARB) to maintain a very low level of H_2 (reaction 3 or reaction 6 in Table 7.1, respectively) in order to make the overall reaction thermodynamically favorable (Angelidaki et al. 2011; Stams and Plugge, 2009). In the absence of other electron acceptors, such as nitrate and sulfate, the produced H_2 is most likely routed to CH_4 through hydrogenotrophic methanogenesis, since ARB are known of being poor H_2-consumers (Lee and Rittmann, 2010; Parameswaran et al., 2009). So far, nothing is known about the SAO process in MECs fed with high FAN concentration.

My overarching goal is to investigate the effect of different FAN levels on the interactions among ARB and other members of the communities, particularly the fermenters and methanogens. I document the microbial interactions through a combination of chemical, electrochemical, and genomic tools. In order to study electron-flow and synergies in an MEC's anode, I use a fixed concentration of glucose (5 mM) as the sole electron-donor substrate, and I vary the influent FAN concentration (i.e., 0.02, 0.18, and 0.37 g FAN/L) going into the anode during batch and semi-continuous (hydraulic retention time of 2 days) MECs. Key is that I establish electron-equivalent mass balances. I also characterize the relative abundance and composition of bacteria and Archaea by Illumina sequencing, and I track homoacetogens and methanogens by targeting the formyltetrahydrofolate synthetase (FTHFS) gene – a conserved gene involved in their CO_2 fixation pathway – and *mcr*A gene, respectively, by quantitative real-time PCR (qPCR).

7.2 Materials and Methods

7.2.1 MEC design and operation

For my experiments to understand the fundamentals of how the microbial community changes in response to high FAN concentration, I used half-cell MECs with its anode potential controlled using a potentiostat. Each MEC held ~320 mL in each chamber and had a square graphite anode having a total surface area of ~11.6 cm^2, and a 0.8-cm OD graphite rod as cathode. This setup excluded any interference from potential losses at the cathode or due to a large distance between the anode and the cathode; fixing the anode potential allowed me to focus only on the anodic reactions. In order to ensure that the ARB were not limited by a low anode potential, I poised the anode at a fixed potential of –0.3 V vs. Ag/AgCl (or ~ –0.04 V vs. standard hydrogen electrode (SHE) in my media) using a VMP3 digital potentiostat (Bio-Logic USA, Knoxville, TN) by placing an Ag/AgCl reference electrode (BASI Electrochemistry, west Lafayette, IN) about 0.5 cm away from the anode. I separated the anode chamber from the cathode chamber with an anion exchange membrane (AMI 7001, Membranes International, Glen Rock, NJ). The pH of the cathode chamber was adjusted to 12 by addition of 10 N NaOH.

I inoculated the MEC's anode chamber with 2 mL of biofilm inoculum from a previously operated MEC fed with 5 mM glucose as the sole electron donor. After sparging the MEC with ultra-high purity N_2 gas (≥99.9%) for ~45 min, I fed the MEC with autoclaved (for 90 min at 121°C) glucose medium (initial pH of 8.1) containing: 5 mM glucose (or 38.4 me^-eq), 100 mM phosphate buffer (KH_2PO_4/Na_2HPO_4), 2.1 g $NaHCO_3$, and 10 mL of trace minerals as outlined in Parameswaran et al. (2009). I added different amounts of ammonium chloride as the sole N-source, giving FAN (and TAN) concentrations of 0.02 g FAN/L (0.2 g TAN/L), 0.18 g FAN/L (2 g TAN/L), and 0.37 g FAN/L (4 g TAN/L). Prior to the MEC's electron balance experiments, I

acclimated the inoculum by continuously feeding the developed biofilm with 5 mM glucose medium as the sole electron donor at relatively short hydraulic retention time (i.e., 24 h), followed by performing 2 consecutive batch cycles to select for a microbial community that was efficient at consuming glucose and producing electrical current. I controlled the temperature at 30°C in a temperature-controlled room, and the liquid in both chambers was mixed using a magnetic stirrer at 220 rpm. I performed all batch MEC experiments in duplicate.

In order to confirm and expand the results from the batch MEC experiments, I evaluated MEC performance with semi-continuous operation. I operated two independent MECs in parallel and fed in a semi-continuous mode once every 2 days. The MECs were operated at a fixed temperature of 30°C and fed with a 5-mM glucose medium having the same composition as mentioned in the previous paragraph. The liquid in both chambers was mixed using a magnetic stirrer at 220 rpm. I tested the MECs with different FAN concentration achieved with different combination of TAN concentration and pH: (1) 0.003 g FAN/L (pH = 7 and TAN = 0.2 g/L), (2) 0.02 g FAN/L (pH = 8.1 and TAN = 0.2 g/L), 0.18 g FAN/L (pH = 8.1 and 2 g/L), and (4) 0.37 g FAN/L (pH = 8.1 and TAN = 4 g/L).

7.2.2 Chemical analyses

I measured TAN, in duplicate, using HACH kits (HACH, Ames, IA) after filtration through a 0.22-µm membrane filter (PVDF GD/X, Whatman, GE Healthcare, Ann Arbor, MI). I quantified liquid samples for organic fermentation products and glucose using high-performance liquid chromatography (HPLC; Model LC-20AT, Shimadzu, Columbia, MD) with an Aminex HPX-87H column (Bio-Rad Laboratories, Hercules, CA) after filtration through a 0.22-µm membrane filter according the method described in

Mahmoud et al. (2014). Briefly, I used 2.5 mM sulfuric acid and 18-MΩ reverse-osmosis water as eluents for determining organic fermentation products and glucose, respectively, at a constant flow rate of 0.6 mL/min. I developed a five-point calibration curve for every set of analyses, performed duplicate assays, and report the average concentrations.

I measured the volume of gas produced with a friction-free glass syringe of 10- or 25-mL volume (Popper & Sons, Inc., New Hyde Park, NY, USA). I estimated gas percentages of H_2, CH_4, and CO_2 in samples taken with a gas-tight syringe (SGE 500 μL, Switzerland) using a gas chromatograph (GC 2010, Shimadzu Corporation, Columbia, MD) equipped with a thermal conductivity detector and a packed column (Carboxen™ 1010 PLOT Capillary Column, Supleco, Inc.). Helium was the carrier gas at a constant flow rate of 10 mL/min and pressure of 42.3 kPa. Temperature conditions for column, injection, and detector were 80, 150, and 220 °C, respectively. I employed analytical grade H_2, CH_4, and CO_2 gases for standard curves, carried out gas analyses in duplicate, and averaged the two values.

7.2.3 Microbial community analyses

7.2.3.1 DNA extraction. At the end of each batch experiment, I harvested the entire biofilm biomass from each MEC anode by scraping it off with a sterilized pipette tip and suspending the biomass sample in a sterile centrifuge tube containing DNA-free water. I then centrifuged the contents at 10,000g (Eppendorf Centrifuge 5414 D, USA) for 10 min to concentrate the biomass, which I stored at −20 °C prior to DNA extraction. I also centrifuged the entire liquid of the MEC chamber to concentrate the suspended phase for extraction. I extracted the total genomic DNA using the MOBIO Powersoil DNA extraction kit according to manufacturer's instructions, and determined the quality

and quantity of the extracted DNA using a nanodrop spectrophotometer (ND 1000, Thermo Scientific) by measuring absorbance at 260 and 280 nm.

7.2.3.2 quantitative real-time PCR (qPCR). I evaluated the presence and abundance of methanogenic Archaea and homoacetogens by targeting the *mcr*A and FTHFS genes, respectively, using qPCR. I carried out all PCR reactions in optically clear tubes with caps in an Eppendorf Realplex 4S realcycler with a 20 μL total reaction volume. I performed all qPCR reactions in triplicate along with a six-point standard curve by following modified assays for FTHFS gene (Parameswaran et al., 2010) and *mcr*A gene (Steinberg and Regan, 2009). I performed negative-control assays by using DNA-free water instead of DNA templates. I reported the results as the number of gene copies per reactor, after calculating the number of 16S rRNA genes per the entire biofilm or suspended phase of each MEC.

7.2.3.3 Illumina sequencing. I amplified the extracted DNA using 16S rRNA gene-targeting forward and reverse fusion primers at MR DNA laboratory (www.mrdnalab.com, Shallowater, TX, USA). I performed bacterial and archaeal sequence using the bar-coded primer set 515F (5′–GTGCCAGCMGCCGCGGTAA–3′)/806R (5′–GGACTACHVGGGTWTCTAAT–3′) (Caporaso et al., 2012) and 349F (5′–GYGCASCAGKCGMGAAW–3′)/806R (5′–GGACTACVSGGGTATCTAAT–3′) (Takai and Horikoshi, 2000), respectively, in a single-step 28 cycle PCR using the HotStarTaq Plus Master Mix Kit (Qiagen, USA) with the following conditions: 94°C for 3 min, followed by 28 cycles of 94°C for 30 s, 53°C for 40 s, and 72°C for 1 min, after which a final elongation step at 72°C was for 5 min. In order to determine the amplification success and the relative intensity of bands, PCR products were checked in 2% agarose gel (Werner et al., 2011). Then, the amplified products were pooled in equal proportions based on their molecular weight and DNA concentrations, purified, and used to prepare

DNA libraries following the Illumina TruSeq DNA library preparation protocol. Sequencing was performed on a MiSeq Illumina sequencer (Illumina Inc., USA) following the manufacturer's guidelines.

7.2.3.4 Bioinformatics analysis. I analyzed the sequences data using QIIME software package version 1.9.1 (Caporaso et al., 2010) after trimming off low-quality bases and discarding sequences shorter than 25 bp, longer than 450 bp, or labeled as chimeric sequences. I performed taxonomic classification at 3% sequence divergence (97% sequence similarity) and assigned taxonomy to operational taxonomic units (OTUs) by using the Ribosomal Database Project (RDP) classifier with a 50% confidence threshold (Cole et al., 2009). I performed rarefaction on the OTU table at a depth of 100 sequences in 10 replicates, and I analyzed the rarefaction measures with the same sequence numbers per sample (i.e., 223000 sequences per sample for bacteria population) with a python script in QIIME software (Caporaso et al., 2010). I performed alpha- and beta-diversity calculations, including richness of each samples with Chao1 index (Chao, 1987), the diversity with Shannon and Phylogenetic Distance Whole Tree metrics (Faith, 1992), the evenness with the equitability coefficient on a normalized scale from zero, in which community is perfectly even, to 1, in which community has one dominant OTU and many singlets (Werner et al., 2011), and principal-coordinates analysis (PCoA) using python script in QIIME software. Sequence data sets are available at NCBI/Sequence Read Archive (SRA) under study with BioProject accession number PRJNA343831.

7.2.4 Electron balance and electron flow into various sinks

I established electron balances by estimating the electron equivalents of experimentally measured glucose and fermentation products with the following

equivalences (Rittmann and McCarty, 2001): 24 me^- eq per mmole glucose, 8 me^- eq per mmole acetate, 14 me^- eq per mmole propionate, 20 me^- eq per mmole butyrate, 12 me^- eq per mmole lactate, 25 me^- eq per mmole valerate, 0.32 me^- eq per mL CH_4 (@30°C), and 0.08 me^- eq per mL H_2 (@30°C).

Figure 7.1 shows the different paths for electron flow from glucose when hydrogenotrophic methanogens are not suppressed (Figure 7.1A) or are completely suppressed (Figure 7.1B). I assumed stoichiometric fermentation of glucose (24 me^- eq) into 2 moles of acetate (16 me^- eq) and 4 moles of H_2 (8 me^- eq). Acetate is efficiently consumed by acetate-consuming ARB to generate electric current, while H_2 is consumed by hydrogenotrophic methanogens that have thermodynamic, kinetic, and metabolic advantages over H_2-consuimng ARB and homoacetogens (Parameswaran et al., 2009). In parallel, a fraction of electrons is utilized by different microbial groups in the MEC's anode to synthesize new microbial cells. I quantify the fraction of electrons used for biomass synthesis based on f_s° (me^- eq biomass per me^- eq substrate) values of 0.18 for fermenters (Rittmann and McCarty, 2001), 0.08 for hydrogen-consuming methanogens (Rittmann and McCarty, 2001), ~0.02 for homoacetogens (Ni et al., 2011b; Graber and Breznak, 2004) and ~0.09 for ARB (my findings in Chapter 6). The resulting CE for the electron flows in Figure 7.1A (when methanogenesis is not suppressed) is 50%, with 25% of the electrons routed to CH_4 gas and 25% to biomass. CE increases to 76% when methanogenesis is completely inhibited, with comparable electrons routed to biomass (24%) (Figure 7.1B).

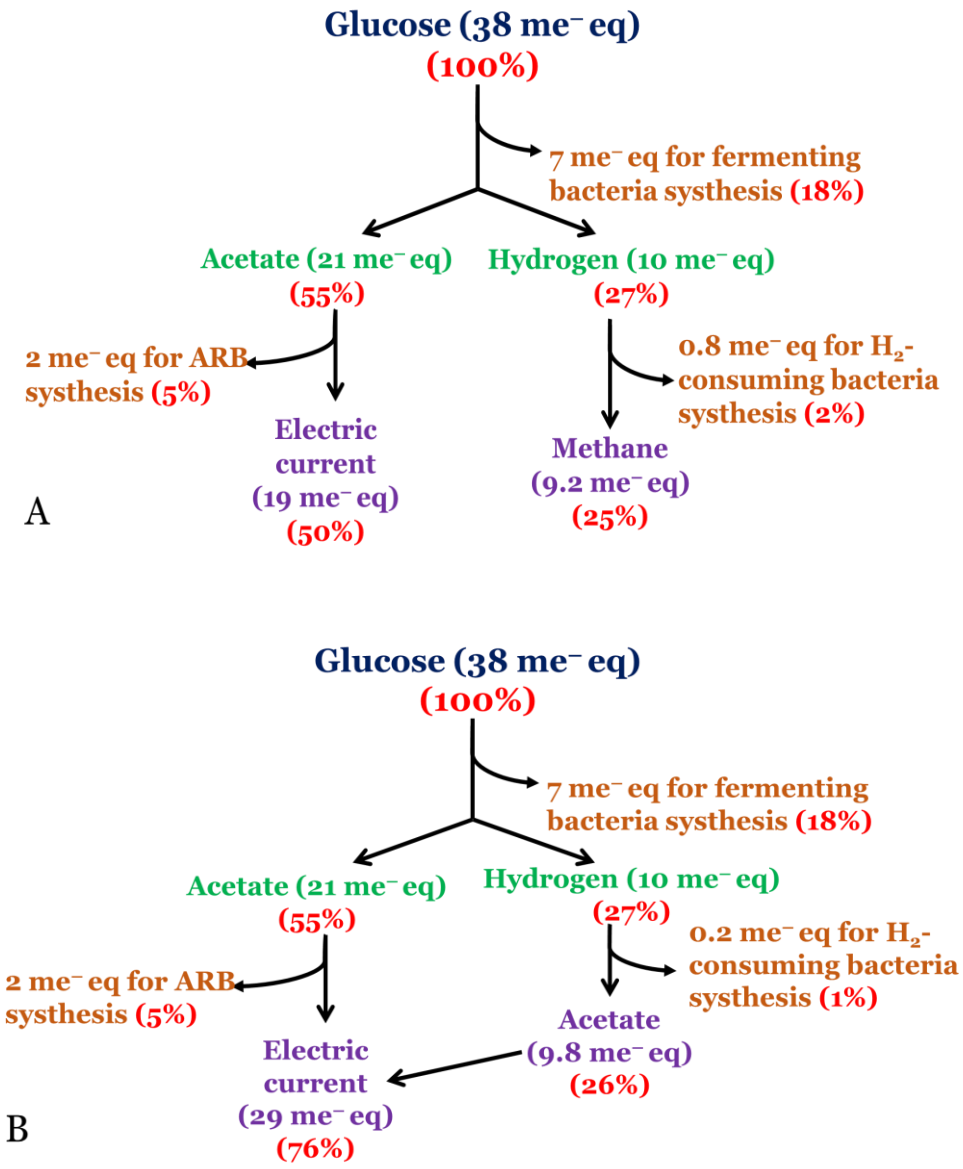

Figure 7.1 Electron flows from glucose into different electron sinks in an MEC's anode. (A) when methanogenesis is not inhibited. (B) when methanogenesis is completely inhibited

7.3. Results and Discussion

7.3.1 Framework for explaining electrons distribution for batch MECs

Figure 7.2 presents the electron distribution from glucose into the possible electron sinks over the course of the experiments with different FAN concentrations. The inoculum had been pre-acclimated to glucose, and then I performed an electron balance on batch experiments with glucose as the sole electron donor. With the lowest initial FAN (i.e., 0.02 g FAN/L), current production increased significantly during the first 2 days (Figure 7.2A). Simultaneously, acetate production increased to ~14% of the total electrons, and the glucose decreased below detection limit. Methane slowly accumulated within 2 days of operation and reached a plateau after day 6, when methane generation accounted for ~15% of the total electrons supplied from glucose. 15% methane is less than the estimate in Figure 7.1A (i.e., 25%), probably due to either H_2 consumption by either ARB or homo-acetogenesis. The total electrons contained in other fermentation products were small: ~3.3 % for propionate and ~3.1% for butyrate within the first 4 days of operation. Propionate and butyrate were completely consumed at day 17 and day 8, respectively.

I detected no H_2 in the headspace gas of the MEC's anode. Thus, H_2 produced during glucose fermentation was quickly channeled to methane by H_2-consuming methanogens, to current by ARB, or to acetate and then current by homoacetogens and ARB (Parameswaran et al., 2009; Lee et al., 2009). The Coulombic recovery at the end of batch cycle (~57%) was slightly greater than the estimated value in Figure 7.1A, which suggests that a modest flow of electron where routed through H_2 to the anode.

Figure 7.2B shows the distribution of electrons from glucose during 20 days of batch operation with 0.18 g FAN/L, where methane generation was partly inhibited. Compared to the MEC fed with 0.02 g FAN/L (Figure 7.2A), current slowly increased

during the first 2 days and was associated with complete glucose fermentation. However, lactate started to increase to become the largest electron sink (~30%) at day 2, followed by acetate (~13%), propionate (~5%), and iso-butyrate (~2%). Since the lactate is unlikely to be consumed by ARB, its fermentation was proceeded rapidly so that current increased to become the largest electron sink after day 6, at which time methane accounted for ~9% of the total electrons supplied from glucose. Although I did not detect any H_2 in the headspace gas, formate was detected in low concentration (0.67 mM), accounting for nearly 2% of glucose's total electrons. These results support that that 0.18 g FAN/L delayed lactate fermentation, rather than glucose fermentation, and significantly inhibited methanogenesis. A key finding is that CE was ~76%, which illustrates the benefit to inhibiting methanogenesis.

Further increasing the initial FAN concentration to 0.37 g FAN/L (Figure 7.2C) had a more pronounced effect on fermentation, although the impact on methanogenesis was not much greater than for 0.18 g FAN/L. Similar to the lower FAN concentration, the rate of glucose consumption did not change; however, 0.37 g FAN-N/L altered the fermentation kinetics and pathway. During the first 4 days, lactate, iso-butyrate, propionate, butyrate, and acetate accumulated, collectively accounting for ~25% of glucose's electrons. After 4 days, fermentation proceeded rapidly with concurrent increases in electric current, which became the largest electron sink by the end of the batch cycle (~62%), suggesting that this high FAN concentration might partially inhibit ARB. However, methanogenesis was not completely inhibited, as it accounted for ~6% of glucose's electrons.

As a result of organic-acids accumulation, the pH at the end of all batch cycles decreased from their initial pH value (i.e., 8.1) to a narrow range of 6.85–7.10. Since the

pH values were not much different from each other, variations in pH should have had a minimal effect on fermentation pathway and kinetics (Lee et al., 2008).

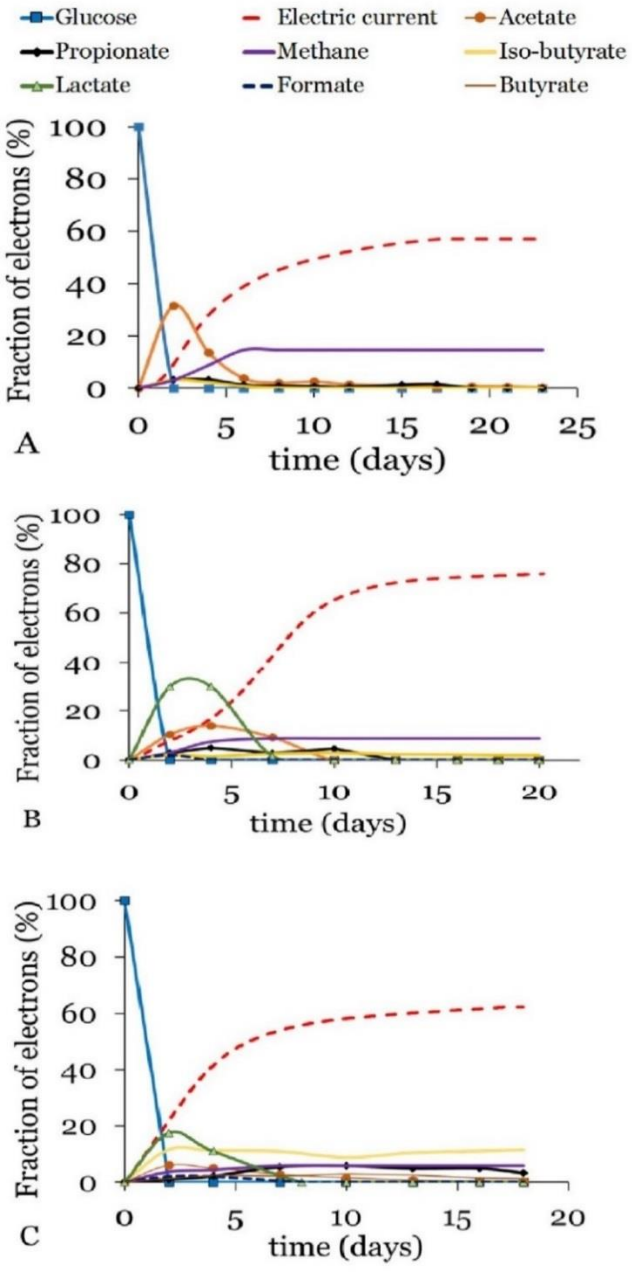

Figure 7.2 Electron distributions in MECs fed with 5-mM glucose at an initial pH of 8.1: (A) 0.02 g FAN/L or 0.2 g TAN/L (final pH = 6.85), (B) 0.18 g FAN/L or 2 g TAN/L (final pH = 7.10), and (C) 0.37 g FAN-N/L or 4 g TAN/L (final pH = 6.89).

7.3.2. Electron balances for batch MECs

Figure 7.3 presents the electron balance at the end of batch-cycle operation. Approximately 57%, 76%, and 62% of the total electrons from glucose ended up as electric current for MECs fed with 0.02, 0.18, and 0.37 g FAN/L, respectively. Theoretically, ~25% (or 9.7 me^- eq) of glucose's electrons (i.e., 38.4 me^- eq) should have been ended up as methane, if all the generated H_2 were utilized by H_2-consuming methanogens (Figure 7.1A). However, I detected as methane only about 15%, 9%, and 6%, respectively, of the original electrons.

Electrons ending up as organic acids at the end of the experiment were by far the highest for the MEC fed with 0.37 g FAN/L: ~16% of the influent electrons, versus ~0.2% and ~2% for MECs fed 0.02 and 0.18 g FAN-N/L, respectively. Approximately 28%, 13%, and 16% of the electron from glucose were unaccounted by directly measured components. Unidentified components include biomass, soluble microbial products, and fermentation products not measured by HPLC. Figure 7.1 shows an estimate of 25 and 24% of electrons ending up in biomass when methanogenesis is active versus completely inhibited.

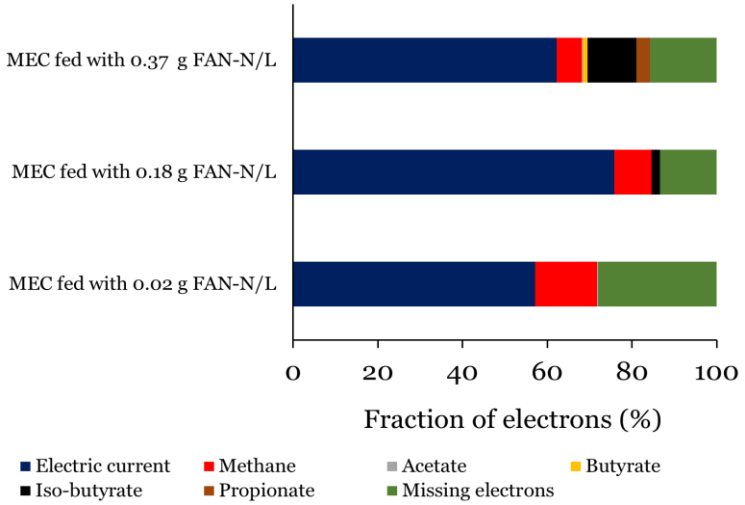

Figure 7.3 Electron balance of MECs at the end of batch-cycle operation.

7.3.3. Semi-continuous glucose fermentation in MECs

To examine whether high FAN concentration affected fermentation, methanogenesis, or both, I performed MEC experiments using semi-continuous operation by replacing the feed medium (i.e., 5 mM glucose) once every two days. Figure 7.4 summarizes the results for both MECs, which showed similar trends. The current density was stable over the influent FAN range of 0.003 to 0.18 g FAN-N/L (Figure 7.4A), but a further increase of influent FAN to 0.37 g N/L led to a gradual decrease in the current density after 2 semi-continuous cycles. This pattern suggests that higher FAN slowed acetate oxidation by ARB, since acetate accumulated at the end of semi-continuous cycle (Figure 7.4B).

Similar to the batch MECs, glucose was completely fermented for all FAN conditions, confirming that high FAN concentration did not affect the first fermentation step. As the FAN concentration increased, more electrons ended up in organic acids, and this was associated with 17–29% decreases in methane yield. Perhaps high FAN altered the fermenters' intracellular pH homeostasis, leading them to divert electrons away from H_2 production and toward formation of more-reduced organic products (González-Cabaleiro et al., 2015). A shift from H_2 to organic acids is consistent with high FAN maintaining a low H_2 concentration in the MEC, a change that should be beneficial for syntrophic interactions not involving hydrogenotrophic methanogens.

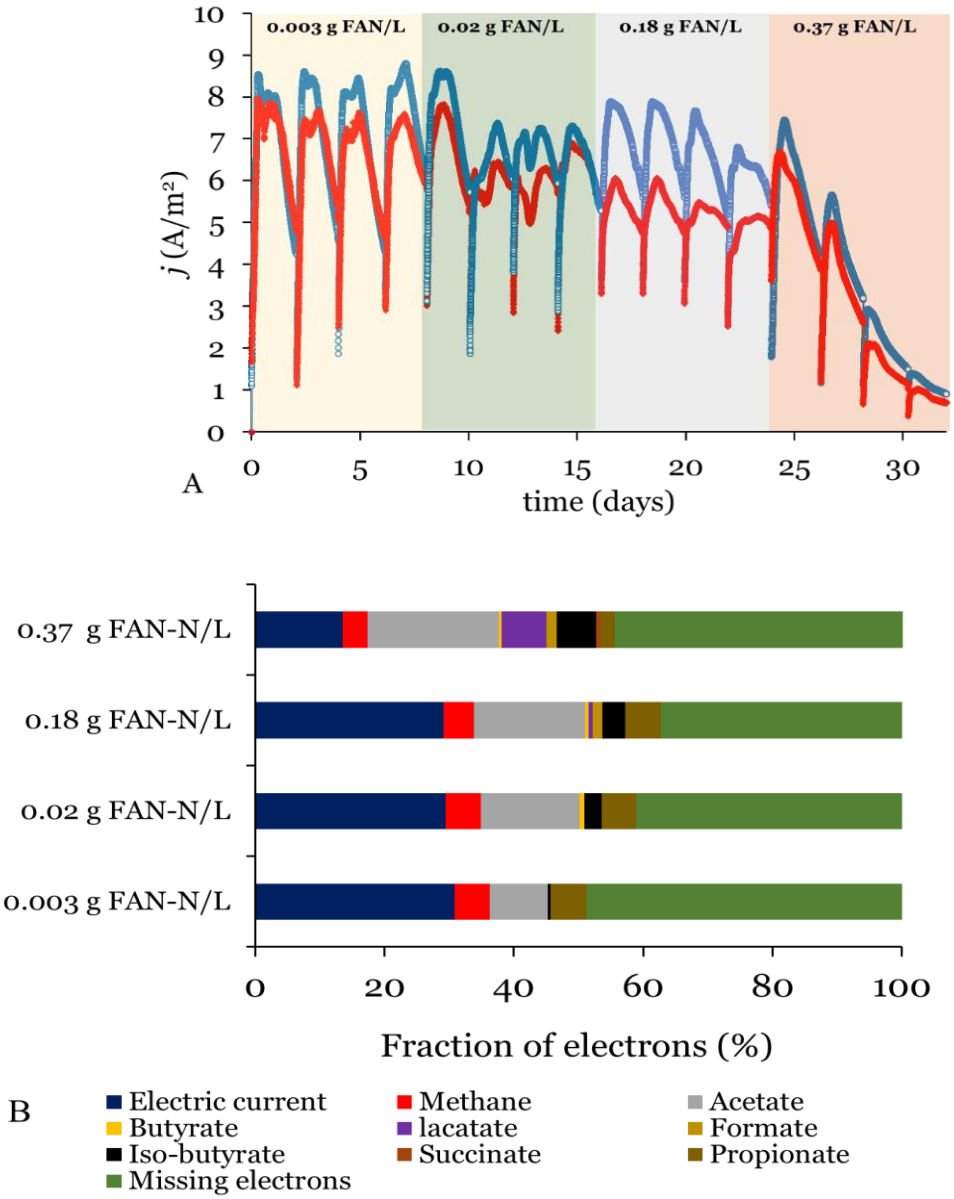

Figure 7.4 Performance of semi-continuous MECs fed with different FAN concentrations. (A) Current generation profile of duplicate MECs versus time. (B) Electron balance of MECs at the end of semi-continuous cycle operation in panel A.

7.3.4 Distribution of bacterial population in batch MECs

Figure 7.5 and Figure D.1 (in appendix D) report the sequence analyses of the V4 region in the bacterial 16S rRNA gene in the batch-MEC samples. The majority of bacterial 16S rRNA genes in all samples belonged to 3 phyla: *Proteobacteria, Firmicutes*, and *Bacteroidetes* (Figure 7.5A), which is consistent with previous studies (Mahmoud et al., 2016; Sanchez-Herrera et al., 2014; Parameswaran et al, 2010). Several members of phyla *Bacteroidetes* and *Firmicutes* are known to ferment sugar, whereas many members of *Proteobacteria* are known to perform anode respiration (Siegert et al., 2015; Rismani-Yazdi et al., 2013; Zhang et al., 2012). The lower abundance of *Proteobacteria* in the suspended-phase (SP) samples agrees with the fact that most of ARB can only use the anode surface as terminal electron acceptor.

Among the *Proteobacteria, Deltaproteobacteria* were the largest sub-group. The predominant genus among *Deltaproteobacteria* was *Geobacter,* and their relative abundance increased with higher FAN. Whereas biofilm (Bf) samples from 0.02 g FAN/L had ~2.6% of the total genus sequences in *Geobacter*, samples from 0.18 and 0.37 g FAN/L had 34.5% and 62% of the total genus sequences, respectively (Figure 7.5B). The high abundance of *Geobacter* in 0.18 and 0.37 g FAN/L Bf samples agrees with their higher CEs compared to the control MEC, and it confirms that the relatively high FAN concentration gave the ARB an ecological advantage that enhance electron flow towards anode respiration versus methanogenesis.

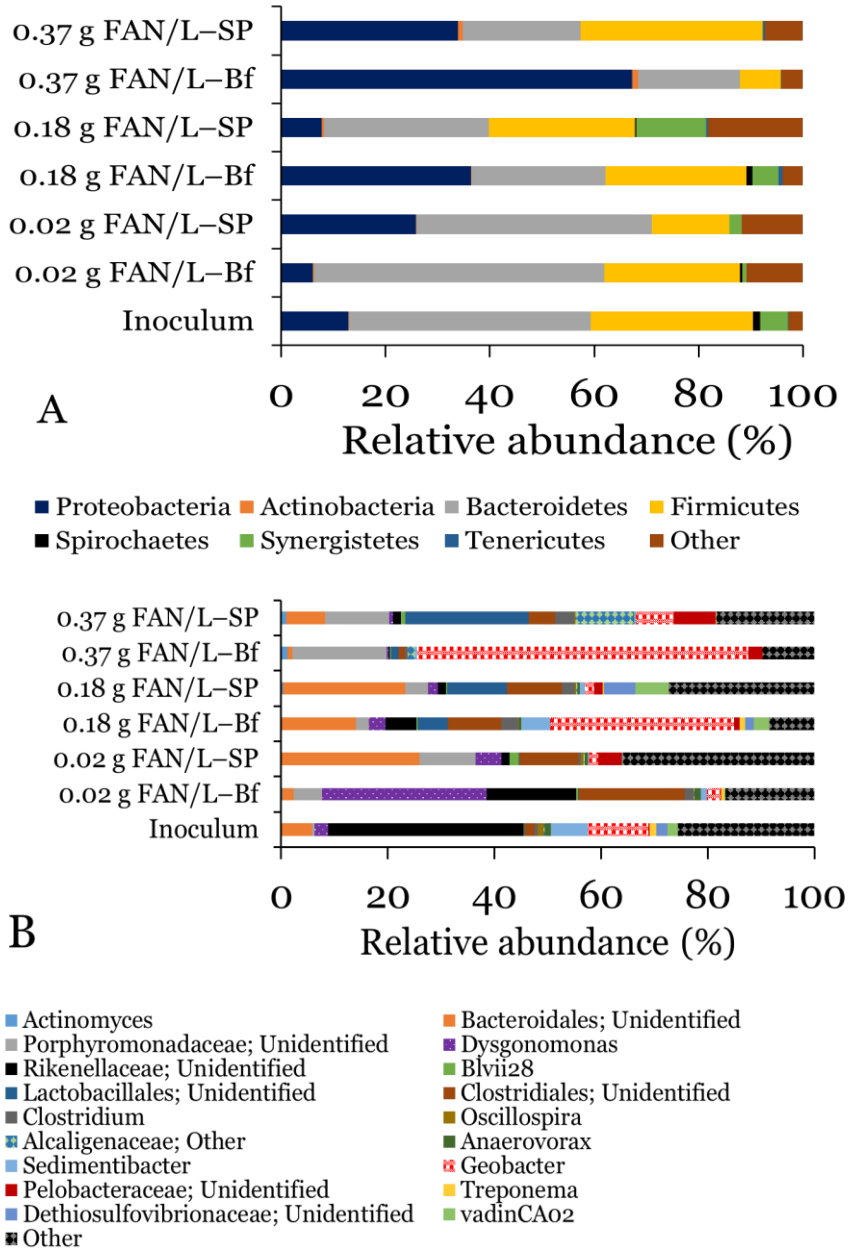

Figure 7.5 Bacterial community sequencing results. (A) bacterial community distribution at the phylum level. Phyla with less than 1% of total sequences are grouped as "others". (B) bacterial community distribution at the genus level. Genera with less than 1% of total sequences are grouped as "others".

The relative abundance of *Firmicutes* was similar in all samples except for 0.37 g FAN/L Bf, but their compositions varied significantly. Figure 7.6 shows community breakdown at the family level within the phylum *Firmicutes*. An increase in FAN

concentration led to the emergence of *Clostridiaceae* and *Ruminococcaceae* families, which belong to the order *Clostridiale*s. Compensating losses occurred for the family *Tissierellaceae*. Recently, Müller et al. (2016) revealed that several members of the *Clostridia* class, mainly belonging to the orders *Clostridiales*, can perform syntrophic acetate oxidation (SAO) (See Table 7.1), which was the predominant pathway for methane production with elevated ammonia levels (Müller et al., 2016; Westerholm et al., 2012).

I also detected an increase in the relative abundance of *Lactobacillales*, which include genera *Lactobacillus* and *Enterococcus*, at the highest FAN conditions (0.18 and 0.37 g FAN/L). *Lactobacillales* are reported to play a major role in lactic-acid production in fermentation (De Vrieze et al., 2015), and this is consistent with my observation of lactate accumulation during glucose fermentation in MECs fed with 0.18 and 0.37 g FAN/L (Figure 7.2).

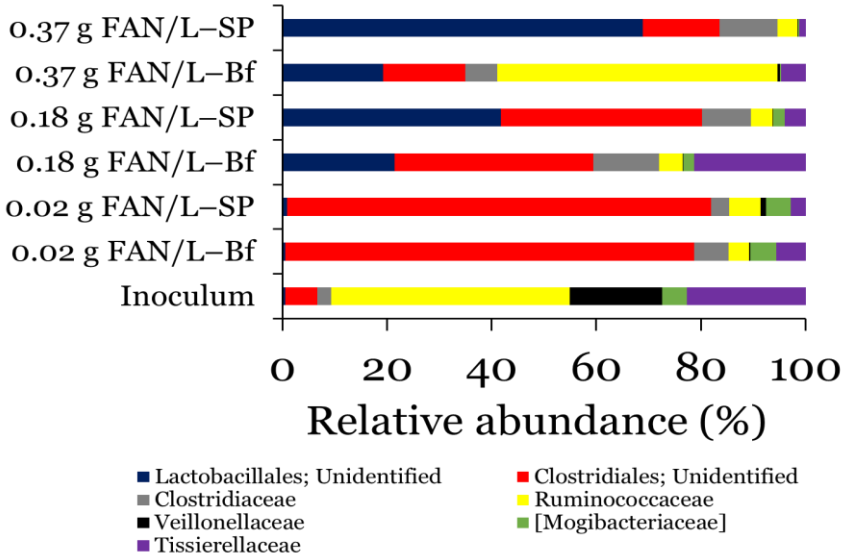

Figure **7.6** The composition of phylum *Firmicutes* at the family level. Bacterial community diversity results.

Supplementary Table D.1 and Figure D.2A shows all the values for the bacterial community diversity metrics for Bf and SP samples. The Chao1, Shannon, and PD values reflect that the Bf samples developed more diverse bacterial community than the corresponding SP samples. Also, the bacterial diversity of Bf and SP samples from 0.18 g FAN/L-fed MEC, which achieved the highest CE (Figure 7.2), was greater than from the other two MECs. Consistent with the diversity results and based on the equitability coefficient, the evenness increased as FAN concentration increased from 0.02 to 0.18 g FAN/L, while the 0.37 g FAN/L-fed MEC was least even (Figure D.2B). Previous studies (Werner et al., 2011; Wittebolle et al., 2009) revealed that microbial communities with greater evenness are often associated with more robustness and functional stability compared to less even microbial communities.

The results of weighted PCoA analysis show that principal components (PC) 1 and 2 explained 33.7% and 29.8% of the total bacterial community variations, respectively (Figure 7.7). Increasing FAN concentration correlated with the PC2 vector, whereas the type of sample (Bf versus SP) correlated with the PC1 vector.

The trend along PC2 was associated with the emergence of the orders *Desulfuromonadales*, *Lactobacillales*, and *Synergistales* at elevated FAN concentration; to compensate, the relative abundances of other orders, such as *Clostridiales* and *Bacteroidales*, decreased in response in change in FAN concentration (Figure 7.7). Several members of *Desulfuromonadales*, a sub-group of *Deltaproteobacteria*, and *Lactobacillales* are well-known ARB and lactic acid producers, respectively. Although *Synergistales*, a sub-group of phylum *Synergistetes*, have been detected in anaerobic digesters treating different wastewater, their functions are still mysterious (Zamanzadeh et al., 2016; Militon et al., 2015; Delbès et al., 2001). One study suggested that members of this order are potential propionate consumers (Hagen et al., 2014), but another study

suggested that they might be SAOB (Ito et al., 2011). The emergence of those orders, coupled with the decreases of *Clostridiales* and *Bacteroidales*, well-known acetic acid-producing fermenters, supports that higher FAN altered glucose fermentation towards the production of higher organic acids (e.g., lactate) and away from H_2, rather than the formation of 2 moles of acetate and 4 moles of H_2 per mole of glucose, as illustrated in Figure 7.1.

The trend along PC1 was associated with the emergence of the orders *Bacteroidales* and *Lactobacillales,* which play an important role in fermentation of complex substrates. Compensating for these increases, the relative abundance of *Desulfuromonadales* decreased along PC1 vector. These results confirm that most of fermentation occurred in the suspension phase, since I operated MECs in batch mode; ARB dominated the MECs' biofilm.

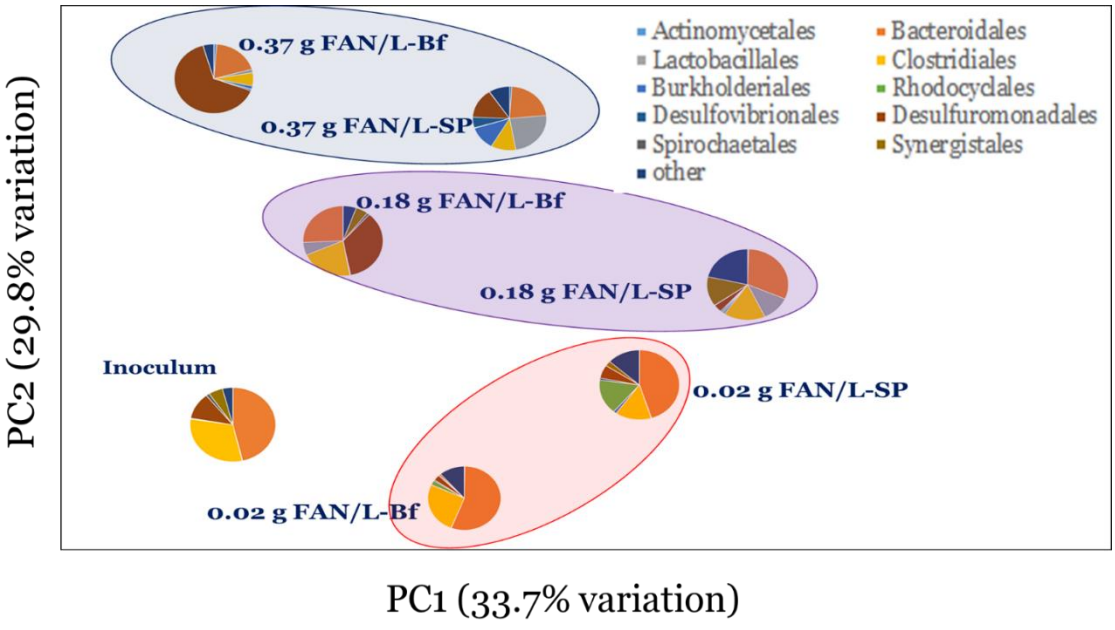

Figure 7.7 Weighted Unifrac analysis shows that the relative abundance of order-level phylotypes on the Principal Coordinates. FAN concentration determined the main phylotypes that drove the community structures in MECs.

7.3.5 Distribution of Archaea population in batch MECs

Figure 7.8 summarizes the sequencing results for Archaea. Hydrogenotrophic methanogens dominated all Bf and SP Archaea communities, regardless the FAN concentration, which is consistent with previous work (Siegert et al., 2015; Rismani-Yazdi et al., 2013; Shehab et al., 2013; Parameswaran et al., 2010). The percentage of Archaea relative to bacteria, based on the prokaryotic library results, decreased as FAN increased, supporting that the methanogens were partially inhibited by higher FAN (Figure D.3). For example, the percentage of Archaea relative to Bacteria in Bf samples was about 10.8%, 3.8%, and 4.0% for 0.02 g FAN/L, 0. 18 g FAN/L, and 0.37 g FAN/L, respectively. The percentage of Archaea to bacteria was higher for all SP samples than for Bf samples, confirming that the methanogens were predominantly in the suspended phase of MECs operated in batch mode. This trend is reinforced by the qPCR results targeting the *mcrA* gene (Figure 7.8A) and by the gradual decrease in CH_4 production in the MECs' headspace (Figure 7.2).

All Bf and SP samples were dominated by hydrogenotrophic methanogens (i.e., *Methanobacterium* and *Methanobrevibacter*) (Figure 7.8B), and I did not detect any acetoclastic methanogens. For the 0.02 g FAN/L bf, *Methanobacterium* was dominant (~ 83% of sequence), while *Methanobrevibacter* (74% for 0.18 g FAN/L biofilm and 91% for 0.37 g FAN/L biofilm) and *Methanobacterium* (16% for 0.18 g FAN/L biofilm and 11% for 0.37 g FAN/L biofilm) shared the archaeal community for higher FAN concentrations. Several members of both genera are reported to be resistant to ammonia inhibition up to 400 mM (i.e., 5.6 g TAN/L or ~ 0.04 g FAN/L at pH 6.8) (Sprott and Patel, 1986).

The higher relative abundance of *Methanobrevibacter* with higher FAN suggests that they contained the strains more resistant to FAN inhibition. Following the FAN

increase, *Methanobacterium* started to outcompete *Methanobrevibacter* (Figure 7.8B). A new uncultured Archaea, classified as a candidate genus vadinCA11 (*Thermoplasmata* sp.), emerged as FAN decreased. This genus was detected in an anaerobic fluidized bed fed with wine-distillation waste (Godon et al., 1997), and it is potentially halophilic (Durbin and Teske, 2012). The results suggest that the community shifted toward methanogens tolerant to FAN.

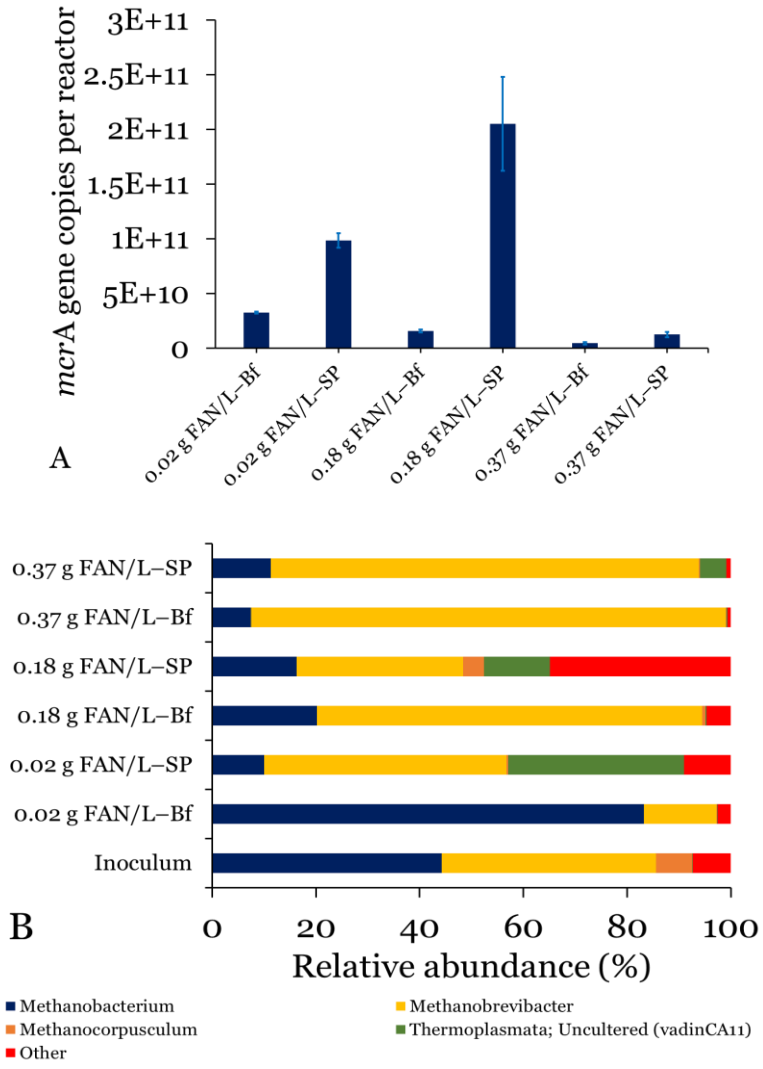

Figure 7.8 Archaeal community analyses. (A) *mcr*A gene copies per reactor determined by qPCR at the end of batch cycles. All error bars show standard deviations of triplicate measurements. (B) Archaeal community distribution at the genus level. Genera with less than 1% of total sequences are grouped as "others".

7.3.6 High FAN did not affect homo-acetogens

Previous work revealed that suppressing methanogenesis was the main reason that high CEs were achieved in MECs (Rago et al., 2015; Parameswaran, et al., 2010). Suppressing methanogenesis should promote homoacetogens, which convert H_2 and CO_2 into acetate, the ideal substrate for ARB. If this scenario were true, I should have observed a larger population of homoacetogens with higher FAN concentration. To test this hypothesis, I tracked the relative abundance of homoacetogens by targeting the FTHFS gene using qPCR; the results are in Figure 7.9. FTHFS gene copies for all Bf and SP samples were comparable, regardless of the FAN concentration. The qPCR data also are consistent with bacterial 16S rRNA gene sequence data, where I detected genus *Treponema*, a well-known homoacetogenic *Spirochaetes* (Figure 7.5B), but at low relative abundance (< 1% of total sequences) for all samples. Thus, homoacetogens were consistently present, and changes in their numbers likely were not responsible for enhancing CE.

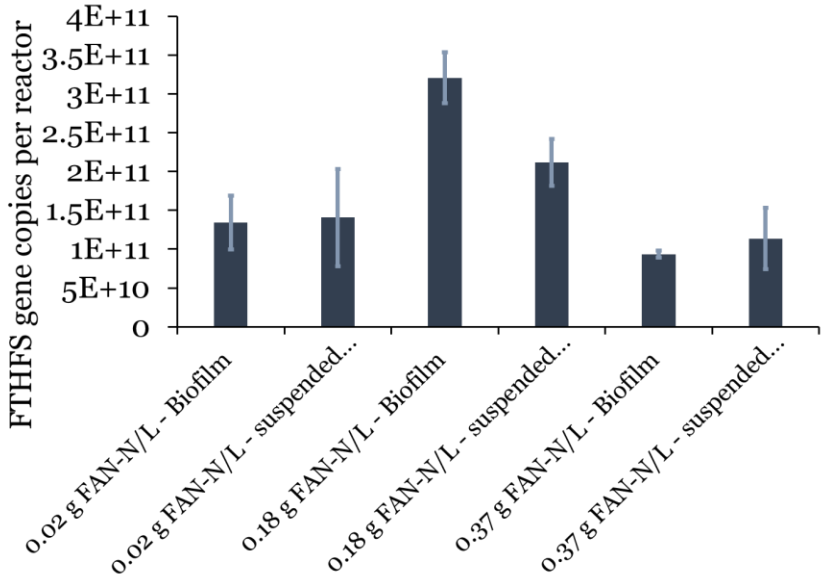

Figure 7.9 FTHFS gene copies per reactor determined by qPCR at the end of batch cycles. All error bars show standard deviations of triplicate measurements.

7.3.7 New insights into metabolic flexibility in MECs

My results add new insights for possible way to decrease CH_4 production by controlling the fermentation step using FAN instead of inhibiting methanogens using expensive or toxic chemical inhibitors. Altering fermentation led to less production of H_2, which is the "fuel" for methanogens, resulting in less CH_4 production and higher CE, even though methanogenesis was not completely suppressed. The lowering of H_2 generation was accompanied by more production of short-chain organic acids. However, relatively-high FAN (0.37 g FAN/L in my study) might promote SAOB, which are competitors for acetoclastic ARB, introducing the possibility of a new pathway for acetate consumption in MECs fed with fermentable substrates; it is a pathway to be avoided.

SAO might be the reason for the lower CE I observed with the MEC fed with 0.37 g FAN/L, compared to MEC fed with 0.18 g FAN/L. Although acetate-based anode respiration is thermodynamically favorable compared to SAO (See Table 7.1), the half-maximum-rate concentration (K_s) for SAOB ranges from 4.7 to 13 mM (Rivera-Salvador et al., 2014; Ito et al., 2011), values ~2.5- to 7-fold higher than the maximum K_s reported for mixed-culture ARB (1.86 mM) (Lee et al., 2009). Despite the higher K_s value for acetate, the SAOB may be more tolerant to high FAN, which would give them a kinetic advantage compared to ARB, since ARB often are susceptible to a high FAN concentration. This observation coincides with emergence of *Clostridiaceae* and *Ruminococcaceae* families, which are potential SAOB. Further investigation of SAOB in MECs is warranted.

7.4 Conclusion

My results reveal that FAN can help promoting desired syntrophy in MECs fed with a fermentable substrate, leading to less methanogenesis and higher CE. In MECs fed with glucose as the sole electron donor, an elevated FAN concentration partially inhibited H_2-consuming methanogens and altered electron flow from glucose towards more production of organic acids and less H_2. In addition, archaeal sequence analysis showed lower relative abundance of hydrogenotrophic methanogens in biofilm and suspended-phase samples with high FAN concentration. Although the effects of FAN were not as dramatic as from methanogenesis inhibitors like BES, FAN was able to promote syntrophic interactions among fermenters and ARB. However, relatively high FAN also might be a risky strategy if it promotes SAOB, which compete with homo-acetogens by oxidizing acetate and producing H_2.

An important implication of this study is that methanogenesis does not need to be completely suppressed to achieve high current production and CE from MECs fed with fermentable substrates. Using FAN to suppress methanogenesis is a realistic option for scaling-up MECs during the biodegradation of fermentable substrates, particularly when the feed stream has a high nitrogen content, such as animal manures and landfill leachate.

CHAPTER 8

SUMMARY, CONCLUSIONS, AND RECOMMENDATIONS FOR FUTURE WORK

8.1 Summary and Conclusions

When I started my research, the performance of MXCs fed with real wastewater was beginning to be studied, and the results were poor. The main problems were a slow rate of hydrolysis and fermentation of complex organic matter and electrons being diverted away from anode respiration, particularly to methane production. Thus, I wanted to gain a deeper understanding of both steps limiting the degradation of organic matter in MXCs. I used landfill leachate as the organic-bearing waste stream. Leachate is known to contain high concentrations of recalcitrant organics, making it a treatment challenge. However, leachate also has a low solid content and high buffering capacity, which are positives for MXCs.

To lay out the foundation for my research, I used Chapter 1 to overview the fundamentals of MXCs and how organic compounds get degraded in the MXC's anode, and then I used Chapter 2 to provide an extensive background on wastewater treatment in MXCs, the limited factors affected the anode performance, and the main microbial processes occurred in mixed-culture MXCs. Then, Chapters 3–7 presented a series of experimental studies that answered specific research questions on the two limiting steps.

In Chapter 3, I demonstrated that inhibition of fermentation, not anode respiration, was the main factor causing poor COD removal and current density in MXCs. Applying Fenton pre-treatment of landfill leachate overcame these fermentation bottlenecks by decreasing the complexity of the biodegradable-organic matter and the presence of inhibitors, leading to high CE, current density, and organic matter removal; an increase in biofilm dry weight; and emergence of phylotypes closely related to anode

respiration (i.e., *Proteobacteria*) and fermentation (i.e., *Firmicutes*, *Bacterioidetes*, *Spirochaetes*, and *Actinobacteria*). These results shed the light on the importance to speed-up fermentation kinetics for the development of efficient MXCs for treatment of complex organic matter.

I used Chapter 4 to investigate the impacts of doing most of the fermentation in an independent reactor that preceded the MEC. Allowing the fermentation to occur in a separate reactor promoted transformation of the complex organic matter in the leachate to simple volatile fatty acids, leading to much better MEC performance compared to control MEC fed with raw leachate: 14.8- and 9.2-fold increase in BOD_5 removal and current density, respectively. These results provide further support that the fermentation is the rate-limiting step in the biodegradation of organic matter in an MXCs

In Chapter 5, I systematically studied how fermentation pathways and kinetics changed as a result of altering the landfill leachate's BOD_5/COD and carbohydrate-to-protein ratios. I observed that increasing the BOD_5/COD and carbohydrate-to-protein ratios significantly improved fermentation efficiency and the distribution of fermentation organic acids, with acetate, butyrate, and propionate being the dominant products.

I explored how to minimize electrons being diverted away from anode respiration to methane production in Chapter 6. Previous studies demonstrated that methanogenesis can be completely inhibited by adding 2-bromoethanesulfonate, and this led to higher CEs. Here, I tested my hypothesis that ammonium be a tool to manage the competition between methanogens and ARB in MXCs. Ideally, the ammonia concentration is high enough to inhibit methanogens, but has no inhibitory effect on ARB and fermenters. Using a controlled experimental design, I reveal that ARB are

resistant to relatively high total ammonia-nitrogen (TAN) concentrations, but the concentrations are similar to those that methanogens can tolerate; thus, TAN cannot be used alone to favor ARB over methanogens. However, operating at a somewhat higher pH (~8.1) increased the free ammonia-nitrogen (FAN) concentration to a level (~ 200 mg FAN/L) that favored ARB over methanogens, opening up the opportunity to use FAN as a practical and effective tool for suppressing methanogens in waste streams with a high TAN concentration, such a landfill leachate.

In Chapter 7, I use a combination of chemical, electrochemical, and genomic tools to document ecological interactions between ARB and non-ARB in batch and semi-continuous MXCs fed with glucose as the sole electron donor and influent FAN from low to high concentrations (0.02 to 0.37 g FAN/L). High FAN shifted the glucose fermentation pathways toward accumulation of higher organic acids and less H_2. This change in fermentation pathways yielded higher CE and lower CH_4 production, although methanogenesis was not completely suppressed. Illumina sequencing results showed that MEC's anodes fed with higher FAN concentration were dominated with phylotypes that are most closely related to anode respiration (*Geobacteraceae*), lactic-acid production (*Lactobacillales*), and syntrophic acetate oxidation (*Clostridiaceae*). In summary, I could achieve high current density and CE from a fermentable substrate when high FAN altered the community of fermenting bacteria in a way that minimized the flow of electrons to methanogenesis.

In summary, my findings address both limitations associated with poor MXCs performance treating real wastewater. They point towards practical means to overcome both limitations and will help pave the way toward tomorrow's energy-positive, sustainable treatment of waste streams, particularly those containing complex, recalcitrant organics.

8.2 Recommendations for Future Work

In this following sections, I suggest additional follow-up research studies that stem from my findings presented in Chapters 3–7. This new research studies will lead to deeper understanding on how we can improve the efficiency of MXCs treating complex organic substrates, in terms of treatment efficiency and energy recovery.

8.2.1 Research study 1: Recalcitrant organic removal at the cathode of MXCs

In Chapters 3 and 5, I used the Fenton oxidation process as a tool to alter the composition of organic matter in landfill leachate in ways to allow me understanding the main limiting step in the biodegradation of organic matter in MXCs. Although using advanced oxidation processes, including Fenton oxidation process, is an effective approach to improve the biodegradability of recalcitrant organic compounds, including landfill leachate, it would not be economically feasible for large-scale applications due to the high cost of H_2O_2. However, recent research studies revealed that H_2O_2 can be electro-generated sustainably in MXCs in a relatively-high concentration (up to ~74 mM H_2O_2) via partial reduction of O_2 using inexpensive carbon cathode materials (Fu et al., 2010; Rozendal et al., 2009). Combining this possibility of self-generation of H_2O_2 with performing *in-situ* Fenton oxidation reaction in cathode of MXCs may offer a truly sustainable means of enhancing treatment and energy capture from recalcitrant organic matter. Despite the previous efforts to develop bioelectro—Fenton process driven by MXCs (Feng et al., 2010; Li et al., 2010; Zhu and Ni, 2009), no study showed long-term evaluation of this process, particularly the effect of $OH^{\cdot}$ on MXC's materials, including membranes and electrodes stability.

For doing so, I would set-up flat-plate MEC such as those described in Young et al. (2016) to study the H_2O_2 generation and the efficacy of *in-situ* Fenton oxidation process at the cathode when landfill leachate used as the sole electron donor. I would not use the basic H-type MEC setup, as illustrated in Chapters 3–7, due to high potential losses associated with this design. I would start by inoculating the MEC's anode chamber with anaerobic digester sludge, which guarantees fermenters and ARB in the inoculum, and I would feed a synthetic anaerobic medium with acetate as the sole electron donor – having a good buffer strength and trace mineral components (as described in Chapters 6 and 7) – in order to develop a thick biofilm on the anode surface. Once the anode biofilm reaches steady-state condition, as evidenced from stable current density generation, I would start feed raw leachate to the cathode generating H_2O_2 with either adding a source for Fe^{2+} or using fixed Fe-catalyst. First, oxidation of recalcitrant organic matter in leachate will mainly occur in the cathode chamber. Then, this treated leachate will be recirculated to anode chamber to generate electric current simultaneously.

8.2.2 Research study 2: Understanding the role of syntrophic acetate oxidizing bacteria in MXCs fed with fermentable and non-fermentable organic substrates

In Chapter 7, I was able to control the ecological interactions between ARB and non-ARB in mixed-culture MXCs fed with glucose to achieve high CE by minimizing the activity of methanogens. In this research, I used two different FAN concentrations (0.18 and 0.37 g FAN/L) compared to control condition (i.e., 0.02 g FAN/L). At 0.18 g FAN/L, I observed ~1.33-fold increase in CE and higher abundance ARB. Further increase in FAN concentration led to decrease in CE, even though CE was still higher than the

control MEC. Illumina sequencing analysis of 0.37 g FAN/L-fed MECs clearly showed emergence of phylotypes related to SAO. SAOB, which are competitors for acetoclastic ARB, might promote a new pathway for acetate consumption in MECs fed with fermentable substrates, which has to be avoided. Although acetate-based anode respiration is thermodynamically more favorable compared to SAO, SAOB have metabolic and kinetic advantages over ARB: (1) have much higher K_s value than ARB (Rivera-Salvador et al., 2014; Ito et al., 2011; Lee et al., 2009) and (2) are more tolerant to high FAN.

To understand under which conditions SAOB are favored over ARB, and to verify if SAOB are r-strategists microorganisms that are capable to grow and take up electron donors rapidly under high substrate conditions, whereas ARB are oligotrophs or K-strategists microorganisms that are capable to grow and compete for substrate under scarce substrate conditions, I propose to use MECs with similar design as those described in my dissertation research Chapters 3–7, which should be run in duplicates. I would inoculate my MECs with pre-acclimated inoculum to high ammonia concentrations (i.e., > 4 g TAN/L). After several transfer of inoculum, I would provide MECs with either glucose or acetate as the sole electron donor. After achieving steady-state current generation, I would spike ^{13}C–acetate and track the percentage ^{13}C–acetate, which would end up as electric current using a potentiostat or CH_4 using gas chromatography–mass spectrometry (GC-MS). I would also perform metagenomics and metatranscriptomics analysis to document the change in the microbial community structure after introducing high ammonia concentration. While this study seems to be fundamental in nature, it would shed light on ecological interactions in MXCs fed with fermentable and non-fermentable substrates in which SAOB are a real risk for ARB.

8.2.3 Research study 3: Production of soluble microbial products in mixed-culture anode biofilm enriched with Geobacteraceae

Because one of the main goals of an MXCs is to treat wastewater, the final effluent quality has to meet discharge limits (i.e., <30 mg 5-day BOD_5/L). Recent research revealed that high energy recovery and organic matter removal are not likely to occur simultaneously (Akman et al., 2013; Zhuang et al., 2012). Despite the recent efforts to improve the MXC's effluent quality, we still lack complete understanding for how MXCs could not produce an effluent with low organic concentration, even though the MXCs were usually operated with very long HRTs (up to 30 days) (my findings in Chapter 4). A large fraction of donor substrate is often lost to undesired electron-sinks that do not produce electric current. In addition to well-known undesired electron sinks (i.e., methane production and biomass synthesis) (my findings in Chapter 7), a likely reason for electron losses and high effluent organic matter concentration is the release of soluble microbial products (SMP) and/or extracellular polymeric substances (EPS) during normal biomass metabolism and decay (Ni et al., 2011a). Although only one study examined the SMP production in mixed-culture MXC (An and Lee, 2013), no comprehensive research studies have linked the dynamics of SMP production to normal operation of MXCs. Because the SMP production in inevitable in mixed-culture environmental biotechnology systems, including MXCs (Ni et al., 2011a), understanding the composition of SMP produced by ARB is of great importance toward scaling-up MXCs. For doing so, I would develop a mature ARB biofilm in the same MECs as described in Chapters 3–7 by controlling the anode potential with a potentiostat. I would also estimate the SMP at different operating conditions (i.e., flow rates and anode potentials) by subtracting the effluent soluble chemical oxygen demand (SCOD) measured by HACH kits from the effluent acetate concentration measured by HPLC.

My preliminary results showed that SMP concentrations at different operating conditions represent at least ~25% of the influent COD. Approximately 20% of SMP concentrations was recalcitrant with BOD_5/COD ratio of <0.1, which represents biomass-associated products (BAP) fraction of SMP.

REFERENCES

Ail, S.S. and Dasappa, S., 2016. Biomass to liquid transportation fuel via Fischer Tropsch synthesis – Technology review and current scenario. Renew. Sustain. Energy Rev. 58, 267–286.

Akman, D., Cirik, K., Ozdemir, S., Ozkaya, B. and Cinar, O., 2013. Bioelectricity generation in continuously-fed microbial fuel cell: effects of anode electrode material and hydraulic retention time. Bioresour. Technol. 149, 459–464.

Alibardi, L. and Cossu, R., 2016. Effects of carbohydrate, protein and lipid content of organic waste on hydrogen production and fermentation products. Waste Manag. 47, 69–77.

Amat, A.M., Arques, A., Galindo, F., Miranda, M.A., Santos-Juanes, L., Vercher, R.F. and Vicente, R., 2007. Acridine yellow as a solar photocatalyst for enhancing biodegradability and eliminating ferulic acid as model pollutant. Appl. Catalysis B Environ. 73, 220–226.

An, J. and Lee, H.S., 2013. Implication of endogenous decay current and quantification of soluble microbial products (SMP) in microbial electrolysis cells. RSC Adv. 3, 14021–14028.

Angelidaki, I. and Ahring, B.K., 1993. Thermophilic anaerobic digestion of livestock waste: effect of ammonia. Appl. Microbiol. Biotechnol. 38, 560–564.

Angelidaki, I., Karakashev, D., Batstone, D.J., Plugge, C.M. and Stams, A.J., 2011. Biomethanation and its potential. Methods Enzymol. 494, 327–351.

Angenent, L.T., Karim, K., Al-Dahhan, M.H., Wrenn, B.A. and Domíguez-Espinosa, R., 2004. Production of bioenergy and biochemicals from industrial and agricultural wastewater. Trends Biotechnol. 22, 477–485.

APHA, 1998. Standard Methods for the Examination of Water and Wastewater, 18th Ed., American Public Health Association, Washington, DC.

Argelier, S., Delgenes, J.P. and Moletta, R., 1998. Design of acidogenic reactors for the anaerobic treatment of the organic fraction of solid waste. Bioproc. Eng. 18, 309–315.

Arredondo, M.R., Kuntke, P., Jeremiasse, A.W., Sleutels, T.H.J.A., Buisman, C.J.N. and ter Heijne, A., 2015. Bioelectrochemical systems for nitrogen removal and recovery from wastewater. Environ. Sci.: Water Res. Technol. 1, 22–33.

Badalamenti, J.P., Krajmalnik-Brown, R. and Torres, C.I., 2013. Generation of high current densities by pure cultures of anode-respiring *Geoalkalibacter* spp. under alkaline and saline conditions in microbial electrochemical cells. mBio 4, e00144-13.

Ball, H.A. and Reinhard, M., 1996. Monoaromatic hydrocarbon transformation under anaerobic conditions at seal beach, California: Laboratory studies. Environ. Toxicol. Chem. 15, 114–122.

Baolan, H., Shuai, L., Lidong, S., Ping, Z., Xiangyang, X. and Liping, L., 2012. Effect of different ammonia concentrations on community succession of ammonia-oxidizing microorganisms in a simulated paddy soil column. PLoS One 7, e44122.

Behera, M. and Ghangrekar, M.M., 2009. Performance of microbial fuel cell in response to change in sludge loading rate at different anodic feed pH. Bioresour. Technol. 100, 5114–5121.

Berndes, G., Hoogwijk, M. and van den Broek, R., 2003. The contribution of biomass in the future global energy system: a review of 17 studies. Biomass and Bioenergy 25, 1–28.

Bird, L.J., Bonnefoy, V. and Newman, D.K., 2011. Bioenergetic challenges of microbial iron metabolisms. Trends Microbiol. 19, 330–340.

Bligh, E. and Dyer, W., 1959. A rapid method for total lipid extraction and purification. Canadian J. Biochem. Physiol. 37, 911-917.

Bond, D.R. and Lovley, D.R., 2003. Electricity production by Geobacter sulfurreducens attached to electrodes. Appl. Environ. Microbiol. 69, 1548–1555.

Bond, D.R. and Lovley, D.R., 2005. Evidence for involvement of an electron shuttle in electricity generation by *Geothrix fermentans*. Appl. Environ. Microbiol. 71, 2186–2189.

Borole, A.P., Reguera, G., Ringeisen, B., Wang, Z.W., Feng, Y. and Kim, B.H., 2011. Electroactive biofilms: Current status and future research needs. Energy Environ. Sci. 4, 4813–4834.

Bretschger, O., Obraztsova, A., Sturm, C.A., Chang, I.S., Gorby, Y.A., Reed, S.B., Culley, D.E., Reardon, C.L., Barua, S., Romine, M.F., Zhou, J., Beliaev, A.S., Bouhenni, R., Saffarini, D., Mansfeld, F., Kim, B.H., Fredrickson, J.K. and Nealson, K.H., 2007. Current production and metal oxide reduction by *Shewanella oneidensis* MR-1 wild type and mutants. Appl. Environ. Microbiol. 73, 7003–7012.

British Petroleum (BP), 2011. Statistical review of world energy. Brit Pet, London.

Budini, R., Tonelli, D. and Girotti, S., 1980. Analysis of total phenols using the Prussian blue method. J. Agricul. Food Chem. 28 (6), 1236-1238.

Call, D.F., Wagner, R.C. and Logan, B.E., 2009. Hydrogen production by Geobacter species and a mixed consortium in a microbial electrolysis cell. Appl. Environ. Microbiol. 75, 7579–7587.

Caporaso, J.G., Kuczynski, J., Stombaugh, J., Bittinger, K., Bushman, F.D., Costello, E.K., Fierer, N., Pena, A.G., Goodrich, J.K., Gordon, J.I., Huttley, G.A., Kelley, S.T., Knight, D., Koenig, J.E., Ley, R.E., Lozupone, C.A., McDonald, D., Muegge, B.D., Pirrung, M., Reeder, J., Sevinsky, J.R., Tumbaugh, P.J., Walters, W.A., Widmann, J., Yatsunenko, T., Zaneveld, J. and Knight, R., 2010. QIIME allows analysis of high-throughput community sequencing data. Nature Methods 7, 335–336.

Caporaso, J.G., Lauber, C.L., Walters, W.A., Berg-Lyons, D., Huntley, J., Fierer, N., Owens, S.M., Betley, J., Fraser, L., Bauer, M., Gormley, N., Gilbert, J.A., Smith, G. and Knight, R., 2012. Ultra-high-throughput microbial community analysis on the Illumina HiSeq and MiSeq platforms. The ISME J. 6, 1621–1624.

Chae, K.J., Choi, M.J., Kim, K.Y., Ajayi, F.F., Park, W., Kim, C.W. and Kim, I.S., 2010. Methanogenesis control by employing various environmental stress conditions in two-chambered microbial fuel cells. Bioresour. Technol. 101, 5350–5357.

Chao, A., 1987. Estimating the population-size for capture recapture data with unequal catchability. Biometrics 43, 783–791.

Chaudhuri, S.K. and Lovley, D.R., 2003. Electricity generation by direct oxidation of glucose in mediatorless microbial fuel cells. Nature Biotechnol. 21, 1229–1232.

Cheng, H.Y., Liang, B., Mu, Y., Cui, M.H., Li, K., Wu, W.M., and Wang, A.J., 2015. Stimulation of oxygen to bioanode for energy recovery from recalcitrant organic matter aniline in microbial fuel cells (MFCs). Water Res. 81, 72–83.

Clauwaert, P., Tolêdo, R., van der Ha, D., Crab, R., Verstraete, W., Hu, H., Udert, K.M. and Rabaey, K., 2008. Combining biocatalyzed electrolysis with anaerobic digestion. Water Sci. Technol. 57, 575–579.

Cole, J.R., Wang, Q., Cardenas, E., Fish, J., Chai, B., Farris, R.J., Kulam-Syed-Mohideen, A.S., McGarrell, D.M., Marsh, T., Garrity, G.M. and Tiedje, J.M., 2009. The Ribosomal Database Project: improved alignments and new tools for rRNA analysis. Nucleic Acids Res. 37(suppl 1), D141–D145.

Conrad, R. and Wetter, B., 1990. Influence of temperature on energetics of hydrogen metabolism in homoacetogenic, methanogenic, and other anaerobic bacteria. Arch. Microbiol. 155, 94–98.

Conrad, R., Bak, F., Seitz, H.J., Thebrath, B., Mayer, H.P. and Schütz, H., 1989. Hydrogen turnover by psychrotrophic homoacetogenic and mesophilic methanogenic bacteria in anoxic paddy soil and lake sediment. FEMS Microbiol. Ecol. 62, 285–294.

Cruz-Garcia, C., Murray, A.E., Klappenbach, J.A., Stewart, V. and Tiedje, J.M., 2007. Respiratory nitrate ammonification by *Shewanella oneidensis* MR-1. J. Bacteriol. 189, 656– 62.

Cusick, R.D. and Logan, B.E., 2012. Phosphate recovery as struvite within a single chamber microbial electrolysis cell. Bioresour. Technol. 107, 110–115.

Cusick, R.D., Bryan, B., Parker, D.S., Merrill, M.D., Mehanna, M., Kiely, P.D., Liu, G. and Logan, B.E., 2011. Performance of a pilot-scale continuous flow microbial electrolysis cell fed winery wastewater. Appl. Microbiol. Biotechnol. 89, 2053–2063.

Damiano, L., Jambeck, J.R., and Ringelberg, D.B., 2014. Municipal solid waste landfill leachate treatment and electricity production using microbial fuel cells. Appl. Biochem. Biotechnol. 173, 472–485.

De Vrieze, J., Saunders, A.M., He, Y., Fang, J., Nielsen, P.H., Verstraete, W. and Boon, N., 2015. Ammonia and temperature determine potential clustering in the anaerobic digestion microbiome. Water Res. 75, 312–323.

Delbès, C., Moletta, R. and Godon, J.-J., 2001. Bacterial and archaeal 16S rDNA and 16S rRNA dynamics during an acetate crisis in an anaerobic digestor ecosystem. FEMS Microbiol. Ecol. 35, 19–26.

Deng, Y., 2007. Physical and oxidative removal of organics during Fenton treatment of mature municipal landfill leachate. J. Haz. Mat. 146, 334–340.

Deng, Y. and Englehardt, J.D., 2006. Treatment of landfill leachate by the Fenton process. Water Res. 40, 3683–3694.

Díaz, E.E., Stams, A.J.M., Amils, R. and Sanz, J.L., 2006. Phenotypic properties and microbial diversity of methanogenic granules from a full-scale upflow anaerobic sludge bed reactor treating brewery wastewater. Appl. Environ. Microbiol. 72, 4942–4949.

Diekert, G. and Wohlfarth, G., 1994. Metabolism of homoacetogens. Antonie van Leeuwenhoek 66, 209–221.

DuBois, M., Gilles, K.A., Hamilton, J.K., Rebers, P.A. and Smith, F., 1956. Colorimetric method for determination of sugar and related substances. Anal. Chem. 28, 350–356.

Duesterberg, C.K., and Waite, T.D., 2006. Process optimization of Fenton oxidation using kinetic modeling. Environ. Sci. Technol. 40, 4189–4195.

Durbin, A.M. and Teske, A., 2012. Archaea in organic-lean and organic-rich marine subsurface sediments: an environmental gradient reflected in distinct phylogenetic lineages. Front. Microbiol. 3, 168.

Elefsiniotis, P. and Oldham, W.K., 1994. Anaerobic acidogenesis of primary sludge: the role of solids retention time. Biotechnol. Bioeng. 44, 7–13.

Erable, B., Féron, D. and Bergel, A., 2012. Microbial catalysis of the oxygen reduction reaction for microbial fuel cells: a review. ChemSusChem 5, 975–987.

Erisman, J.W., Sutton, M.A., Galloway, J., Klimont, Z. and Winiwarter, W., 2008. How a century of ammonia synthesis changed the world. Nature Geosci. 1, 636–639.

Escapa, A., Mateos, R., Martínez, E.J. and Blanes, J., 2016. Microbial electrolysis cells: An emerging technology for wastewater treatment and energy recovery. From laboratory to pilot plant and beyond. Renew. Sustain. Energy Rev. 55, 942–956.

Esteve-Nunéz, A., Rothermich, M., Sharma, M. and Lovley, D.R., 2005. Growth of *Geobacter sulfurreducens* under nutrient limiting conditions in continuous culture. Environ. Microbiol. 7, 641–648.

Faaij, A., 2006. Modern biomass conversion technologies. Mitigation and adaptation strategies for global change. 11, 335–367.

Faith, D.P., 1992. Conservation evaluation and phylogenetic diversity. Biol. Cons. 61, 1–10.

Fan, Y., Hu, H. and Liu, H., 2007. Enhanced coulombic efficiency and power density of air-cathode microbial fuel cells with an improved cell configuration. J. Power Sources 171, 348–354.

Feng, C.H., Li, F.B., Mai, H.J. and Li, X.Z., 2010. Bio-electro-Fenton process driven by microbial fuel cell for wastewater treatment. Environ. Sci. Technol. 44, 1875–1880.

Feng, L., Chen, Y. and Zheng, X., 2009. Enhancement of waste activated sludge protein conversion and volatile fatty acids accumulation during waste activated sludge anaerobic fermentation by carbohydrate substrate addition: The effect of pH. Environ. Sci. Technol. 43, 4373–4380.

Fischer, G. and Schrattenholzer, L., 2001. Global bioenergy potentials through 2050. Biomass and Bioenergy 20, 151–159.

Fornero, J.J., Rosenbaum, M. and Angenent, L.T., 2010. Electric power generation from municipal, food, and animal wastewaters using microbial fuel cells. Electroanalysis 22, 832–843.

Forster, P., Ramaswamy, V., Artaxo, P., Berntsen, T., Betts, R., Fahey, D.W., Haywood, J., Lean, J., Lowe, D.C., Myhre, G., Naganga, J., Prinn, R., Raga, G., Schutz, M. and Van Dorland, R., 2007. Changes in atmospheric constitutents and in radiative forcing. In Climate change 2007: The Physical Science Base, Fourth Assessment Report of the Intergovernmental Panel on Climate Change, Soloman, S., Qin, D.; Manning, M.; Chen, Z.; Marquis, M.; Averyt, K. B.; Tignor, M.; Miller, H. L., Eds.; Cambridge University Press: Cambridge.

Franks, A.E. and Nevin, K.P., 2010. Microbial fuel cells, A current review. Energies 3, 899–919.

Freguia, S., Rabaey, K., Yuan, Z. and Keller, J., 2008. Syntrophic processes drive the conversion of glucose in microbial fuel cell anodes. Environ. Sci. Technol. 42, 7937–7943.

Fu, L., You, S.J., Yang, F., Gao, M., Fang, X. and Zhang, G., 2010. Synthesis of hydrogen peroxide in microbial fuel cell. J. Chem. Technol. Biotechnol. 85, 715–719.

Ganesh, K. and Jambeck, J.R., 2013. Treatment of landfill leachate using microbial fuel cells: alternative anodes and semi-continuous operation. Bioresour. Technol. 139, 383–387.

Gao, Y., Ryu, H., Santo Domingo, J.W. and Lee, H.S., 2014. Syntrophic interactions between H_2-scavenging and anode-respiring bacteria can improve current density in microbial electrochemical cells. Bioresour. Technol. 153, 245–253.

Ge, Z., Li, J., Xiao, L., Tong, Y. and He, Z., 2014. Recovery of electrical energy in microbial fuel cells. Environ. Sci. Technol. Lett. 1, 137–141.

Ge, Z., Zhang, F, Grimaud, J., Hurst, J. and He, Z., 2013. Long-term investigation of microbial fuel cells treating primary sludge or digested sludge. Bioresour. Technol. 136, 509–514.

Godon, J.J., Zumstein, E., Dabert, P., Habouzit, F. and Moletta, R., 1997. Molecular microbial diversity of an anaerobic digestor as determined by small-subunit rDNA sequence analysis. Appl. Environ. Microbiol. 63, 2802–2813.

Gogate, P.R. and Pandit, A.B., 2004. A review of imperative technologies for wastewater treatment I: oxidation technologies at ambient conditions. Adv. Environ. Res. 8, 501–551.

Gómez, X., Fernández, C., Fierro, J., Sánchez, M.E., Escapa, A. and Morán, A., 2011. Hydrogen production: two stage processes for waste degradation. Bioresour. Technol. 102, 8621–8627.

Gonçalves, M.R., Costa, J.C., Marques, I.P. and Alves, M.M., 2012. Strategies for lipids and phenolics degradation in the anaerobic treatment of olive mill wastewater. Water Res. 46, 1684–1692.

González-Cabaleiro, R., Lema, J.M. and Rodríguez, J., 2015. Metabolic energy-based modelling explains product yielding in anaerobic mixed culture fermentations. PLoS One 10, e0126739.

Graber, J.R. and Breznak, J.A., 2004. Physiology and nutrition of *Treponema primitia*, an H2/CO2-acetogenic spirochete from termite hindguts. Appl. Environ. Microbiol. 70, 1307–1314.

Graf, E. and Penniston, J.T., 1980. Method for determination of hydrogen peroxide, with its application illustrated by glucose assay. Clin. Chem. 26, 658–660.

Greene, A.C., Patel, B.K. and Yacob, S., 2009. *Geoalkalibacter subterraneus* sp. nov., an anaerobic Fe(III)- and Mn(IV)-reducing bacterium from a petroleum reservoir, and emended descriptions of the family *Desulfuromonadaceae* and the genus *Geoalkalibacter*. Int. J. Syst. Evol. Microbiol. 59, 781– 785.

Greenman, J., Gálvez, A., Giusti, L. and Ieropoulos, I., 2009. Electricity from landfill leachate using microbial fuel cells; comparison with a biological aerated filter. J. Enzyme Microb. Technol. 44, 112–119.

Gunaseelan, V.N., 1997. Anaerobic digestion of biomass for methane production: A review. Biomass and Bioenergy 13, 83–114.

Hafez, H., Nakhla, G. and El Naggar, H., 2010. An integrated system for hydrogen and methane production during landfill leachate treatment. Int. J. Hydrogen Energy 35, 5010–5014.

Hagen, L.H., Vivekanand, V., Linjordet, R., Pope, P.B., Eijsink, V.G.H. and Horn, S.J., 2014. Microbial community structure and dynamics during co-digestion of whey permeate and cow manure in continuous stirred tank reactor systems. Bioresour. Technol. 171, 350–359.

Hall, D.O. and Scrase, J.I., 1998. Will biomass be the environmentally friendly fuel of the future? Biomass and Bioenergy 15, 357–367.

Hallenbeck, P.C., 2009. Fermentative hydrogen production: Principles, progress, and prognosis. Int. J. Hydrogen Energy 34, 7379–7389.

Hamelers, H.V.M., ter Heijne, A., Stein, N., Rozendal, R.A. and Buisman, C.J.N., 2011. Butler-Volmer-Monod model for describing bio-anode polarization curves. Bioresour. Technol. 2011, 102, 381–387.

Hansen, K.H., Angelidaki, I. and Ahring, B.K., 1998. Anaerobic digestion of swine manure: inhibition by ammonia. Water Res. 32, 5–12.

Hao, T., Xiang, P., Mackey, H.R., Chi, K., Lu, H., Chui, H., van Loosdrecht, M.C.M. and Chen, G.H., 2014. A review of biological sulfate conversions in wastewater treatment. Water Res. 65, 1–21.

Hatti-Kaul, R. and Mattiasson, B., 2016. Anaerobes in industrial- and environmental biotechnology. Adv. Biochem. Eng. Biotechnol. Springer International Publishing Switzerland, pp 1–31.

Hatti-Kaul, R., Tornvall, U., Gustafsson, L. and Borjesson, P., 2007. Industrial biotechnology for the production of bio-based chemicals – a cradle-to-grave perspective. Trends Biotechnol. 25, 119–124.

Heidenreich, S. and Foscolo, P.U., 2015. New concepts in biomass gasification. Prog. Energy Comb. Sci. 46, 72–95.

Heidrich, E.S., Curtis, T.P. and Dolfing, J., 2011. Determination of the internal chemical energy of wastewater. Environ. Sci. Technol. 45, 827–832.

Heidrich, E.S., Edwards, S.R., Dolfing, J., Cotterill, S.E. and Curtis, T.P., 2014. Performance of a pilot scale microbial electrolysis cell fed on domestic wastewater at ambient temperatures for a 12 month period. Bioresour. Technol. 173, 87–95.

Heilmann, J. and Logan, B.E., 2006. Production of electricity from proteins using a microbial fuel cell. Water Environ. Res. 78, 531–537.

Holdren, J.P. and Smith, K.R., 2000. Energy, the environment and health. J. Goldemberg (Ed.), World energy assessment, UNDP, Washington, DC, pp. 61–110.

Holmes, D.E., Nicoll, J.S., Bond, D.R. and Lovley, D.R., 2004. Potential role of a novel psychrotolerant member of the family *Geobacteraceae*, *Geopsychrobacter electrodiphilus* gen. nov., sp. nov., in electricity production by a marine sediment fuel cell. Appl. Environ. Microbiol. 70, 6023–6030.

Hoogwijk, M., Faaij, A., Eickhout, B., de Vries, B. and Turkenburg, W., 2005. Potential of biomass energy out to 2100, for four IPCC SRES land-use scenarios. Biomass and Bioenergy 29, 225–257.

Ichihashi, O. and Hirooka, K., 2012. Removal and recovery of phosphorus as struvite from swine wastewater using microbial fuel cell. Bioresour. Technol. 114, 303–307.

International Energy Agency (IEA), 2015. Key world energy statistics. Available online: https://www.iea.org/publications/freepublications/publication/KeyWorld_Statistics_2015.pdf.

IPCC, 2014. Climate Change 2014: Impacts, adaptation, and vulnerability. Part A: Global and sectoral aspects. Contribution of working group II to the Fifth assessment report of the intergovernmental panel on climate change, Cambridge University Press, Cambridge.

Iranpour, R., Stenstrom, M., Tchobanoglous, G., Miller, D., Wright, J. and Vossoughi, M., 1999. Environmental engineering: Energy value of replacing waste disposal with resource recovery. Science 285, 706–711.

Ishii, S., Suzuki, S., Norden-Krichmar, T.M., Nealson, K.H., Sekiguchi, Y., Gorby, Y.A. and Bretschger, O., 2012. Functionally stable and phylogenetically diverse microbial enrichments from microbial fuel cells during wastewater treatment. PLoS One 7, e30495.

Ishii, S., Shimoyama, T., Hotta, Y. and Watanabe, K., 2008a. Characterization of a filamentous biofilm community established in a cellulose-fed microbial fuel cell. BMC Microbiol. 8, 1–12.

Ishii, S., Watanabe, K., Yabuki, S., Logan, B.E. and Sekiguchi, Y., 2008b. Comparison of electrode reduction activities of Geobacter sulfurreducens and an enriched

consortium in an air-cathode microbial fuel cell. Appl. Environ. Microbiol. 74, 7348–7355.

Ito, T., Yoshiguchi, K., Ariesyady, H.D. and Okabe, S., 2011. Identification of a novel acetate-utilizing bacterium belonging to *Synergistes* group 4 in anaerobic digester sludge. ISME J. 5, 1844–1856.

Johansson, T.B., Kelly, H., Reddy, A.K.N. and Williams, R.H., 1993. Renewable energy: sources for fuels and electricity, Island Press, Washington, DC (1993), pp. 1–71.

Jones, W.J., Nagle, D.P. Jr. and Whitman, W.B., 1987. Methanogens and the diversity of archaebacteria. Microbiol. Rev. 51, 135–177.

Kamm, B. and Kamm, M., 2004. Principles of biorefineries. Appl. Microbiol. Biotechnol. 64, 137–145.

Kang, Y.W. and Hwang, K.Y., 2000. Effects of reaction conditions on the oxidation efficiency in the Fenton process. Water Res. 34, 2786–2790.

Karamanev, D.G., Nikolov, L.N. and Mamatarkova, V., 2002. Rapid simultaneous quantitative determination of ferric and ferrous ions in drainage waters and similar solutions. Miner. Eng. 15, 341–346.

Kashima, H. and Regan, J.M., 2015. Facultative nitrate reduction by electrode-respiring *Geobacter metallireducens* biofilms as a competitive reaction to electrode reduction in a bioelectrochemical system. Environ. Sci. Technol. 49, 3195–3202.

Kato, S., Sasaki, K., Watanabe, K., Yumoto, I. and Kamagata, Y., 2014. Physiological and transcriptomic analyses of the thermophilic, aceticlastic methanogen Methanosaeta thermophila responding to ammonia stress. Microbes Environ. 29, 162–167.

Katuri, K.P., Werner, C.M., Jimenez-Sandoval, R.J., Chen, W., Jeaon, S., Logan, B.E., Lai, Z. Amy, G.L. and Saikaly, P.E., 2014. A novel anaerobic electrochemical membrane bioreactor (AnEMBR) with conductive hollow-fiber membrane for treatment of low-organic strength solutions. Environ. Sci. Technol. 48, 12833–12841.

Katuri, K.P., Rengaraj, S., Kavanagh, P., O'Flaherty, V. and Leech, D., 2012. Charge transport through *Geobacter sulfurreducens* biofilms grown on graphite rods. Langmuir 28, 7904–7913.

Katuri, K.P., Kavanagh, P., Rengaraj, S. and Leech, D., 2010. Geobacter sulfurreducens biofilms developed under different growth conditions on glassy carbon electrodes: insights using cyclic voltammetry. Chem. Commun. 46, 4758–4760.

Kazumi, J., Caldwell, M.E., Suflita, J.M., Lovley, D.R. and Young, L.Y., 1997. Anaerobic degradation of benzene in diverse anoxic environments. Environ. Sci. Technol. 31, 813–818.

Kelly, P.T. and He, Z., 2014. Nutrients removal and recovery in bioelectrochemical systems: A review. Bioresour. Technol. 153, 351–360.

Kennedy, K.J. and Lentz, E.M., 2000. Treatment of landfill leachate using sequencing batch and continuous flow upflow anaerobic sludge blanket (UASB) reactors. Water Res. 34, 3640–3656.

Kheshgi, H.S., Prince, R.C. and Marland, G., 2000. The potential of biomass fuels in the context of global climate change: Focus on transportation fuels. Annu. Rev. Energy Environ. 25, 199–244.

Ki, D., Parameswaran, P., Popat, S.C., Rittmann, B.E. and Torres, C.I., 2015. Effects of pre-fermentation and pulsed-electric-field treatment of primary sludge in microbial electrochemical cells. Bioresour. Technol. 195, 83–88.

Kiely, P.D. Regan, J.M. and Logan, B.E., 2011. The electric picnic: synergistic requirements for exoelectrogenic microbial communities. Curr. Opin. Biotechnol. 22, 378–385.

Kim, K.Y., Yang, W. and Logan, B.E., 2015. Impact of electrode configurations on retention time and domestic wastewater treatment efficiency using microbial fuel cells. Water Res. 80, 41–46.

Kim, J., Kim, K., Ye, H., Lee, E., Shin, C., McCarty, P.L. and Bae, J., 2011a. Anaerobic fluidized bed membrane bioreactor for wastewater treatment. Environ. Sci. Technol. 45, 576– 581.

Kim, H.W., Nam, J.Y. and Shin, H.S., 2011b. Ammonia inhibition and microbial adaptation in continuous single-chamber microbial fuel cells. J. Power Sources 196, 6210–6213.

Kim, B.H., Park, H.S., Kim, H.J., Kim, G.T., Chang, I.S., Lee, J. and Phung, N.T., 2004. Enrichment of microbial community generating electricity using a fuel-cell-type electrochemical cell. Appl. Microbiol. Biotechnol. 63, 672–681.

Kim, J.S., Kim, H.Y., Won, C.H. and Kim, J.G. 2001. Treatment of leachate produced in stabilized landfills by coagulation and Fenton oxidation process. J. Chin. Inst. Chem. Eng. 32, 425–429.

Kim, Y.K. and Huh, I.R. 1997. Enhancing biological treatability of landfill leachate by chemical oxidation. Environ. Eng. Sci. 14, 73–79.

Kjeldsen, P., Barlaz, M.A., Rooker, A.P., Baun, A., Ledin, A. and Christensen, T.H., 2002. Present and long-term composition of MSW landfill leachate: A review. Crit. Rev. Environ. Sci. Technol. 32, 297–336.

Kotloski, N.J. and Gralnick, J.A., 2013. Flavin Electron Shuttles Dominate Extracellular Electron Transfer by *Shewanella oneidensis*. mBio 4, e00553–12.

Kotsyurbenko, O.R., Glagolev, M.V., Nozhevnikova, A.N. and Conrad, R., 2001. Competition between homoacetogenic bacteria and methanogenic archaea for hydrogen at low temperature. FEMS Microbiol. Ecol. 38, 153–159.

Kovárová-Kovar, K, and Egli, T., 1998. Growth kinetics of suspended microbial cells: from single-substrate-controlled growth to mixed-substrate kinetics. Microbiol. Mol. Biol. Rev. 62, 646–666.

Kuntke, P., Śmiech, K.M., Bruning, H., Zeeman, G., Saakes, M., Sleutels, T.H.J.A., Hamelers, H.V.M. and Buisman, C.J.N., 2012. Ammonium recovery and energy production from urine by a microbial fuel cell. Water Res. 46, 2627–2636.

Kuntke, P., Geleji, M., Bruning, H., Zeeman, G., Hamelers, H.V.M. and Buisman, C.J.N., 2011. Effects of ammonium concentration and charge exchange on ammonium recovery from high strength wastewater using a microbial fuel cell. Bioresour. Technol. 102, 4376–4382.

Lai, Y.J.S., Parameswaran, P., Li, A., Aguinaga, A. and Rittmann, B.E., 2016. Selective fermentation of carbohydrate and protein fractions of *Scenedesmus*, and biohydrogenation of its lipid fraction for enhanced recovery of saturated fatty acids. Biotechnol. Bioeng. 113, 320–329.

Lashof, D.A. and Tirpak, D.A., 1990. Policy options for stabilizing global climate, Hemisphere Publishing Corporation, New York, Washington, Philadelphia, London.

Laspidou, C.S. and Rittmann, B.E., 2002. A unified theory for extracellular polymeric substances, soluble microbial products, and active and inert biomass. Water Res. 36, 2711–2720.

Lazarus, M., 1993. Towards a fossil free energy future: the next energy transition Stockholm Environment Institute, Boston.

Lee, D.J., Lee, C.Y. and Chang, J.S., 2012. Treatment and electricity harvesting from sulfate/sulfide-containing wastewaters using microbial fuel cell with enriched sulfate-reducing mixed culture. J. Haz. Mat. 243, 67–72.

Lee, H.S. and Rittmann, B.E., 2010. Significance of biological hydrogen oxidation in a continuous single-chamber microbial electrolysis cell. Environ. Sci. Technol. 44, 948–954.

Lee, H.-S., Torres, C.I. and Rittmann, B.E., 2009. Effects of substrate diffusion and anode potential on kinetic parameters for anode-respiring bacteria. Environ. Sci. Technol. 43, 7571–7577.

Lee, H.S., Parameswaran, P., Marcus, A.K., Torres, C.I. and Rittmann, B.E., 2008. Evaluation of energy-conversion efficiencies in microbial fuel cells (MFCs) utilizing fermentable and non-fermentable substrates. Water Res. 42, 1501–1510.

Lehninger, A.L., Cox, M.M. and Nelson, D.L., 1993. Principles of biochemistry. Worth Publishers, New York, N.Y.

Levar, C.E., Chan, C.H., Mehta-Kolte, M.G. and Bond, D.R., 2014. An inner membrane cytochrome required only for reduction of high redox potential extracellular electron acceptors. mBio 5, e02034–14.

Lever, M.A., 2012. Acetogenesis in the energy-starved deep biosphere–a paradox? Front. Microbiol. 2, 284.

Li, L., He, Q., Ma, Y., Wang, X. and Peng, X., 2016. A mesophilic anaerobic digester for treating food waste: process stability and microbial community analysis using pyrosequencing. Micro. Cell Fac. 15, 65.

Li, W.-W., Yu, H.-Q. and He, Z., 2014. Towards sustainable wastewater treatment by using microbial fuel cells-centered technologies. Energy Environ. Sci. 7, 911–924.

Li, W.W., Yu, H.Q. and Rittmann, B.E., 2015. Chemistry: Reuse water pollutants. Nature, available online: http://www.nature.com/news/chemistry-reuse-water-pollutants-1.18899.

Li, X.M., Cheng, K.Y., Selvam, A. and Wong, J.W.C., 2013. Bioelectricity production from acidic food waste leachate using microbial fuel cells: Effect of microbial inocula. Process Biochem. 48, 283–288

Li, Z., Yao, L., Kong, L. and Liu, H., 2008. Electricity generation using a baffled microbial fuel cell convenient for stacking. Bioresour. Technol. 99, 1650–1655.

Li, Y., Lu, A., Ding, H., Wang, X., Wang, C., Zeng, C. and Yan, Y., 2010. Microbial fuel cells using natural pyrrhotite as the cathodic heterogeneous Fenton catalyst towards the degradation of biorefractory organics in landfill leachate. Electrochem. Comm. 12, 944–947.

Liew, K.B., Daud, W.R.W., Ghasemi, M., Leong, J.X., Lim, S.S. and Ismail, M., 2014. Non-Pt catalyst as oxygen reduction reaction in microbial fuel cells: A review. Int. J. Hydrogen Energy 39, 4870–4883.

Liu, J., Wu, W., Chen, C., Sun, F. and Chen, Y., 2011. Prokaryotic diversity, composition structure, and phylogenetic analysis of microbial communities in leachate sediment ecosystems. Appl. Microbiol. Biotechnol. 91, 1659–1675.

Liu, Y. and Whitman, W.B., 2008. Metabolic, phylogenetic, and ecological diversity of the methanogenic archaea. Ann. New York Acad. Sci. 1125, 171–189.

Liu, Y., Xu, H.-L., Yang, S.-F. and Tay, J.-H., 2003. Mechanisms and models for anaerobic granulation in upflow anaerobic sludge blanket reactor. Water Res. 37, 661–673.

Logan, B.E., Wallack, M.J., Kim, K.Y., He, W., Feng, Y. and Saikaly, P.E., 2015. Assessment of microbial fuel cell configurations and power densities. Environ. Sci. Technol. Lett. 2, 206–214.

Logan, B.E. and Rabaey, K., 2012. Conversion of wastes into bioelectricity and chemicals using microbial electrochemical technologies. Science 337, 686-690.

Logan, B.E., 2010. Scaling up microbial fuel cells and other bioelectrochemical systems. Appl. Microbiol. Biotechnol. 85, 1665–1671.

Logan, B.E. and Regan, J.M., 2006. Electricity-producing bacterial communities in microbial fuel cells. Trends Microbiol. 14, 512–518.

Lovley, D.R., 2008. The microbe electric: conversion of organic matter to electricity. Curr. Opin. Biotechnol. 19, 564–571.

Lovley, D.R., 2006. Bug juice: harvesting electricity with microorganisms. Nature Rev. Microbiol. 4, 497–508.

Lovley, D.R. and Coates, J.D., 2000. Novel forms of anaerobic respiration of environmental relevance. Opin. Microbiol. 3, 252–256.

Lovley, D.R., Giovannoni, S.J., White, D.C., Champine, J.E., Phillips, E., Gorby, Y.A. and Goodwin, S., 1993. *Geobacter metallireducens* gen. nov. sp. nov., a microorganism capable of coupling the complete oxidation of organic compounds to the reduction of iron and other metals. Arch. Microbiol. 159, 336–344.

Lü, F., Hao, L., Guan, D., Qi, Y., Shao, L. and He, P., 2013. Synergetic stress of acids and ammonium on the shift in the methanogenic pathways during thermophilic anaerobic digestion of organics. Water Res. 47, 2297–2306.

Lusk, B.G., Khan, Q.F., Parameswaran, P., Hameed, A., Ali, N., Rittmann, B.E. and Torres, C.I., 2015. Characterization of electrical current-generation capabilities from thermophilic bacterium *Thermoanaerobacter pseudethanolicus* using xylose, glucose, cellobiose, or acetate with fixed anode potentials. Environ. Sci. Technol. 49, 14725–14731.

Macfarlane, S. and Macfarlane, G.T., 2003. Regulation of short-chain fatty acid production. Proc. Nut. Soc. 62, 67–72.

Mahadevan, R., Bond, D.R., Butler, J.E., Esteve-Nuñez, A., Coppi, M.V., Palsson, B.O., Schilling, C.H. and Lovley, D.R., 2006. Characterization of metabolism in the Fe(III)-reducing organism Geobacter sulfurreducens by constraint-based modeling. Appl. Environ. Microbiol. 72, 1558–1568.

Mahmoud, M., Parameswaran, P., Torres, C.I. and Rittmann, B.E., 2014. Fermentation pre-treatment of landfill leachate for enhanced electron recovery in a microbial electrolysis cell. Bioresour. Technol. 151, 151–158.

Mahmoud, M., Parameswaran, P., Torres, C.I. and Rittmann, B.E., 2016. Relieving the fermentation inhibition enables high electron recovery from landfill leachate in a microbial electrolysis cell. RSC Adv. 6, 6658–6664.

Malki, M., De Lacey, A.L., Rodríguez, N., Amils, R. and Fernandez, V.M., 2008. Preferential use of an anode as an electron acceptor by an acidophilic bacterium in the presence of oxygen. Appl. Environ. Microbiol. 74, 4472–4476.

Malvankar, N.S. and Lovley, D.R., 2014. Microbial nanowires for bioenergy applications. Curr. Opin. Biotechnol. 27, 88–95.

Marsili, E., Sun, J. and Bond, D.R., 2010. Voltammetry and growth physiology of Geobacter sulfurreducens biofilms as a function of growth stage and imposed electrode potential. Electroanalysis 22, 865–874.

Marsili, E., Baron, D.B., Shikhare, I.D., Coursolle, D., Gralnick, J.A. and Bond, D.R., 2008. *Shewanella* secretes flavins that mediate extracellular electron transfer. Proc. Natl. Acad. Sci. U.S.A. 105, 3968–3973.

McCarty, P.L., Bae, J. and Kim, J., 2011. Domestic wastewater treatment as a net energy producer–can this be achieved? Environ. Sci. Technol. 45, 7100–7106.

McInerney, M.J., Struchtemeyer, C.G., Sieber, J., Mouttaki, H., Stams, A.J., Schink, B., Rohlin, L. and Gunsalus, R.P., 2008. Physiology, ecology, phylogeny, and genomics of microorganisms capable of syntrophic metabolism. Ann. New York Acad. Sci. 1125, 58–72.

McKinlay, J.B., Vieille, C. and Zeikus, J.G., 2007. Prospects for a bio-based succinate industry. Appl. Microbiol. Biotechnol. 76, 727–740.

Meckenstock, R.U., Warthmann, R.J. and Schäfer, W., 2004. Inhibition of anaerobic microbial o-xylene degradation by toluene in sulfidogenic sediment columns and pure cultures. FEMS Microbiol. Ecol. 47, 381–386.

Metcalf and Eddy, 2003. Wastewater engineering–treatment and reuse, revised by Tchobanoglous, G., Burton, F.L., Stensel, H.D, 4th edition, McGraw-Hill Inc., New York.

Miceli, J.F., Garcia-Peña, I., Parameswaran, P., Torres, C.I. and Krajmalnik-Brown, R., 2014. Combining microbial cultures for efficient production of electricity from butyrate in a microbial electrochemical cell. Bioresour. Technol. 169, 169–174.

Miceli, J.F., Parameswaran, P., Kang, D.W., Krajmalnik-Brown, R. and Torres, C.I., 2012. Enrichment and analysis of anode-respiring bacteria from diverse anaerobic inocula. Environ. Sci. Technol. 46, 10394–10355.

Militon, C., Hamdi, O., Michotey, V., Fardeau, M.L., Ollivier, B., Bouallagui, H., Hamdi, M. and Bonin, P., 2015. Ecological significance of Synergistetes in the biological treatment of tuna cooking wastewater by an anaerobic sequencing batch reactor. Environ. Sci. Poll. Res. 22, 18230–18238.

Min, B. and Logan, B.E., 2004. Continuous electricity generation from domestic wastewater and organic substrates in a flat plate microbial fuel cell. Environ. Sci. Technol. 38, 5809–5814.

Min, B., Kim, J.R., Oh, S.E., Regan, J.M. and Logan, B.E., 2005. Electricity generation from swine wastewater using microbial fuel cells. Water Res. 39, 4961–4968.

Mrkva, M., 1983. Evaluation of correlations between absorbance at 254 nm and COD of rivers waters. Water Res. 17, 231–235.

Müller, T., Walter, B., Wirtz, A. and Burkovski, A., 2006. Ammonium Toxicity in Bacteria. Curr. Microbiol. 52, 400–406.

Müller, B., Sun, L., Westerholm, M. and Schnürer, A., 2016. Bacterial community composition and *fhs* profiles of low- and high-ammonia biogas digesters reveal novel syntrophic acetate-oxidising bacteria. Biotechnol. Biofuels. 9, 48.

Muyzer, G. and Stams, A.J.M., 2008. The ecology and biotechnology of sulphate-reducing bacteria. Nature Rev. Microbiol. 6, 441–454.

Nakasaki, K., Tran, L.T.H., Idemoto, Y., Abe, M. and Rollon, A.P., 2009. Comparison of organic matter degradation and microbial community during thermophilic composting of two different types of anaerobic sludge. Bioresour. Technol. 100, 676–682.

Nam, J.Y., Kim, H.W., Lim, K.H. and Shin, H.S., 2010a. Effects of organic loading rates on the continuous electricity generation from fermented wastewater using a single-chamber microbial fuel cell. Bioresour. Technol. 101, S33–S37.

Nam, J.Y., Kim, H.W. and Shin, H.S., 2010b. Ammonia inhibition of electricity generation in single-chambered microbial fuel cells. J. Power Sources 195, 6428–6433.

Nevin K.P., Richter, H., Covalla, S.F., Johnson, J.P., Woodard, T.L., Orloff, A.L., Jia, H., Zhang M. and Lovley, D.R., 2008. Power output and columbic efficiencies from biofilms of Geobacter sulfurreducens comparable to mixed community microbial fuel cells. Environ. Microbiol. 10, 2505–2514.

Ni, B.J., Rittmann, B.E. and Yu, H.Q., 2011a. Soluble microbial products and their implications in mixed culture biotechnology. Trends Biotechnol. 29, 454–463.

Ni, B.J., Liu, H., Nie, Y.Q., Zeng, R.J., Du, G.C., Chen, J. and Yu, H.Q., 2011b. Coupling glucose fermentation and homoacetogenesis for elevated acetate production: Experimental and mathematical approaches. Biotechnol. Bioeng. 108, 345–353.

Ni, B.J., Rittmann, B.E., Fang, F., Xu, J. and Yu, H.Q., 2010. Long-term formation of microbial products in a sequencing batch reactor. Water Res. 44, 3787–3791.

Oh, S. and Logan, B.E., 2005. Hydrogen and electricity production from a food processing wastewater using fermentation and microbial fuel cell technologies. Water Res. 39, 4673–4682.

Owen, W. F., 1982. Energy in wastewater treatment, Prentice-Hall, Inc.: Englewood Cliffs.

Palatsi, J., Viñas, M., Guivernau, M., Fernandez, B. and Flotats, 2011. Anaerobic digestion of slaughterhouse waste: Main process limitations and microbial community interactions. Bioresour. Technol. 102, 2219–2227.

Pant, D., Singh, A., Van Bogaert, G., Olsen, S.I., Nigam, P.S., Diels, L. and Vanbroekhoven, K., 2012. Bioelectrochemical systems (BES) for sustainable energy production and product recovery from organic wastes and industrial wastewaters. RSC Adv. 2, 1248–1263.

Pant, D., Van Bogaert, G., Diels, L. and Vanbroekhoven, K., 2010. A review of the substrates used in microbial fuel cells (MFCs) for sustainable energy production. Bioresour. Technol. 101, 1533–1543.

Parameswaran, P., Bry, T., Popat, S.C., Lusk, B.G., Rittmann, B.E. and Torres, C.I., 2013. Kinetic, electrochemical, and microscopic characterization of the thermophilic, anode-respiring bacterium Thermincola ferriacetica. Environ. Sci. Technol. 47, 4934–4940.

Parameswaran, P., Torres, C.I., Lee, H.S., Krajmalnik-Brown, R. and Rittmann, B.E., 2009. Syntrophic interactions among anode respiring bacteria (ARB) and Non-ARB in a biofilm anode: electron balances. Biotechnol. Bioeng. 103, 513–523.

Parameswaran, P. and Rittmann, B.E., 2012. Feasibility of anaerobic co-digestion of pig waste and paper sludge. Bioresour. Technol. 124, 163–168.

Parameswaran, P., Zhang, H., Torres, C.I., Rittmann, B.E. and Krajmalnik-Brown, R., 2010. Microbial community structure in a biofilm anode fed with a fermentable substrate: the significance of hydrogen scavengers. Biotechnol. Bioeng. 105, 69–78.

Peccia, J. and Westerhoff, P., 2015. We should expect more out of our sewage sludge. Environ. Sci. Technol. 49, 8271–8276.

Peters, V., Janssen, P.H. and Conrad, R., 1998. Efficiency of hydrogen utilization during unitrophic and mixotrophic growth of *Acetobacterium woodii* on hydrogen and lactate in the chemostat. FEMS Microbiol. Ecol. 26, 317– 324.

Pham, T.H., Rabaey, K., Aelterman, P., Clauwaert, P., De Schamphelaire, L., Boon, N. and Verstraete, W., 2006. Microbial fuel cells in relation to conventional anaerobic digestion technology. Eng. Life Sci. 6, 285–292.

Phelps, T.J. and Zeikus, J.G., 1984. Influence of pH on terminal carbon metabolism in anoxic sediments from a mildly acidic lake. Appl. Environ. Microbiol. 48, 1088–1095.

Picioreanu, C., van Loosdrecht, M.C.M., Curtis, T.P. and Scott, K., 2010. Model based evaluation of the effect of pH and electrode geometry on microbial fuel cell performance. Bioelectrochem. 78, 8–24.

Pignatello, J.J., Oliveros, E. and Mackay, A., 2006. Advanced oxidation processes for organic contaminant destruction based on the Fenton reaction and related chemistry. Crit. Rev. Env. Sci. Technol. 36, 1–84.

Pinto, R.P., Srinivasan, B., Manuel, M.F. and Tartakovsky, B., 2010. A two-population bio-electrochemical model of a microbial fuel cell. Bioresour. Technol. 101, 5256–5265.

Popat, S.C. and Torres, C.I., 2016. Critical transport rates that limit the performance of microbial electrochemistry technologies. Bioresour. Technol. 215, 265–273.

Puig, S., Serra, M., Coma, M., Balaguer, M. and Colprim, J., 2011. Simultaneous domestic wastewater treatment and renewable energy production using microbial fuel cells (MFCs). Water Sci. Technol. 64, 904–909.

Qian, F., Baum, M., Gu, Q. and Morse, D.E., 2009. A 1.5 μL microbial fuel cell for on-chip bioelectricity generation. Lab Chip 9, 3076–3081.

Rabaey, K., Van de Sompel, K., Maignien, L., Boon, N., Aelterman, P., Clauwaert, P., De Schamphelaire, L., Pham, H.T., Vermeulen, J., Verhaege, M., Lens, P. and Verstraete, W., 2006. Microbial fuel cells for sulfide removal. Environ. Sci. Technol. 40, 5218–5224

Ragauskas, A.J., Williams, C.K., Davison, B.H., Britovsek, G., Cairney, J., Eckert, C.A., Frederick, W.J. Jr., Hallett, J.P., Leak, D.J., Liotta, C.L., Mielenz, J.R., Murphy, R., Templer, R. and, Tschaplinski, T., 2006. The path forward for biofuels and biomaterials. Science 311, 484–489.

Rago, L., Guerrero, J., Baeza, J.A. and Guisasola, A., 2015. 2-Bromoethanesulfonate degradation in bioelectrochemical systems. Bioelectrochem. 105, 44–49.

Rajagopal, R., Massé, D.I. and Singh, G., 2013. A critical review on inhibition of anaerobic digestion process by excess ammonia. Bioresour. Technol. 143, 632–641.

Rajeshwari, K.V., Balakrishnan, M., Kansal, A., Lata, K. and Kishore, V.V.N., 2000. State-of-the-art of anaerobic digestion technology for industrial wastewater treatment. Renew. Sustain. Energy Rev. 4, 135–156.

Reeve, J.N., 1992. Molecular biology of methanogens. Annual Rev. Microbiol. 46, 165–191.

Ren, L., Ahn, Y., Hou, H., Zhang, F. and Logan, B.E., 2014a. Electrochemical study of multi-electrode microbial fuel cells under fed-batch and continuous flow conditions. J. Power Sources 257, 454–460.

Ren, L., Ahn, Y. and Logan, B.E., 2014b. A two-stage microbial fuel cell and anaerobic fluidized bed membrane bioreactor (MFC-AFMBR) system for effective domestic wastewater treatment. Environ. Sci. Technol. 48, 4199–4206.

Ren, Z., Ward, T.E. and Regan, J.M., 2007. Electricity production from cellulose in a microbial fuel cell using a defined binary culture. Environ. Sci. Technol. 41, 4781–4786.

Renou, S., Givaudan, J.G., Poulain, S., Dirassouyan, F. and Moulin, P., 2008. Landfill leachate treatment: Review and opportunity. J. Haz. Mat. 150, 468–493.

Rimboud, M., Quemener, E.D., Erable, B., Bouchez, T. and Bergel, A., 2015. Multi-system Nernst–Michaelis–Menten model applied to bioanodes formed from sewage sludge. Bioresour. Technol. 195, 192–169.

Rismani-Yazdi, H., Carver, S.M., Christy, A.D., Yu, Z., Bibby, K., Peccia, J. and Tuovinen, O.H., 2013. Suppression of methanogenesis in cellulose-fed microbial fuel cells in relation to performance, metabolite formation, and microbial population. Bioresour. Technol. 129, 281–288.

Rittmann, B.E., Krajmalnik-Brown, R., and Halden, R.U., 2008. Pre-genomic, genomic and post-genomic study of microbial communities involved in bioenergy. Nature Rev. Microbiol. 6, 604–612.

Rittmann, B.E., 2008. Opportunities for renewable bioenergy using microorganisms. Biotechnol. Bioeng. 100, 203–212.

Rittmann, B.E. and McCarty, P.L., 2001. Environmental biotechnology: Principles and applications; McGraw-Hill: New York.

Rivera-Salvador, V., López-Cruz, I.L., Espinosa-Solares, T., Aranda-Barradas, J.S., Huber, D.H., Sharma, D. and Toledo, J.U., 2014. Application of Anaerobic Digestion Model No. 1 to describe the syntrophic acetate oxidation of poultry litter in thermophilic anaerobic digestion. Bioresour. Technol. 167, 495–502.

Rodríguez, J., Kleerebezem, R., Lema, J.M. and van Loosdrecht, M.C., 2006. Modeling product formation in anaerobic mixed culture fermentations. Biotechnol. Bioeng. 93, 592–606.

Rothausen, S. and Conway, D., 2011. Greenhouse-gas emissions from energy use in the water sector. Nature Climate Change 1, 210–219.

Rozendal, R.A., Leone, E., Keller, J. and Rabaey, K., 2009. Efficient hydrogen peroxide generation from organic matter in a bioelectrochemical system. Electrochem. Comm. 11, 1752–1755.

Rozendal, R.A., Hamelers, H.V.M., Rabaey, K., Keller, J. and Buisman, C.J.N., 2008a. Towards practical implementation of bioelectrochemical wastewater treatment. Trends Biotechnol. 26, 450–459.

Rozendal, R.A., Jeremiasse, A.W., Hamelers, V.M.H. and Buisman, C.J.N., 2008b. Hydrogen production with a microbial biocathode. Environ. Sci. Technol. 42, 629–634.

Sanchez-Herrera, D., Pacheco-Catalan, D., Valdez-Ojeda, R., Canto-Canche, B., Dominguez-Benetton, X., Domínguez-Maldonado, J. and Alzate-Gaviria, L., 2014. Characterization of anode and anolyte community growth and the impact of impedance in a microbial fuel cell. BMC Biotechnol. 14, 102.

Sarria, V., Parra, S., Adler, N., Péringer, P., Benitez, N. and Pulgarin C., 2002. Recent developments in the coupling of photoassisted and aerobic biological processes for the treatment of biorecalcitrant compounds. Cataly. Today 76, 301–315.

Schimel, J., Balser, T.C. and Wallenstein, M., 2007. Microbial stress-response physiology and its implications for ecosystem function. Ecology 88, 1386–1394.

Schink, B. and Stams, A.J.M., 2013. Syntrophism among prokaryotes. In: Rosenberg E, DeLong EF, Lory S, Stackebrandt E, Thompson F (eds.). The Prokaryotes. Springer: Berlin, Germany, pp 471–493.

Schuchmann, K. and Müller, V., 2014. Autotrophy at the thermodynamic limit of life: a model for energy conservation in acetogenic bacteria. Nature Rev. Microbiol. 12, 809–821.

Scott, K., Murano, C. and Rimbu, G., 2007. A tubular microbial fuel cell. J. Appl. Electrochem. 37, 1063–1068.

Shehab, N., Li, D., Amy, G.L., Logan, B.E. and Saikaly, P.E., 2013. Characterization of bacterial and archaeal communities in air-cathode microbial fuel cells, open circuit and sealed-off reactors. Appl. Microbiol. Biotechnol. 97, 9885–9895.

Shell, 1995. The evolution of the world's energy system 1860–2060: extracts of a study by Shell International London.

Shimoyama, T., Yamazawa, A., Ueno, Y., Watanabe, K., 2009. Phylogenetic analyses of bacterial communities developed in a cassette-electrode microbial fuel cell. Microbes Environ. 24(2), 188–92.

Shoener, B.D., Bradley, I.M., Cusick, R.D. and Guest, J.S., 2014. Energy positive domestic wastewater treatment: the roles of anaerobic and phototrophic technologies. Environ. Sci.: Processes Impacts 16, 1204–1222.

Siegert, M., Li, X.F., Yates, M.D. and Logan, B.E., 2015. The presence of hydrogenotrophic methanogens in the inoculum improves methane gas production in microbial electrolysis cells. Front. Microbiol. 5, 778.

Sleutels, T.H.J.A., Molenaar, S.D., Ter Heijne, A. and Buisman, C.J.N., 2016. Low substrate loading limits methanogenesis and leads to high coulombic efficiency in bioelectrochemical systems. Microorganisms 4, 7.

Sleutels, T.H.J.A., Ter Heijne, A., Buisman, C.J.N. and Hamelers, H.V.M., 2012. Bioelectrochemical systems: an outlook for practical applications. ChemSusChem 5, 1012–1019.

Smalley, R.E., 2003. Top ten problems of humanity for next 50 years. Energy & Nanotechnology conference, Rice University, TX, USA.

Smith, A.L., Stadler, L.B., Cao, L., Love, N.G., Raskin, L. and Skerlos, S.J., 2014. Navigating wastewater energy recovery strategies: A life cycle comparison of anaerobic membrane bioreactor and conventional treatment systems with anaerobic digestion. Environ. Sci. Technol. 48, 5972–5981.

Sprott, G.D. and Patel, G.B., 1986. Ammonia toxicity in pure cultures of methanogenic bacteria. Syst. Appl. Microbiol. 7, 358–363.

Srikanth, S., Marsili, E., Flickinger, M.C. and Bond, D.R., 2008. Electrochemical characterization of *Geobacter sulfurreducens* cells immobilized on graphite paper electrodes. Biotechnol. Bioeng. 99, 1065–1073.

Stams, A.J. and Plugge, C.M., 2009. Electron transfer in syntrophic communities of anaerobic bacteria and archaea. Nature Rev. Microbiol. 7, 568–577.

Steinberg, L.M. and Regan, J.M., 2009. *mcrA*-targeted real-time quantitative PCR method to examine methanogen communities. Appl. Environ. Microbiol. 75, 4435–4442.

Stephenson, T., Judd, S., Jeferson, B. and Brindle, K., 2000. Membrane bioreactors for wastewater treatment. London: IWA.

Sukkasem, C., Xu, S., Park, S., Boonsawang, P. and Liu, H., 2008. Effect of nitrate on the performance of single chamber air cathode microbial fuel cells. Water Res. 42, 4743–4750.

Supaphol, S., Jenkins, S.N., Intomo, P., Waite, I.S. and O'Donnell, A.G., 2011. Microbial community dynamics in mesophilic anaerobic co-digestion of mixed waste. Bioresour. Technol. 102, 4021–4027.

Takai, K. and Horikoshi, K., 2000. Rapid detection and quantification of members of the archaeal community by quantitative PCR using fluorogenic probes. Appl. Environ. Microbiol. 66, 5066–5072.

Tay, J., He, Y. and Yan, Y., 2001. Improved anaerobic degradation of phenol with supplemental glucose. J. Environ. Eng., 127, 38–45.

Tchobanoglous, G. and Kreith, F., 2002. Handbook of Solid Waste Management. 2nd ed., McGraw-Hill, New York.

Thauer, R.K., Kaster, A.K., Seedorf, H., Buckel, W. and Hedderich, R., 2008. Methanogenic archaea: Ecologically relevant differences in energy conservation. Nature Rev. Microbiol. 6, 579–591.

Thauer, R.K., Jungermann, K. and Decker, K., 1977. Energy conservation in chemotrophic anaerobic bacteria. Bacteriol. Rev. 41, 100–180.

Tice, R.C. and Kim, Y., 2014. Influence of substrate concentration and feed frequency on ammonia inhibition in microbial fuel cells. J. Power Sources 271, 360–365.

Timur, H. and Özturk, I., 1999. Anaerobic sequencing batch reactor treatment of landfill leachate. Water Res. 33, 3225–3230.

Torres, C.I., 2014. On the importance of identifying, characterizing, and predicting fundamental phenomena towards microbial electrochemistry applications. Curr. Opin. Biotechnol. 27, 107–114.

Torres, C.I., Marcus, A.K., Lee, H.S., Parameswaran, P., Krajmalnik-Brown, R., Rittmann, B.E., 2010. A kinetic perspective on extracellular electron transfer by anode-respiring bacteria. FEMS Microbiol. Rev. 34, 3–17.

Torres, C.I., Krajmalnik-Brown, R., Parameswaran, P., Marcus, A.M., Wanger, G., Gorby, Y.A. and Rittmann, B.E., 2009. Selecting anode-respiring bacteria based on anode potential: phylogenetic, electrochemical, and microscopic characterization. Environ. Sci. Technol. 43, 9519–9524.

Torres, C.I., Marcus, A.K. and Rittmann, B.E., 2008. Proton transport inside the biofilm limits electrical current generation by anode-respiring bacteria. Biotechnol. Bioeng. 100, 872–881.

Torres, C.I., Marcus, A.K. and Rittmann, B.E., 2007. Kinetics of consumption of fermentation products by anode-respiring bacteria. Appl. Microbiol. Biotechnol. 77, 689–697.

Tota-Maharaj, K. and Paul, P., 2015. Performance of pilot-scale microbial fuel cells treating wastewater with associated bioenergy production in the Caribbean context. Int. J. Energy Environ. Eng. 6, 213–220.

USEPA (US Environmental Protection Agency), 2000. CFR 445 - Protection of the Environment chapter, landfills point source category, available online: http://www.gpo.gov/fdsys/pkg/CFR-2012-title40-vol31/pdf/CFR-2012-title40-vol31-part445.pdf.

van Wyk, J.P.H., 2001. Biotechnology and the utilization of biowaste as a resource for bioproduct development. Trends Biotechnol. 19, 172–177.

von Canstein, H., Ogawa, J., Shimizu, S. and Lloyd. J.R., 2008. Secretion of flavins by Shewanella species and their role in extracellular electron transfer. Appl. Environ. Microbiol. 74, 615–623.

Wang, A., Sun, D., Cao, G., Wang, H., Ren, N., Wu, W.-M. and Logan, B.E., 2011. Integrated hydrogen production process from cellulose by combining dark fermentation, microbial fuel cells, and a microbial electrolysis cell. Bioresour. Technol. 102, 4137–4143.

Wang, X., Feng, Y., Wang, H., Qu, Y., Yu, Y., Ren, N., Li, N., Wang, E., Lee, H. and Logan, B.E., 2009. Bioaugmentation for electricity generation from corn stover biomass using microbial fuel cells. Environ. Sci. Technol. 43, 6088–6093.

Weiner, J.M. and Lovley, D.R., 1998. Rapid benzene degradation in methanogenic sediments from a petroleum-contaminated aquifer. Appl. Environ. Microbiol. 64, 1937–1939.

Wen, Q., Wu, Y., Zhao, L., Sun, Q. and Kong, F., 2010. Electricity generation and brewery wastewater treatment from sequential anode-cathode microbial fuel cell. J. Zhejiang Univ. Sci. B. 11, 87–93.

Werf, M.J., Vander, Guettler, M.V., Jain, M.K. and Zeikus, J.G., 1997. Environmental and physiological factors affecting the succinate product ratio during carbohydrate fermentation by Actinobacillus sp. 130Z. Arch. Microbiol. 167:332–342.

Werner, J.J., Garcia, M.L., Perkins, S.D., Yarasheski, K.E., Smith, S.R., Muegge, B.D., Stadermann, F.J., DeRito, C.M., Floss, C., Madsen, E.L., Gordon, J.I. and Angenent L.T., 2014. Microbial community dynamics and stability during an ammonia induced shift to syntrophic acetate oxidation. Appl. Environ. Microbiol. 80, 3375–3383.

Werner, J.J., Knights, D., Garcia, M.L., Scalfone, N.B., Smith, S., Yarasheski, K., Cummings, T.A., Beers, A.R., Knight, R. and Angenent, L.T., 2011. Bacterial community structures are unique and resilient in full-scale bioenergy systems. Proc. Natl. Acad. Sci. U.S.A. 108, 4158–4163.

Westerholm, M., Levén, L. and Schnürer, A., 2012. Bioaugmentation of syntrophic acetate-oxidizing culture in biogas reactors exposed to increasing levels of ammonia. Appl. Environ. Microbiol. 78, 7619–7625.

Williams, R.H., 1995. Variants of a low CO_2-emitting energy supply system (LESS) for the world—prepared for the IPCC Second Assessment Report Working Group IIa, energy supply mitigation options Pacific Northwest Laboratories, Richland, p. 39.

Wiszniowski, J., Robert, D., Surmacz-Gorska, Miksch, K. and Weber, J.V., 2006. Landfill leachate treatment methods: A review. Environ. Chem. Lett. 4, 51–61.

Wittebolle, L., Marzorati, M., Clement, L., Balloi, A., Daffonchio, D., Heylen, K., De Vos, P., Verstraete, W. and Boon, N., 2009. Initial community evenness favours functionality under selective stress. Nature 458, 623–626.

Xafenias, N. and Mapelli, V., 2014. Performance and bacterial enrichment of bioelectrochemical systems during methane and acetate production. Int. J. Hydrogen Energy 39, 21864–21875.

Xiao, B., Yang, F. and Liu, J., 2013. Evaluation of electricity production from alkaline pretreated sludge using two-chamber microbial fuel cell. J. Haz. Mat. 254/255, 57–63.

Xing, D., Zuo, Y., Cheng, S., Regan, J.M. and Logan, B.E., 2008. Electricity generation by *Rhodopseudomonas palustris* DX-1. Environ. Sci. Technol. 42, 4146–4151.

Yang, F., Ren, L., Pu, Y. and Logan, B.E., 2013. Electricity generation from fermented primary sludge using single-chamber air-cathode microbial fuel cells. Bioresour. Technol. 128, 784–787.

Yenigün, O. and Demirel, B., 2013. Ammonia inhibition in anaerobic digestion: A review. Process Biochem. 48, 901–911.

Yoho, R.A., Popat, S.C. and Torres, C.I., 2014. Dynamic Potential-Dependent Electron Transport Pathway Shifts in Anode Biofilms of Geobacter sulfurreducens. ChemSusChem 7, 3413–3419.

You, S.J., Zhao, Q.L., Jiang, J.Q., Zhang, J.N. and Zhao, S.Q., 2006. Sustainable approach for leachate treatment: electricity generation in microbial fuel cell. J. Environ. Sci. Health, Part A 41, 2721–2734.

Young, M.N., Links, M.J., Popat, S.C., Rittmann, B.E. and Torres, C.I., 2016. Tailoring microbial electrochemical cells for production of hydrogen peroxide at high concentrations and efficiencies. ChemSusChem (In press; DOI: 10.1002/cssc.201601182).

Yusoff, M.Z.M., Hu, A., Feng, C., Maeda, T., Shirai, Y., Hassan, M.A. and Yu, C.P., 2013. Influence of pretreated activated sludge for electricity generation in microbial fuel cell application. Bioresour. Technol. 145, 90–96.

Zamanzadeh, M., Hagen, L.H., Svensson, K., Linjordet, R. and Horn, S.J., 2016. Anaerobic digestion of food waste – Effect of recirculation and temperature on performance and microbiology. Water Res. 96, 246–254.

Zhang, X., He, W., Ren, L., Stager, J., Evans, P.J. and Logan, B.E., 2015. COD removal characteristics in air-cathode microbial fuel cells. Bioresour. Technol. 176, 23–31.

Zhang, H., Chen, X., Braithwaite, D., and He, Z., 2014a. Phylogenetic and metagenomic analyses of substrate-dependent bacterial temporal dynamics in microbial fuel cells. PLoS One. 9, e107460.

Zhang, C., Yuan, Q., Lu, Y., 2014b. Inhibitory effects of ammonia on methanogen *mcr*A transcripts in anaerobic digester sludge. FEMS Microbiol. Ecol. 87, 368–377.

Zhang, F., Ge, Z., Grimaud, J., Hurst, J. and He, Z., 2013. Long-term performance of liter-scale microbial fuel cells treating primary effluent installed in a municipal wastewater treatment facility. Environ. Sci. Technol. 47, 4941–4948.

Zhang, G., Zhao, Q., Jiao, Y., Wang, K., Lee, D.-J. and Ren, N., 2012. Efficient electricity generation from sewage sludge using biocathode microbial fuel cell. Water Res. 46, 43–52.

Zhang, Y., Min, B., Huang, L. and Angelidaki, I., 2009. Generation of electricity and analysis of microbial communities in wheat straw biomass-powered microbial fuel cells. Appl. Environ. Microbiol. 75, 3389–3395.

Zhang, J.N., Zhao, Q.L., You, S.J., Jiang, J.Q. and Ren, N.Q., 2008. Continuous electricity production from leachate in a novel upflow air cathode membrane free microbial fuel cell. Water Sci. Technol. 57, 1017–1021.

Zhang, H., Choi, H.J. and Huang, C.P., 2005. Optimization of Fenton process for the treatment of landfill leachate. J. Haz. Mat. 125, 166–174.

Zhao, F., Harnisch, F., Schröder, U., Scholz, F., Bogdanoff, P. and Herrmann, I., 2005. Application of pyrolysed iron (II) phthalocyanine and CoTMPP based oxygen reduction catalysts as cathode materials in microbial fuel cells. Electrochem. Comm. 7, 1405–1410.

Zhou, M., Chi, M., Luo, J., He, H. and Jin, T., 2011. An overview of electrode materials in microbial fuel cells. J. Power Sources 196, 4427–4435.

Zhu, X., Siegert, M., Yates, M.D. and Logan, B.E., 2015. Alamethicin suppresses methanogenesis and promotes acetogenesis in bioelectrochemical systems. Appl. Environ. Microbiol. 81, 3863–3868.

Zhu, X. and Ni, J., 2009. Simultaneous processes of electricity generation and p-nitrophenol degradation in a microbial fuel cell. Electrochem. Comm. 11, 274–277.

Zhuang, L., Zheng, Y., Zhou, S., Yuan, Y., Yuan, H. and Chen, Y., 2012. Scalable microbial fuel cell (MFC) stack for continuous real wastewater treatment. Bioresour. Technol. 106, 82–88.

Zinder, S.H. and Koch, M., 1984. Non-aceticlastic methanogenesis from acetate: acetate oxidation by a thermophilic syntrophic coculture. Arch. Microbiol. 138, 263–272.

Zinder, S.H., 1993. Physiological ecology of methanogens. In: Ferry JG, editor. Methanogenesis—Ecology, physiology, biochemistry & genetics. New York, NY: Chapman & Hall. pp 128–206.

APPENDIX A

SUPPLEMENTARY INFORMATION FOR CHAPTER 3

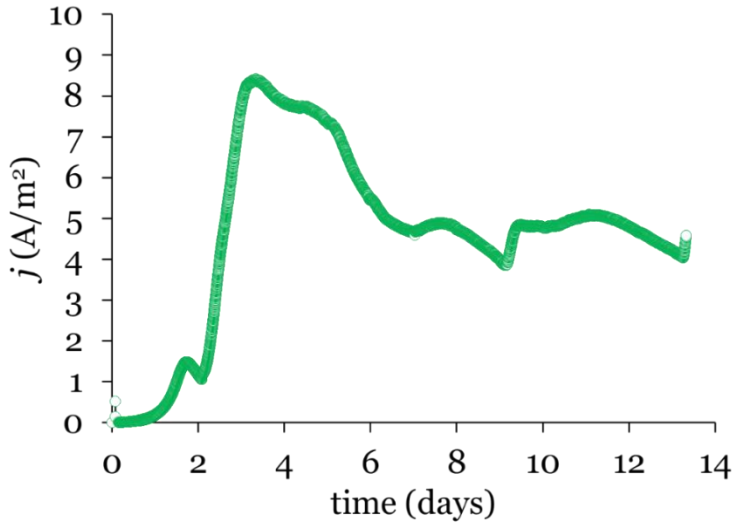

Figure A.1 Current density generation during the initial period of biofilm formation on the anode.

Table A.1 Summary of Fenton oxidation process [a]

Reaction 1:	$Fe^{2+} + H_2O_2 \rightarrow Fe^{3+} + OH^- + OH^{\cdot}$
Reaction 2:	$Fe^{3+} + H_2O_2 \rightarrow Fe^{2+} + HO_2^{\cdot} + H^+$
Reaction 3:	$H_2O_2 + OH^{\cdot} \rightarrow HO_2^{\cdot} + H_2O$
Reaction 4:	$Fe^{2+} + OH^{\cdot} \rightarrow Fe^{3+} + OH^-$
Reaction 5:	$Fe^{3+} + HO_2^{\cdot} \rightarrow Fe^{2+} + HO_2^+$
Reaction 6:	$Fe^{2+} + HO_2^{\cdot} + H^+ \rightarrow Fe^{3+} + H_2O_2$
Reaction 7:	$HO_2^{\cdot} + HO_2^{\cdot} \rightarrow H_2O_2 + O_2$

[a] Adapted from Duesterberg and Waite (2006) and Deng and Englehardt (2006).

APPENDIX B

SUPPLEMENTARY INFORMATION FOR CHAPTER 4

Table B.1 Chemical characteristics of the landfill leachate

Parameter [a]	**Average value (SD** [b]**)**
pH	8.4 (0.59)
COD	2630 (210)
BOD_5	835 (59)
BOD_5/COD ratio	0.32
Carbohydrate	190 (10)
Protein	920 (15)
Lipids	80 (8)
TOC	705 (36)
Phenol	115 (10)
TSS	67 (10)
Total–N	550 (40)
NH_4^+	454 (45)
Organic-N	104 (15)
NO_3–N	0.42 (0.01)
NO_2–N	≤ 0.12
Sulfate	37 (0.5)
Chloride	2990 (13)
Total-P	13.1 (0.6)
Alkalinity, as $CaCO_3$	3890 (190)

[a] All values are in mg/L except pH and BOD_5/COD ratio;
[b] SD: Standard deviation for triplicate measurements

APPENDIX C

SUPPLEMENTARY INFORMATION FOR CHAPTER 6

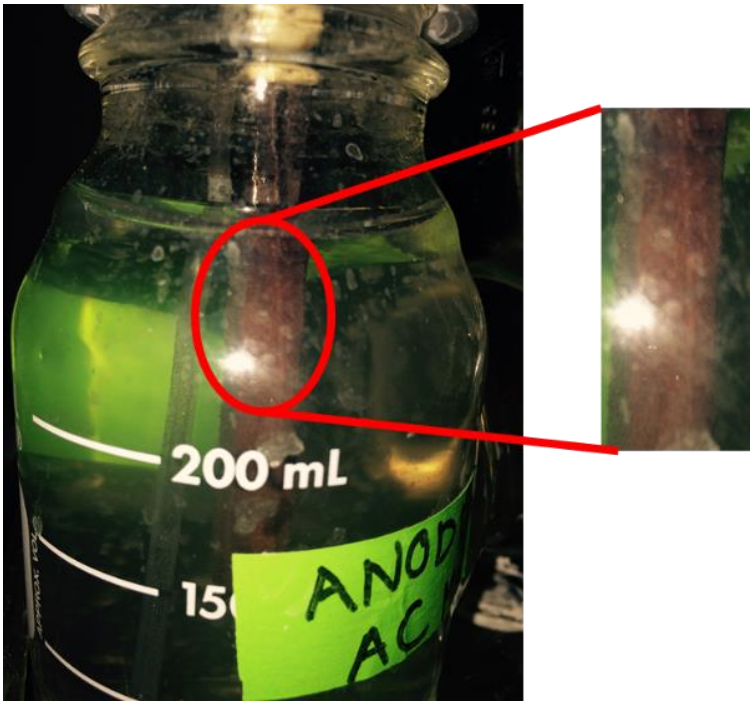

Figure C.1 Photograph shows visibly thick anode biofilms formed after 60 days of continuous feed operation.

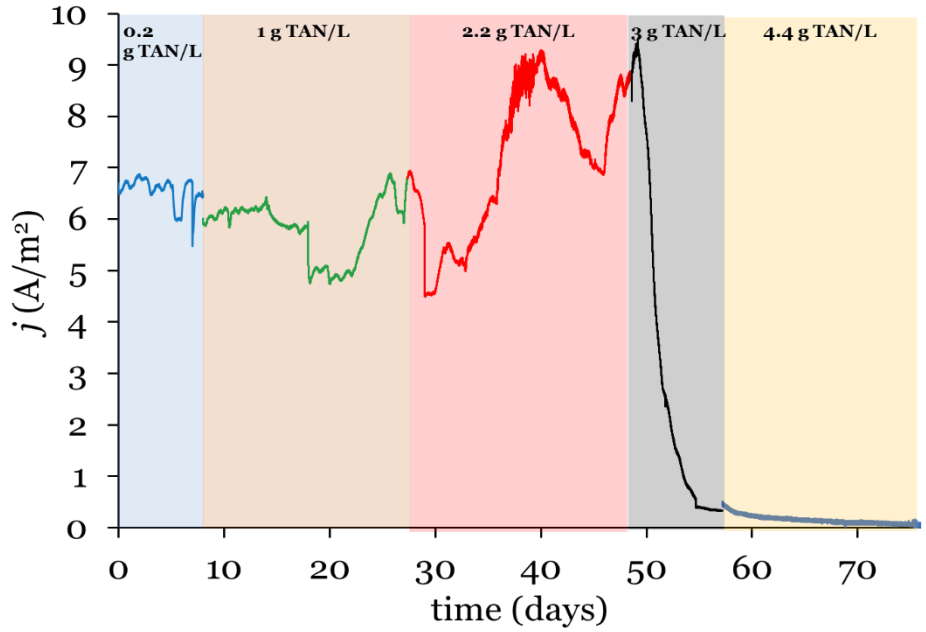

Figure C.2 A second replicate, corresponding to the data presented in Figure 6.1A, showing steady state current generation versus time for MECs fed with different TAN media during continuous operation at an HRT = ~ 18 h.

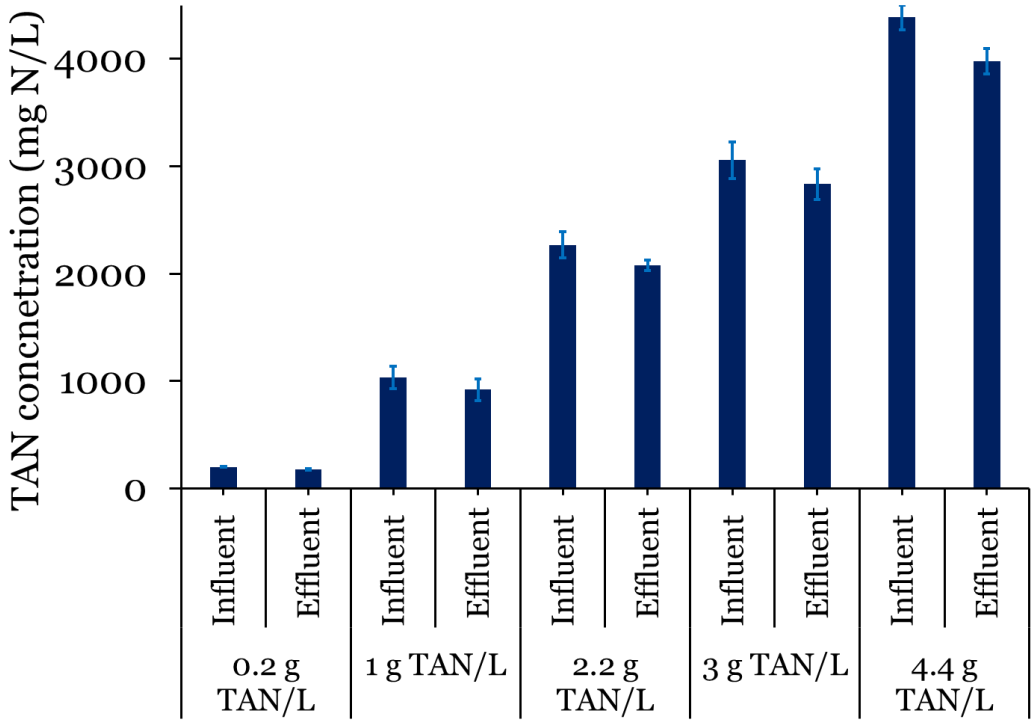

Figure C.3 Average concentration of TAN for MECs during continuous operation at an HRT of ~18 h.

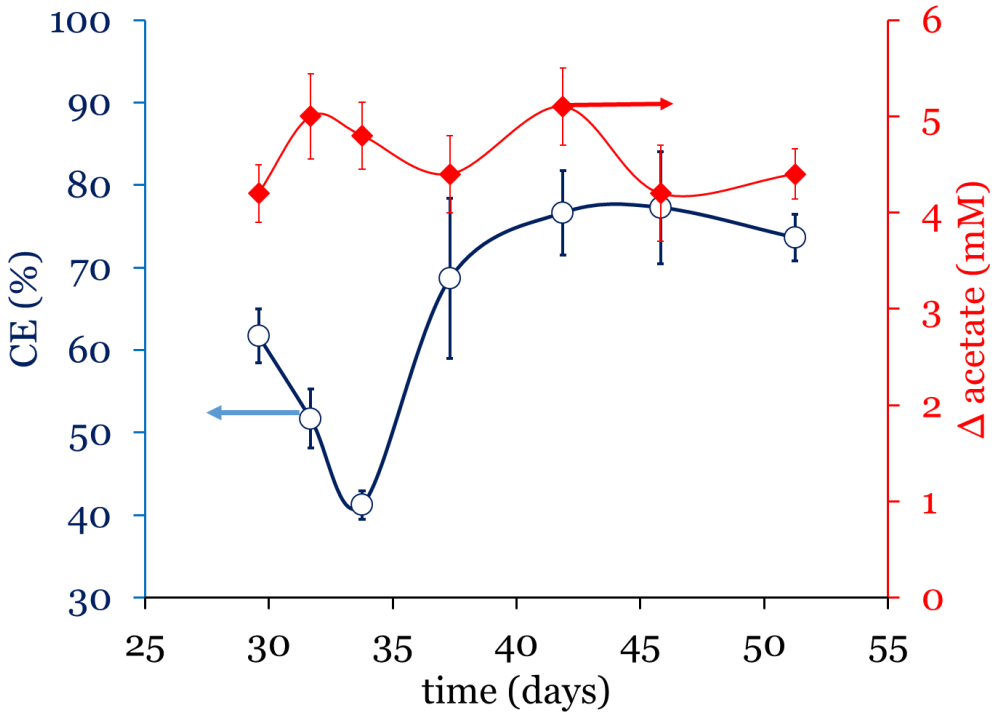

Figure C.4 Coulombic efficiency versus time for an MEC fed with a TAN concentration of 2.2 g N/l, corresponding to the data presented in Figure 6.1A.

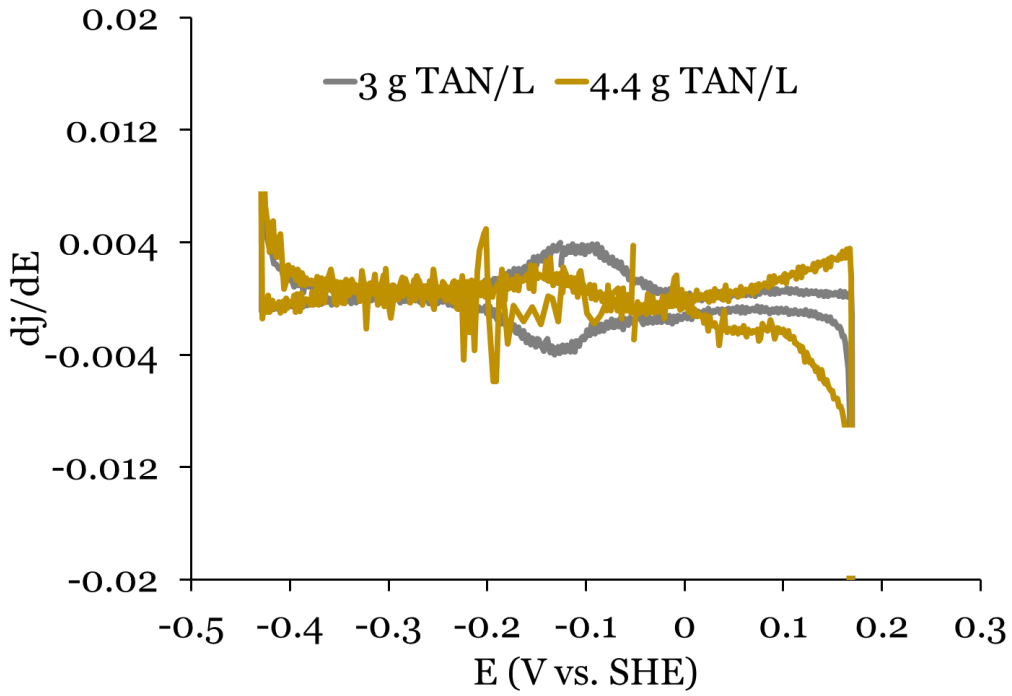

Figure C.5 The first derivative of CVs shown in Figure 6.4A for MEC fed with TAN concentrations of 3 and 4.4 g TAN/L.

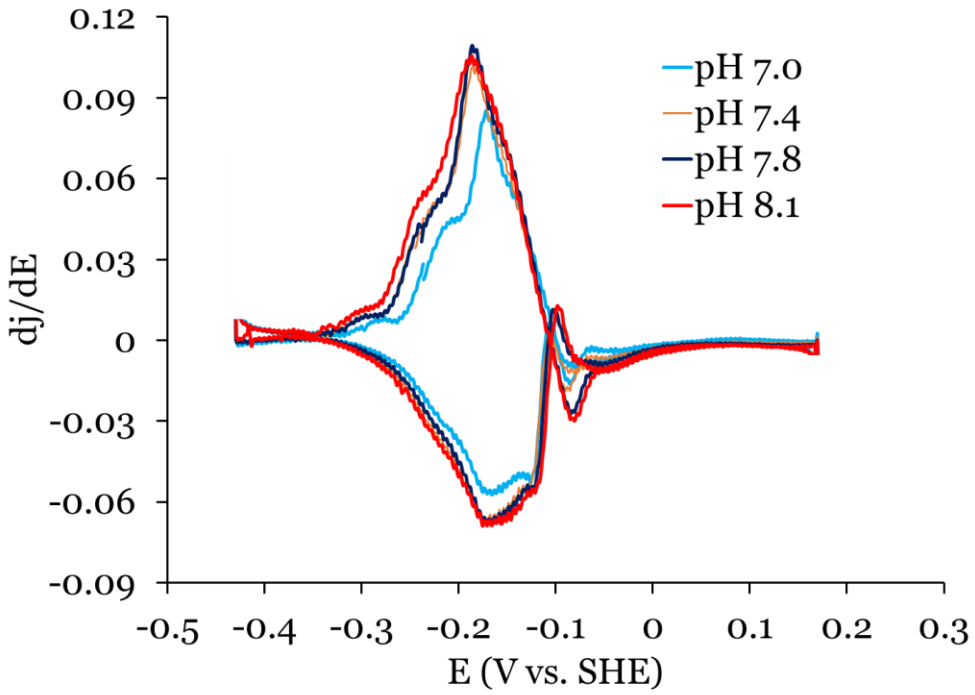

Figure C.6 The first derivatives of the CVs shown in Figure 6.6B for an MEC fed with a TAN concentration of 2.2 g TAN/L at different pH values.

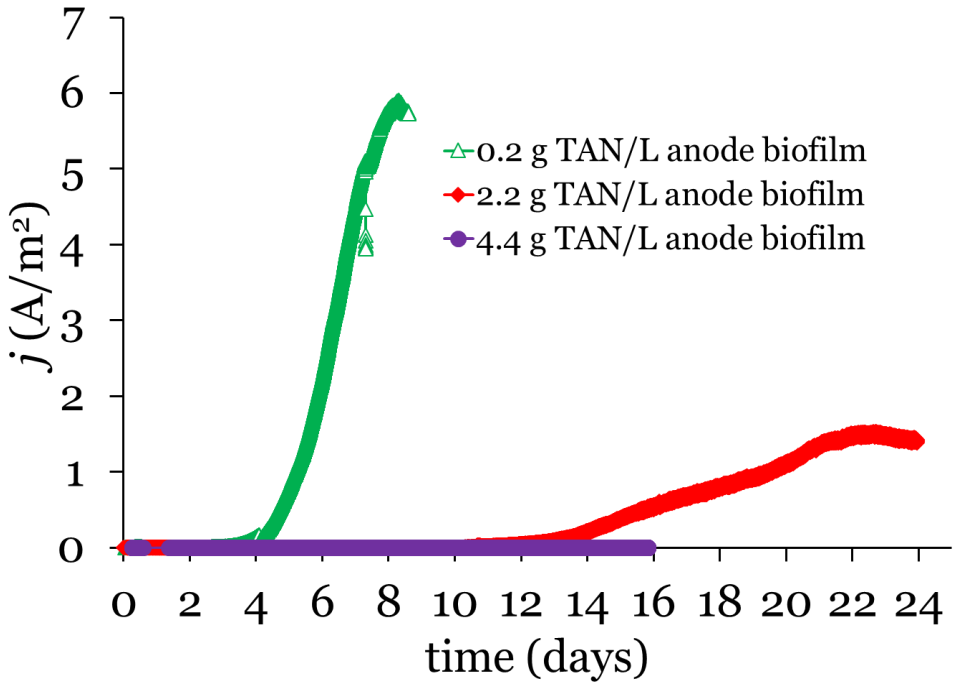

Figure C.7 A second replicate, corresponding to the data presented in Figure 6.7, showing growth-experiment data for MECs fed with different TAN concentrations.

APPENDIX D

SUPPLEMENTARY INFORMATION FOR CHAPTER 7

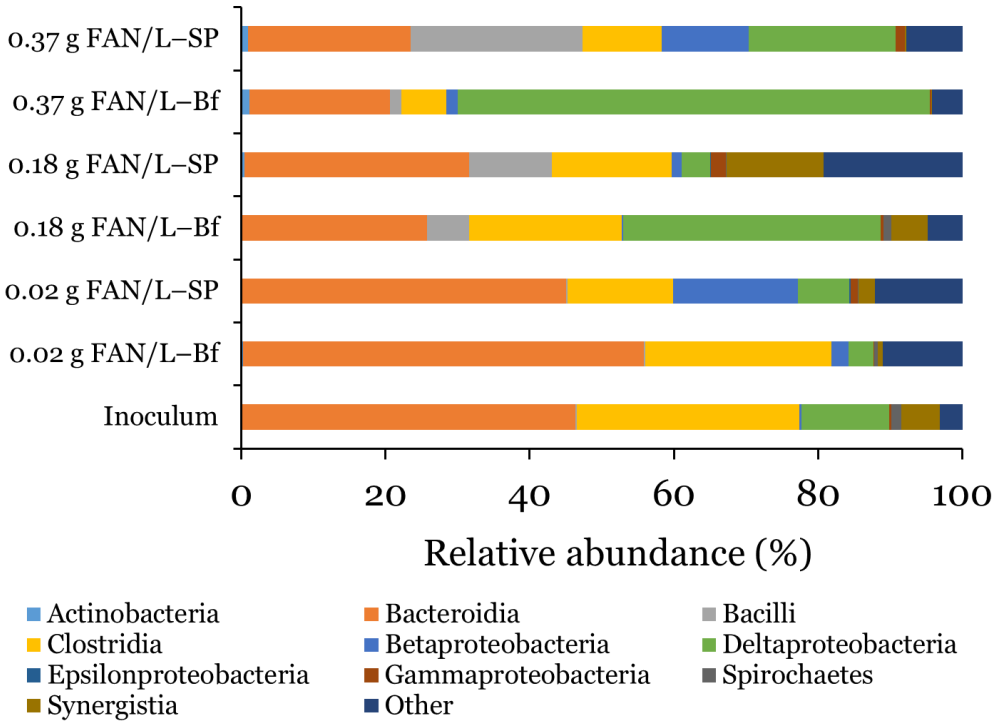

Figure D.1 Bacterial community distribution at the class level. Classes with less than 1% of total sequences are grouped as "others".

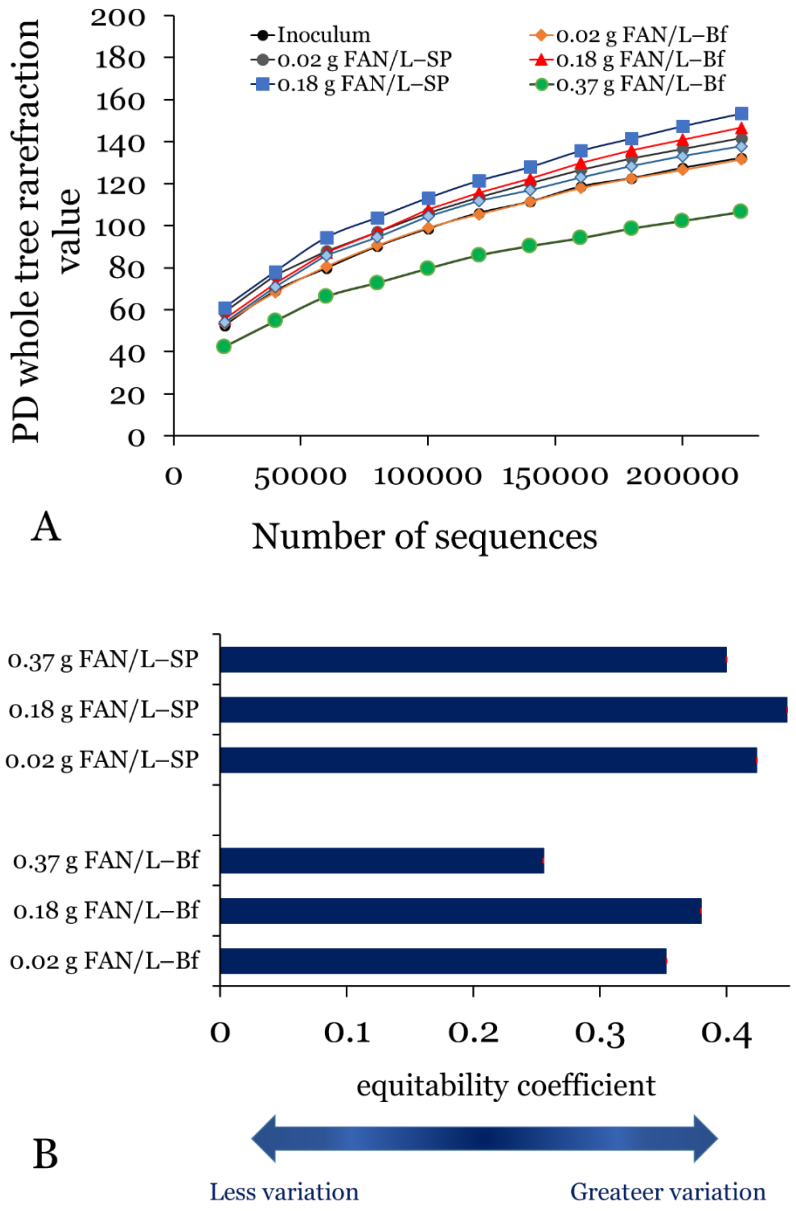

Figure D.2 Bacterial community diversity and richness results. (A) Phylogenetic Diversity (PD) Whole Tree measurements from using trimmed, equal sequencing depth OTUs per sample a 97% similarity. (B) Evenness (measured as the equitability coefficient) of bacterial OTU profiles.

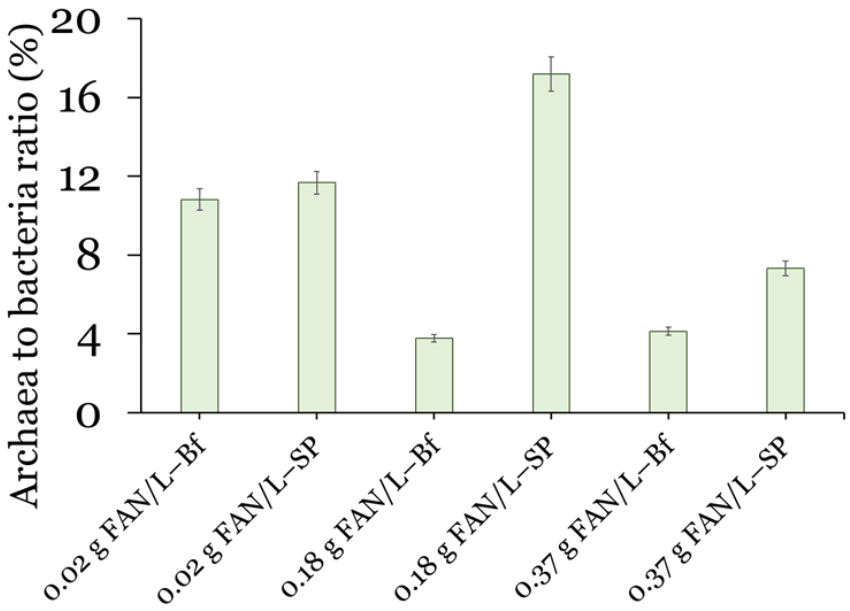

Figure D.3 Archaea-to-bacteria ratio, based on the prokaryotic library results.

Table D.1 Chao1, Shannon, and PD indices for bacterial sequences

Samples	chao1 index	Shannon	PD index
Inoculum	3079±26	4.14±0.0011	132±0.2
0.02 g FAN/L–Bf	3242±30	3.90±0.0010	132±0.7
0.02 g FAN/L–SP	3670±68	4.77±0.0010	141±0.8
0.18 g FAN/L–Bf	4023±62	4.27±0.0009	147±0.6
0.18 g FAN/L–SP	3932±63	5.10±0.00014	153±0.6
0.37 g FAN/L–Bf	2662±32	2.75±0.00085	107±0.4
0.37 g FAN/L–SP	3405±7	4.46±0.00028	137±0.1